An examination of ecosystem dependence on shallow groundwater systems in the Western rivers region, Lake Eyre Basin, South Australia

Volume 2: Supplementary report

DEWNR Technical report 2017/04

Government of South Australia
Department of Environment, Water and Natural Resources

An examination of ecosystem dependence on shallow groundwater systems in the Western Rivers region, Lake Eyre Basin, South Australia

Volume 2: Supplementary report

Mark Keppel[1], Catherine Miles[2], Claire Harding[1], Dorothy Turner[3], Justin Costelloe[4], Kenneth Clarke[3], Megan Lewis[3]

Department of Environment, Water and Natural Resources

October 2017

DEWNR Technical note 2017/04

Department of Environment, Water and Natural Resources

GPO Box 1047, Adelaide SA 5001

Telephone National (08) 8463 6946

International +61 8 8463 6946

Fax National (08) 8463 6999

International +61 8 8463 6999

Website www.environment.sa.gov.au

Disclaimer

The Department of Environment, Water and Natural Resources and its employees do not warrant or make any representation regarding the use, or results of the use, of the information contained herein as regards to its correctness, accuracy, reliability, currency or otherwise. The Department of Environment, Water and Natural Resources and its employees expressly disclaims all liability or responsibility to any person using the information or advice. Information contained in this document is correct at the time of writing.

This work is licensed under the Creative Commons Attribution 4.0 International License.

To view a copy of this license, visit http://creativecommons.org/licenses/by/4.0/.

© Crown in right of the State of South Australia, through the Department of Environment, Water and Natural Resources 2017

ISBN 978-1-925510-63-8

Download this document at: http://www.waterconnect.sa.gov.au

Contents

List of figures

List of tables

1 Introduction

1.1 Background

The western rivers of the Lake Eyre Basin (LEB) are located in the highly arid far north region of South Australia (McMahon et al., 2008). However, despite its aridity, water dependent ecosystems are a notable feature in the region. These include permanent springs fed by the Great Artesian Basin (GAB), permanent and semi-permanent riverine waterholes and extensive riparian and floodplain woodlands.

The project *Ecosystems Dependent on Shallow Groundwater Systems in the Western Rivers* investigates a key knowledge gap in the region: the distribution and characteristics of shallow groundwater in riparian landscapes and the degree to which ecosystems are dependent on that shallow groundwater.

This project uses on-ground research and a multiple lines of evidence approach to address knowledge gaps using:

- Analysis of groundwater and surface water chemistry
- Tree sapflow monitoring
- Tree and soil water potential
- Tree and water isotope analysis
- Remotely sensed imagery analysis.

There are two parts to this report due to the size and multi-faceted nature of this investigation. The main report provides the most pertinent background information, the discussion of findings, the hydroecological conceptual models and conclusions and recommendations stemming from these investigations are provided in the report entitled: "*Examination of Ecosystem Dependence on Shallow Groundwater Systems in the Western Rivers Region, Lake Eyre Basin, South Australian Volume 1: Report*". This report provides supplementary material that helps support the discussion and conclusions presented in the main report. This material includes detailed descriptions of methodology and results from the various field investigations, relevant literature review material, and publically available data used to develop hypotheses.

2 Hydrogeology

The following is a literature review of the hydrogeology of relevant hydrostratigraphic units found within the area that may be affecting potential groundwater dependent ecosystems (GDEs) within the study area and are at potential risk by coal seam gas (CSG) or large coal mining developments.

2.1 Perched aquifers and bank storage

Miles and Costelloe (2015) hypothesized that perched aquifers exist in the upper catchments of the study area; these are regions where the soil or rock may be locally saturated because it overlies a lower permeability unit, and the rate of recharge is greater than the rate of discharge (Richardson et al. 2011). Importantly, perched aquifers are separated by an unsaturated zone from any more-extensive aquifers, although they may leak downwards. Perched aquifers are commonly formed in alluvial and lacustrine environments and the groundwater may be temporary or permanent (Richardson et al. 2011). Because of their isolation from larger aquifers, the risks to ecosystems dependent on perched aquifers tend to be more localised in nature than risks to ecosystems reliant on more extensive groundwater systems. Miles and Costelloe (2015) reasoned that perched aquifers in the riparian/floodplain environments would be recharged by streamflow and they are therefore vulnerable to changes to surface hydrology.

Surface water flows may result in recharge to soil water stores (bank recharge) in zones around channels and waterholes may support riparian trees (Ryu et al. 2014). However, if there is no connection between zones of higher soil moisture and a groundwater system or if moisture occurs within a perched aquifer, associated vegetation is not a GDE.

2.2 Cenozoic alluvials (QTa aquifer)

The uppermost aquifer within the area of the study are the Cenozoic alluvials associated with current-day drainage lines as well as aeolian sediments. As well as recent sediments, palaeochannel sediments associated with the Peake, Lora, Wintinna and Arckaringa Creeks and Neales River form important parts of these aquifers (Figure 2-1). Although there are a number of wells in the area of investigation completed in this aquifer, most of these are located within the western portion (Figure 2-1), nor have these alluvial aquifers been the subject of any hydrochemical investigations. Dunster (1984) observed that these wells usually have large diameters to compensate for low yields and high standing water levels, and notes that some wells may be within the weathered portion of the Bulldog Shale. Dunster (1984), also reported that the salinity of groundwater encountered can be very variable, ranging between 100 and 35 000 mg/l. Similarly, Bowering (1975) noted that good quality groundwater from shallow aquifers could be found in the area of investigation, however small potential yields were observed, particularly in areas north of Wintinna Station (Figure 2-1). Yields of between 0.5 and 1 L/sec from depths up to 40 mbgs were expected. An analysis of water levels in the shallow aquifers within the region (collectively interpreted here as representative of the phreatic groundwater surface) suggests that groundwater within the Cenozoic alluvial flows west to east (Figure 2-1) and therefore correlates to the general topography of the region. However, phreatic groundwater in all aquifers is unlikely to be a continuous unit across the study area due to the limited areal extent of shallow aquifer units and uncertainty concerning lateral connectivity.

2.3 Hamilton Sub-basin (HSB aquifer)

The Hamilton Sub-basin is a small sedimentary basin that occurs between the Alberga River to the south, the Musgrave Ranges to the west and St Johns Anticline to the east (Figure 2-1). The latter structure provides the division between the Hamilton Sub-basin and Lake Eyre geological Basin. Little documentation exists concerning the sediments of the basin are not well documented, as no formal stratigraphic conventions yet assigned. Sediments reach a thickness of 79 m near the western margin (Rogers 1995).

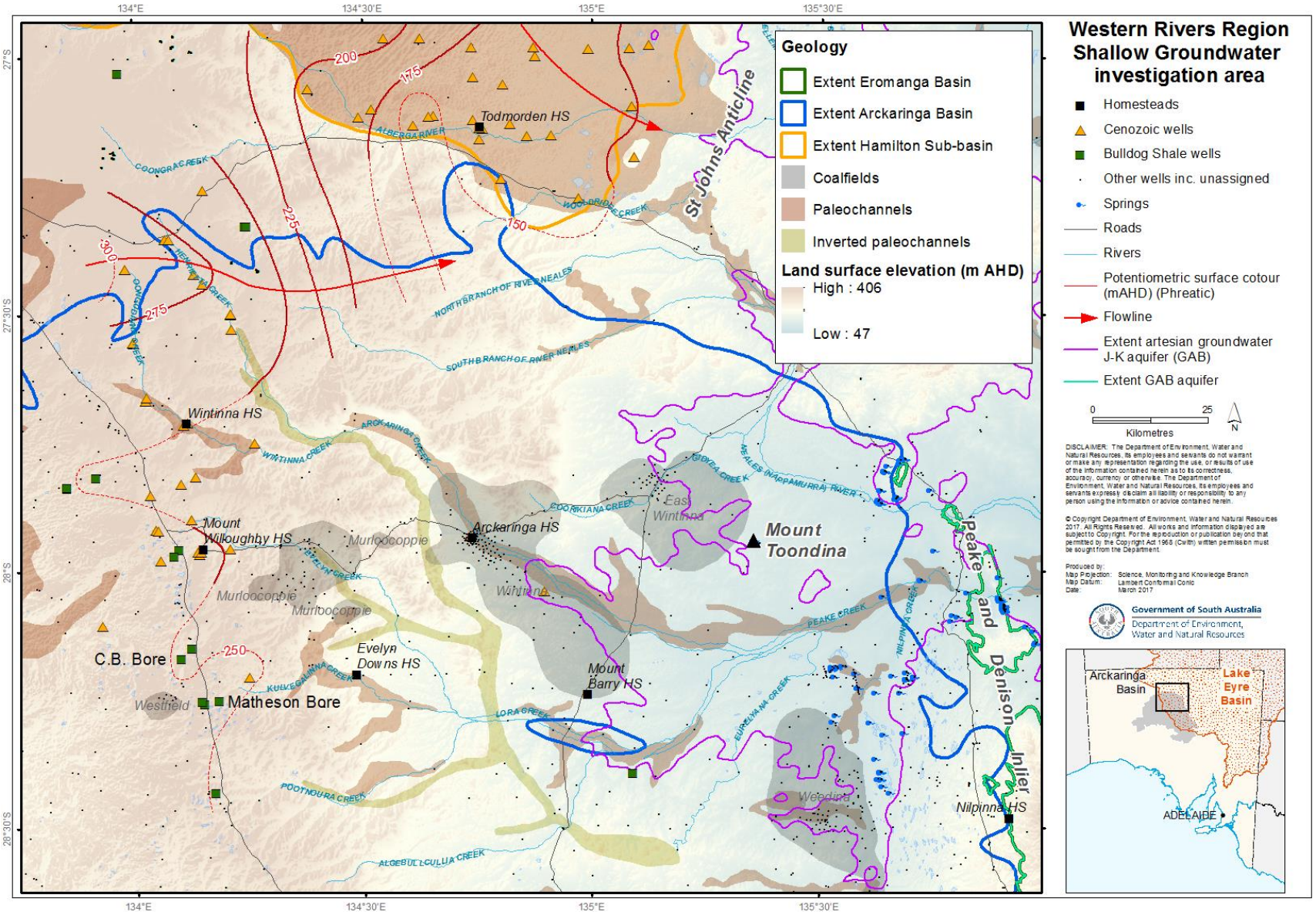

Figure 2-1: Potentiometric surface contour interpretation of phreatic groundwater based on Reduced Standing Water Level (RSWL) (m AHD) data

Little information about groundwater within the Hamilton Sub-basin exists. Herraman and Safta (1977) catalogued a number of wells completed within the Hamilton Sub-basin; these are subsequently included in discussions of wells described as completed in Quaternary alluvials.

2.4 Bulldog Shale

A number of authors (Dunster, 1984; Herraman, 1976; Herraman and Safta, 1977; Smith, 1976) have provided evidence of a groundwater resource within the Bulldog Shale to the south-west of the area of investigation. Smith (1976) describes the existence of a fractured rock aquifer within the Bulldog Shale, in the vicinity the Stuart Highway and Mt Willoughby Station (Figure 2-1). The fractures in question form "unusually continuous" fracture or fissure zone within the weathered near-surface material, which allows for the downward percolation and storage of surface water. This area coincides with the breakaways formed in Bulldog Shale outcrop that mark the margin of the Lake Eyre hydrological Basin in this region.

Dunster (1984) describes a number of wells completed within this aquifer on Mt Willoughby Station, located near the south-east margin of the area of investigation, as generally having good quality water (100–1000 mg/L TDS) but at low yields <0.5 L/sec.). These wells included Matheson Bore and C.B. Bore, although Herraman (1976) describes Matheson Well as completed within Quaternary alluvials. Herraman and Safta (1977) also listed seven wells as completed in only Bulldog Shale. Of these seven, two are abandoned, one not located, one as a capped investigation well and two others (Wellbourne Hill and Ethel Well) were reinterpreted as completed in younger sediments. Ethel Well is still active and was included as a sampling site during this investigation.

Herraman (1976) also says that good quality groundwater can be found within Bulldog Shale aquifers, with salinities less than 1000 mg/L. Smith (1976) summarised results of five wells all completed within the Bulldog Shale fractured rock aquifer; depths varied between 46 and 75 mbgs, standing water levels (SWL) varied between 17 and 30 mbgs, transmissivities varied between 1.7 and 79.1 m^2/day and yields varied between 1.0 and 1.2 L/sec.

Smith (1976) cast doubt on the permanence of groundwater resources in this aquifer, noting that one of the aforementioned wells (B57), which at the time of completion had a yield of 0.9 L/sec, was almost dry two years later. Smith (1976) speculated that such unreliability could be a function of the extension of fracturing into the underlying J-K aquifer, thus providing an effective means of dispersing groundwater from the Bulldog Shale. By extension, this mechanism would also provide additional recharge to the J-K aquifer in addition to that sourced from outcrop.

2.5 GAB (J-K aquifer)

The Great Artesian Basin is one of the largest groundwater basins in the world, underlying approximately 1.7 million km^2, or 22 % of the Australian continent (Habermehl, 1980). Except for the far north and far eastern parts of Queensland and the Northern Territory, the GAB largely occurs in arid and semi-arid regions. Consequently, exploitation of the GAB groundwater resource has played, and continues to play, a vital role in supporting agriculture, mining, industry, civil and cultural communities in Australia (Ah Chee 2002; Leek 2002), inclusive of the area of investigation.

Within the area of investigation, the aquifer units of primary importance are the Algebuckina Sandstone and Cadna-owie Formation. Combined, these units are called the J-K aquifer in South Australia, with the acronym "J-K" derived from the abbreviations for the Jurassic and Cretaceous geological periods. The acronym is a modification of one presented by Habermehl (1980) who referred to the same hydrostratigraphic unit as the "J aquifer." The modification to "J-K' better reflects the true time origins of the aquifer unit in South Australia. Outcrop of these units largely abuts basement outcrop of the Peake and Denison Inlier (Figure 2-2).

Groundwater flow within the J-K aquifer within the study area occurs from areas of recharge near the western margin of the basin towards springs located near the Peake and Denison Inlier (Figure 2-2). For the most part, the J-K aquifer within the area of investigation is either unconfined or sub-artesian, with zones of unsaturated J-K aquifer occurring along the western margin. The hydraulic gradient for groundwater within the J-K aquifer is approximately 0.001. Based on a review of data stored in the Government of South Australia managed database SA Geodata, total dissolved solids (TDS) values for the J-K aquifer within the area of investigation vary between 149 mg/L and 26 384 mg/L. However, all but one well had a concentration of less than 7200

mg/L. Additionally, recorded pH varies from 5.3 to 8.9 although most wells have a pH recorded between 6.5 and 7.9. Yields vary between 0.025 and 44 L/sec, although most yields are less than 4 L/sec.

2.6 Hydrogeological relationships between aquifers

Within the field-survey area of investigation, the Mount Toondina Formation of the Arckaringa Basin (Figure 2-3) directly underlies the majority of the GAB. The upper portion of the Mount Toondina Formation is composed of grey carbonaceous shale, coal and interbedded grey sandstone, siltstone and sandy shale, whereas the lower unit is composed of shale, siltstone, and sandstone. Consequently, the Mount Toondina Formation may be a partial aquifer (Keppel et al. 2015; CSIRO, 2012). The J-K aquifer in other parts of the field area of investigation are underlain by metasediments of the Warburton Basin or Precambrian crystalline basement (Figure 2-3); in such cases, the hydrogeological characteristics of these strata are largely unknown, but are hypothesised to be predominantly controlled by deformation rather than primary depositional textures.

Many of the major drainage channels with well-developed alluvial sedimentary deposits within the field-survey area of investigation occur in regions where groundwater conditions in the J-K aquifer are confined (Figure 2-3). Consequently, the majority of surface water or shallow alluvial aquifer groundwater/deeper groundwater interactions are likely to involve localised or fractured rock aquifers in the Bulldog Shale or groundwater leakage from the J-K aquifer through fractures. Notably, Neogene to Paleogene sediments underlie some areas within the northern portion of the field area of investigation, particularly associated with the Alberga and Neales River. Consequently, aquifers younger than the J-K aquifer are important to consider with respect to interaction with surface water systems in these areas.

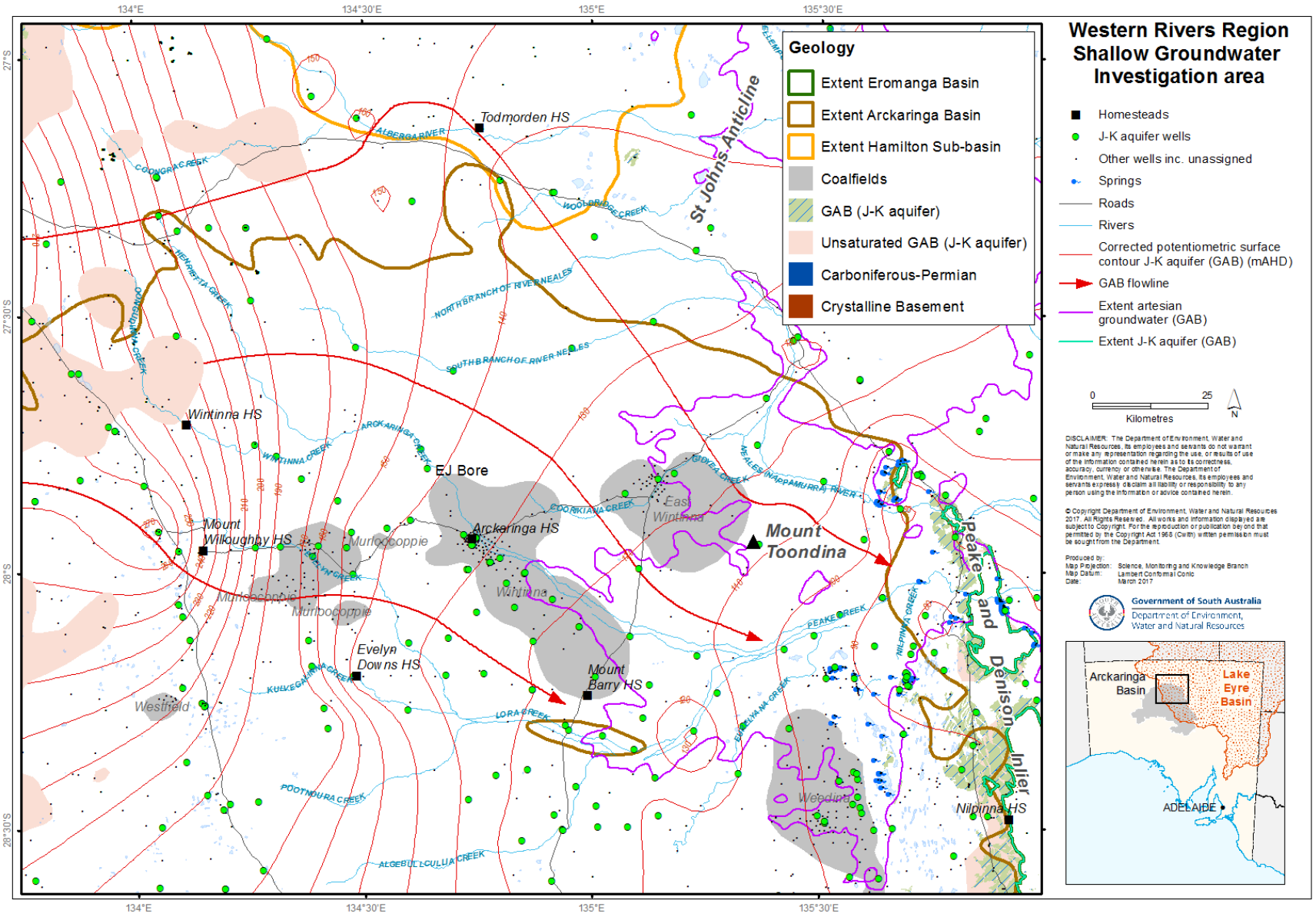

Figure 2-2: Corrected J-K aquifer (GAB) Potentiometric surface contours (m AHD)

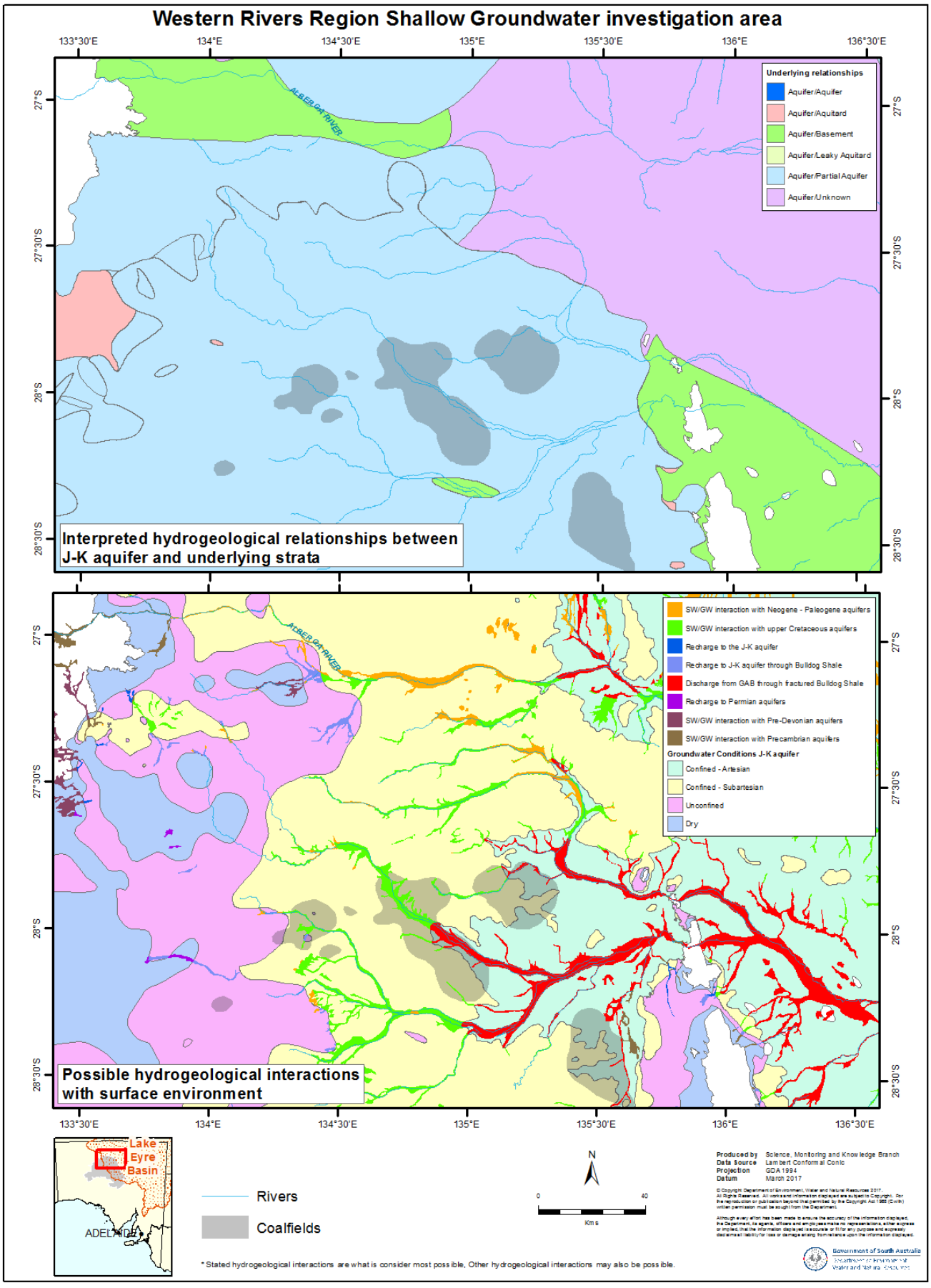

Figure 2-3: Hydrogeological relationships between aquifers

3 Background to identification and classification of groundwater dependent ecosystems and their receptors

3.1 Classification systems for groundwater dependent ecosystems

3.1.1 Interim Australian National Aquatic Ecosystems (ANAE) classification framework

The interim ANAE Classification Framework, is a hierarchical classification system with the following tiered structure:

- Level 1 – large scale national-level regionalisations that provide context for the aquatic ecosystems setting. The ANAE classification framework is flexible in the choice of datasets used in this level.
- Level 2 – subset of the Level 1 classification (i.e. if Level 1 pertains to hydrological basins, Level 2 pertains to catchments), providing more specific but still broad scale context for the aquatic ecosystem setting.
- Level 3 – classifies the class of aquatic ecosystem (surface or subterranean), major types (palustrine, lacustrine, riverine or floodplain) and a pool of habitat level attributes.

In the ANAE classification, there are no pre-determined 'types' of aquatic ecosystems, but aquatic ecosystems can be grouped where they share common attributes depending on which attribute is of interest, or their attribution can be used to assign them to pre-determined types. Under the ANAE classification, a GDE is either partially or entirely dependent on groundwater as a water source and any combination of other level three attributes.

The ANAE classification was applied by Miles and Miles, (2015) to the aquatic ecosystems within the western catchments of the Lake Eyre Basin (LEB) in South Australia with the addition of sub-attributes for water source (to describe the type of groundwater or surface water source) and water regime (to separate frequency of inflows from persistence under cease-to-flow conditions) (Appendix D). At a broad scale, there was insufficient information to classify aquatic ecosystems by most attributes with greater than low confidence. However, at a handful of sites that have been the subject of on-ground investigations, moderate to high confidence with the water source classification exists. Such ecosystems include GAB springs and some waterholes. In contrast, the majority of waterholes are surface water dependent under the classification system, whereas the remainder are dependent on a combination of surface and alluvial groundwater. Most waterholes with groundwater inputs are also saline (brackish to hypersaline) under the classification system (Miles and Miles 2015). Whilst the application of ANAE classification in the LEB and other regions of South Australia and Australia exists, there is currently no single or South Australian-based database to store and receive this information.

3.1.2 National Groundwater Dependent Ecosystems Atlas

The Australian GDE assessment framework (Richardson et al. 2011) is the basis for the national GDE Atlas (BoM 2016). Three broad types of GDEs appear in the GDE Atlas:

1. Aquifers and cave systems (subterranean)
2. Ecosystems dependent on the surface expression of groundwater (surface GDEs)
3. Ecosystems dependent on subsurface presence of groundwater (terrestrial GDEs).

GDE Aquatic ecosystems ratings include their potential of being a GDE as well as the likelihood of being inflow-dependent. Aquatic ecosystems not considered to have any potential to be GDEs in the Atlas are instead inflow-dependent ecosystems (IDEs). Other attributes are included in the Atlas to provide more detail around the type of groundwater systems and the degree of reliance on groundwater but the Atlas classes these as unknown at present.

Table 3-1: Habitat attribute metrics and thresholds used in the classification of SA LEB aquatic ecosystems (Miles and Miles 2015)

Level 3 habitat attributes	Metrics / thresholds	
Landform transport zone (riverine only)	High energy - Upland High energy - Slope Low energy - Upland (plateau) Low energy - Lowland	
Size (palustrine & lacustrine only)	Mega (> 10 000 ha) Macro (100 – 10 000 ha) Meso (25 - 100 ha) Micro (1 - 25 ha) Lepto (0.01 - 1 ha) Nano (< 0.01 ha)	
Soil	Non-porous - Rock (non-soil) Porous - Mineral (soil) Porous - Peat (organic) Porous - Sand (non-soil)	
Vegetation (fringing vegetation)	Woodland Shrub land >1 m Shrub land <1 m Grassland Sedge land Forb land No vegetation Unknown	
Water source	Surface water Groundwater Combined: Surface water dominant Combined: Groundwater dominant Combined: Unknown	
	Groundwater source: Alluvial Fractured Rock Confined Artesian Confined Non-artesian Unconfined (e.g. unconfined GAB)	*Surface water source:* In-stream Overbank Rainfall
Salinity	Fresh (< 1000 mg/L) Brackish (1000 - 3000 mg/L) Saline (3000 - 10 000 mg/L) Hypersaline (>10 000 mg/L)	
Water regime	*Inflow frequency:* Permanent Seasonal (≥ 1 in 1 years) Ephemeral (<1 in 1 to ≥ 1 in 5 years) Highly ephemeral (< 1 in 5 years)	*Persistence:* Permanent Mid-term (≥ 1 year but not permanent) Annual (< = 1 year)
Hydrological connectivity	*Palustrine, lacustrine & floodplain:* Overbank flow Retained Terminal branch Through flow Unconnected	*Riverine:* Always connected Sometimes connected

3.2 Potential for phreatic groundwater use by large woody perrenial plants

There is little knowledge about the likelihood of groundwater use by other species in the region. To address this data gap, the depth to phreatic groundwater required for a selection of large woody perennial plant species was examined by overlying Biological Databases of South Australia (BDBSA) and Atlas of Living Australia (ALA) records of selected plant species (Figure 3-1) with depth to phreatic groundwater (from Miles et al., 2015). Miles et al., 2015 grouped species as follows:

- Studies document use of groundwater ('GDE species'): E. camaldulensis, E. coolabah, Corymbia eremaea (Range Bloodwood) and Atalaya hemiglauca (Whitewood)
- Unlikely to use groundwater ('non-GDE species'): E. socialis (Beaked Red Mallee), Acacia tetragonophylla (Dead Finish) and A. aneura (Mulga)
- Unknown if uses groundwater and commonly growing on floodplains ('unknown'): Acacia ligulata (Umbrella Bush), A. cambagei (gidgee), A. salicina (Broughton Willow), A. estrophiolata (Ironwood), A. stenophylla (River Cooba) and A. oswaldii (Umbrella Wattle).

The results (Figure 3-1) show 'non GDE species' occurred over a greater range of depths to groundwater and *E. socialis* and *A. tetragonophylla* had greater median average depth to groundwater than 'GDE species' and 'unknown' species.

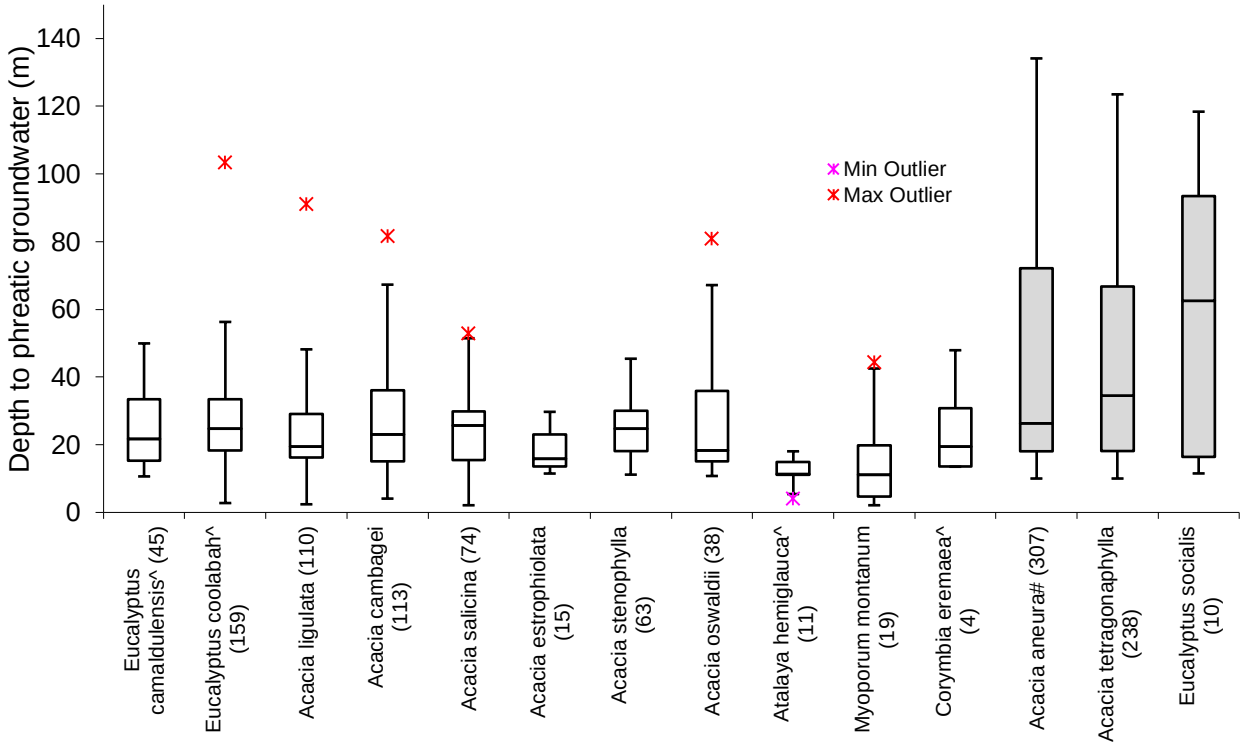

Figure 3-1: Box and whisker plots of depth to phreatic groundwater level for a selection of arid zone species of plants ^ Denotes species for which groundwater use has been documented. Upper and lower whiskers are maximum and minimum values; box is 2nd and 3rd quartile, sample numbers in brackets.

There was little differentiation between the GDE species and unknown GDE species, although A. estrophiolata and Atalaya hemiglauca occurred over notably shallower range of depth to groundwater. Records for these species are few with both only recorded in the Macumba catchment within the study area (Figure 3-2). In addition, despite the restricted distribution of *E. camaldulensis* compared with *E. coolabah*, they are all part of the same association '*E. coolabah*, *Acacia spp*. +/-*E. camaldulensis*' woodland rather than being mapped separately (Figure 3-2). Confusion in interpretation of these results increases with the lack of shallow groundwater bores over the study area and therefore potential for error in depth to groundwater data.

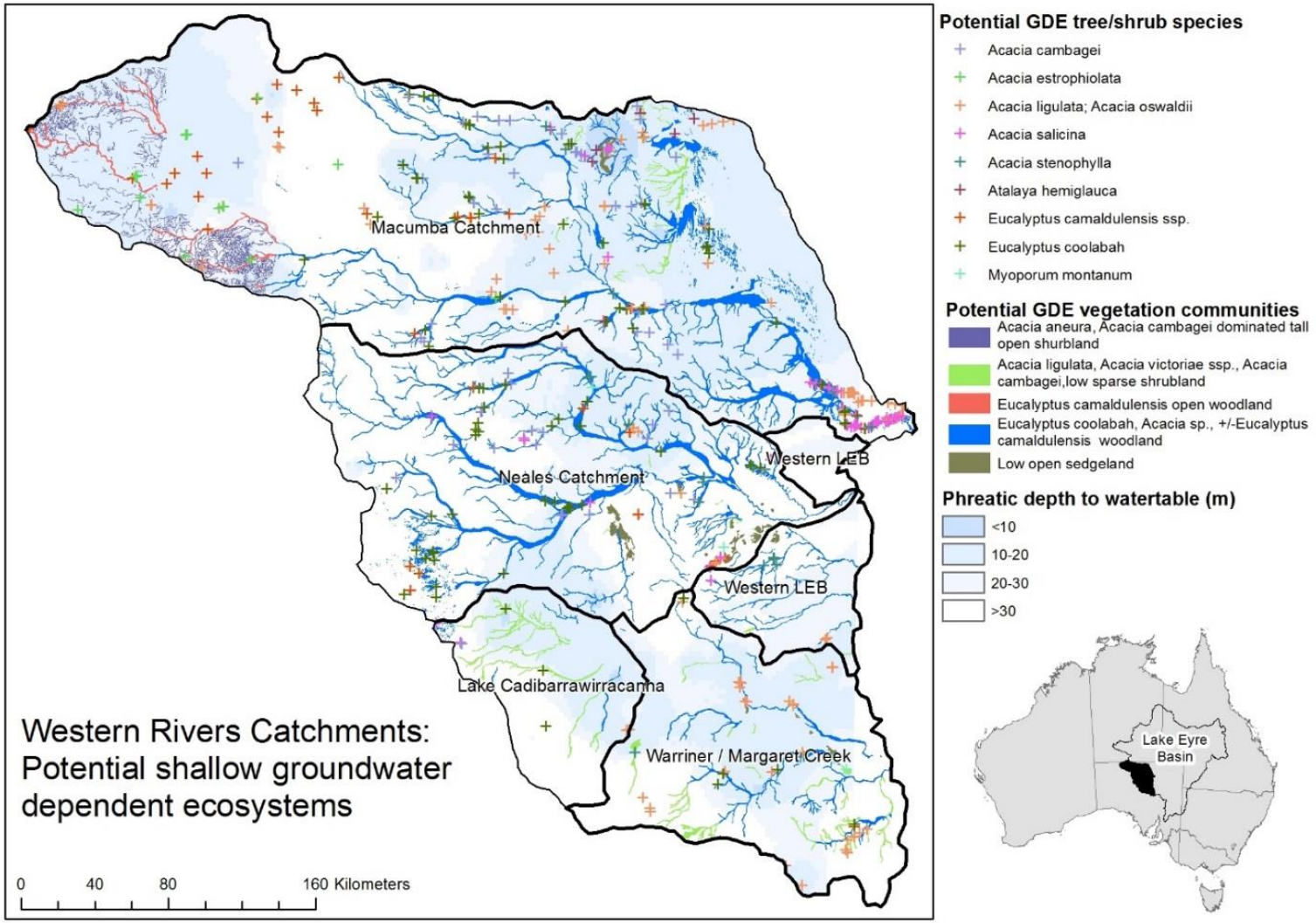

Figure 3-2: Species records for perennial woody vegetation examined for potential groundwater dependency and mapping of potential GDE vegetation communities Note: phreatic depth to watertable is from Miles et al. (2015) which was completed before this study

3.3 Fauna trait groups

An analysis of existing fauna and flora records in both the ALA and BDBSA was undertaken to identify if there were particular fauna that were associated with different vegetation types. The aim of this work was to understand the role of vegetation types that could be groundwater dependent in supporting broader ecosystems of the region and the potential flow-on effects if the composition or character of the riparian and floodplain woodlands were altered (i.e. as a result of surface or groundwater changes). This work did not include an analysis of aquatic species as these have been the focus of recent Coal Seam Gas and Coal Mining Water Knowledge Program Projects. Fauna species were selected on the basis that >10% of all records in the study area were associated with the potential GDE trees and then assigned to trait groups based on six variables from literature review and expert opinion (Table 3-2). The fauna records were then overlaid with the potential GDE tree species records to identify the percent of fauna records in the study area which occur within 100 m of the potential GDE tree species record. Fauna species for which > 10% of records were within 100 m of a given tree species are considered likely to be associated with that tree species.

Table 3-2: Fauna trait group variables

Variables	Vegetation habitat resource classes			
1 Body size	Small	Mid	Large	
2 Nest/shelter place	Tree a) Biomass (high) b) Cavity/hollow c) Colonial	Tree/shrub low biomass	Litter	Burrow
3 Foraging height (predominant)	Top (>8m) -tall vegetation -high biomass	Mid (<8 m) -low (tree/shrub) vegetation -low biomass	Low/Ground (<1 m) -grass/herb understorey - litter/debris	
4 Foraging place (predominant)	a) Air b) Canopy (including crown) c) Perch		d) Bark (including trunk/stem) e) Ground (litter/grasses) f) Water	
5 Food source	a) Insectivorous b) Carnivorous c) Omnivorous d) Herbivorous		e) Aquatic f) Insectivorous + carnivorous g) Insectivorous + nectirovous	
6 Flood responder	Yes: present only during flooding events		No: could be present without flooding	

A broader number of indicator-fauna species were identified for *E. coolabah* woodlands than *A. cambagei* which in turn had more than *E. camaldulensis,* although this may reflect greater sampling effort in *E. coolabah* woodlands. *E. camaldulensis* indicator species were predominantly from the following trait groups:

- Small, arboreal nesting, insectivorous/nectar, canopy foragers
- Mid-small sized, shrub/low foliage foraging/nesting, insectivores/herbivores
- Small-mid-sized, litter/debris foraging/nesting, herbivore/insectivores.

E. coolabah indicator species were predominantly from the following trait groups:

- Small, arboreal nesting, insectivorous/nectar, canopy foragers
- Mid-small sized, shrub/low foliage foraging/nesting, insectivores/ herbivores
- Small-mid-sized, litter/debris foraging/nesting, herbivore/ insectivores
- Mid-large sized, arboreal nesting, perching, carnivores/ insectivores.

A. cambagei indicator species were predominantly from the following trait groups:

- Small, arboreal nesting, insectivorous/nectar, canopy foragers
- Mid-small sized, shrub/low foliage foraging/nesting, insectivores/ herbivores

- Small-mid-sized, litter/debris foraging/nesting, herbivore/ insectivores
- Mid-large sized, arboreal nesting, perching, carnivores/ insectivores.

The results of the indicator species trait group analysis are presented with the box-line models diagrams found in Section 5 of the companion report *"An Examination of Ecosystem Dependence on Shallow Groundwater Systems in the Western Rivers Region, Lake Eyre Basin, South Australia Volume 1: Report."*

There was a strong degree of overlap in the species and trait groups indicative of each of the woodland types which may reflect that most fauna move between vegetation types, utilising different resources in each. Surprisingly few indicator species for *E. camaldulensis* woodlands were from tree hollow nesting trait groups compared with other vegetation types; potentially this is due to low detectability of such species whilst they are in a hollow, however a larger number were identified for *E. coolabah* woodlands. Only one burrowing species (Perentie) was associated with *E. camaldulensis*; this may be due to the higher frequency of inundation likely to be encountered in *E. camaldulensis* habitats as well as this species tending to grow in sandier soils which do not crack as readily as the more clayey and silty soils on which *E. coolabah* and *A. cambagei* occur. Mid-sized, tree hollow nesting/roosting species were associated with both *E. camaldulensis* and *E. coolabah*.

4 Hydrochemistry and environmental isotopes – Method and results

4.1 Methodology

Collection of hydrochemistry samples from 15 wells and 2 waterholes occurred between 17 and 20 November 2015. The study area is situated in northern South Australia, approximately 750 km north-west of Adelaide and covers approximately 38 000 km^2, extending from 20 km north of the Alberga River at the northern end to the Algebullcullia Creek at the southern end. Table 4-1 provides descriptions of sampled wells and Figure 4-1 presents well locations.

Regular water quality measurements were taken using an YSI© multi-parameter meter to ensure stabilisation of water quality prior to sampling. At the time of sampling, a final water quality measurement for pH, electrical conductivity (EC), dissolved oxygen, (DO), redox potential (Eh) and temperature were recorded and a field alkalinity (as $CaCO_3$, using a Hach© titration kit) taken. A number of water samples were collected—the details of sampling, field preparation, and laboratory techniques for each chemical and isotopic species are summarised in Table 4-2.

Additionally, the collection of twig samples for xylem water stable isotopes analysis occurred near sampled wells (see Section 4.1.2).

Table 4-1: Groundwater and surface water sampling sites

Unit no.	Site/Well name	Aquifer	Depth to water m	Latest depth m	Easting	Northing	Sampling date
584000453	Algebullcullia Bore	J-K	15.3	45.5	493835	6846917	17/11/2015
584000056	Junction Bore	J-K	27.1	48.0	485002	6844734	17/11/2015
584100011	Ricky No. 2 Bore	J-K	4.9	244.0	495072	6868539	17/11/2015
	Cootanoorina Waterhole	-	-	-	530317	6883536	18/11/2015
584200008	EJ Bore	J-K	33.0	98.1	464703	6924844	18/11/2015
584200004	McLeod Bore	J-K	20.6	79.3	474021	6909826	18/11/2015
594300020	No. 1 Bore	J-K	10.0	396.0	522150	6972014	19/11/2015
584300036	Homestead 4 (Todmorden)	QTa	?	?	476482	6997977	19/11/2015
584300029	Homestead 2 (Todmorden)	QTa	?	?	476512	6997977	19/11/2015
584300017	Perseverance Bore	HSB	33.0	43.6	474440	7009092	19/11/2015
584300015	Carnegie Bore No. 1	HSB	31.0	43.0	480853	7007381	19/11/2015
584300006	Sheila Bore	HSB	15.2	24.4	486024	6996243	19/11/2015
	Stewart Waterhole	-	-	-	537835	6937709	19/11/2015
574200013	Junction Well (Wintinna)	QTa	6.9	17.8	422467	6954682	20/11/2015
574200018	Ethel Well	QTa	9.0	13.0	404155	6939877	20/11/2015
574200022	Stan Well	QTa	8.1	13.5	412853	6934388	20/11/2015
574200002	Wintinna H.S. No. 2	QTa	?	?	412854	6934311	20/11/2015
594200043	Sanity Bore	J-K	-7.3	206.0	525494	6916941	9/11/2014

J-K: J-K aquifer. HSB: Hamilton Sub-basin aquifer. QTa: Cenozoic alluvial aquifer

Table 4-2: Summary of hydrochemistry collection and analysis techniques

Analyte	Storage	Volume (mL)	Field preparation	Laboratory	Analytical technique
Cations and trace elements	HDPE bottle	125	Filtered -45µm. Addition of HNO_3 (pH<2)	CSIRO Land and Water, Adelaide	Inductively Coupled Plasma Optical Emission Spectrometry (ICP-OES) and Mass Spectrometry (ICP-MS)
Anions, water quality, and total carbon	HDPE bottle	125	Filtered -45µm	CSIRO Land and Water, Adelaide	Dionex ICS–2500 Ion Chromatograph
Stable isotopes of water	McCartney vial	28	Unfiltered	University of California, Davis Campus, USA	Laser Water Isotope Analyser
Strontium $^{87}Sr/^{86}Sr$	HDPE bottle	125	Filtered -45µm	Adelaide Research and Innovation, The University of Adelaide	Finnegan Mat 262 thermal ionisation mass spectrometer
Radiocarbon	HDPE bottle	250	Unfiltered	Rafter Scientific, New Zealand	Accelerator Mass Spectrometry (AMS)
Archive	HDPE bottle	1000	Unfiltered		

4.1.1 Hydrochemistry

4.1.1.1 Major ion and trace metal data

Scatter plots and Piper diagrams were used to determine the broad hydrochemical characteristics of groundwater. This analysis included the interpretation of trends in the data that linked to chemical processes such as the dissolution or precipitation of minerals, water quality conditions or the potential origin of analytes in water. Variations in the proportional concentrations of particular analytes or variations in the concentrations of ions or trace elements were compared to the conserved major ion Chloride (Cl^-), as a means of describing the comparability or otherwise of various groundwater types. Groundwater with comparable major ion and trace metal concentrations may have similar chemical evolutionary histories and therefore be potentially connected. In contrast, notable variations between major ion and trace metal concentrations between groundwater types can be interpreted as differing hydrochemical evolutionary histories and therefore used as a an argument for a lack or limited generally connectivity.

Results previously collected from Sanity Bore, located near eastern margin of the study area, were collated, and assessed in parallel with major ion results obtained during this investigation. Table 4-1 provides locations of wells included in the results compilation. All results had an error of less than ±5%.

.

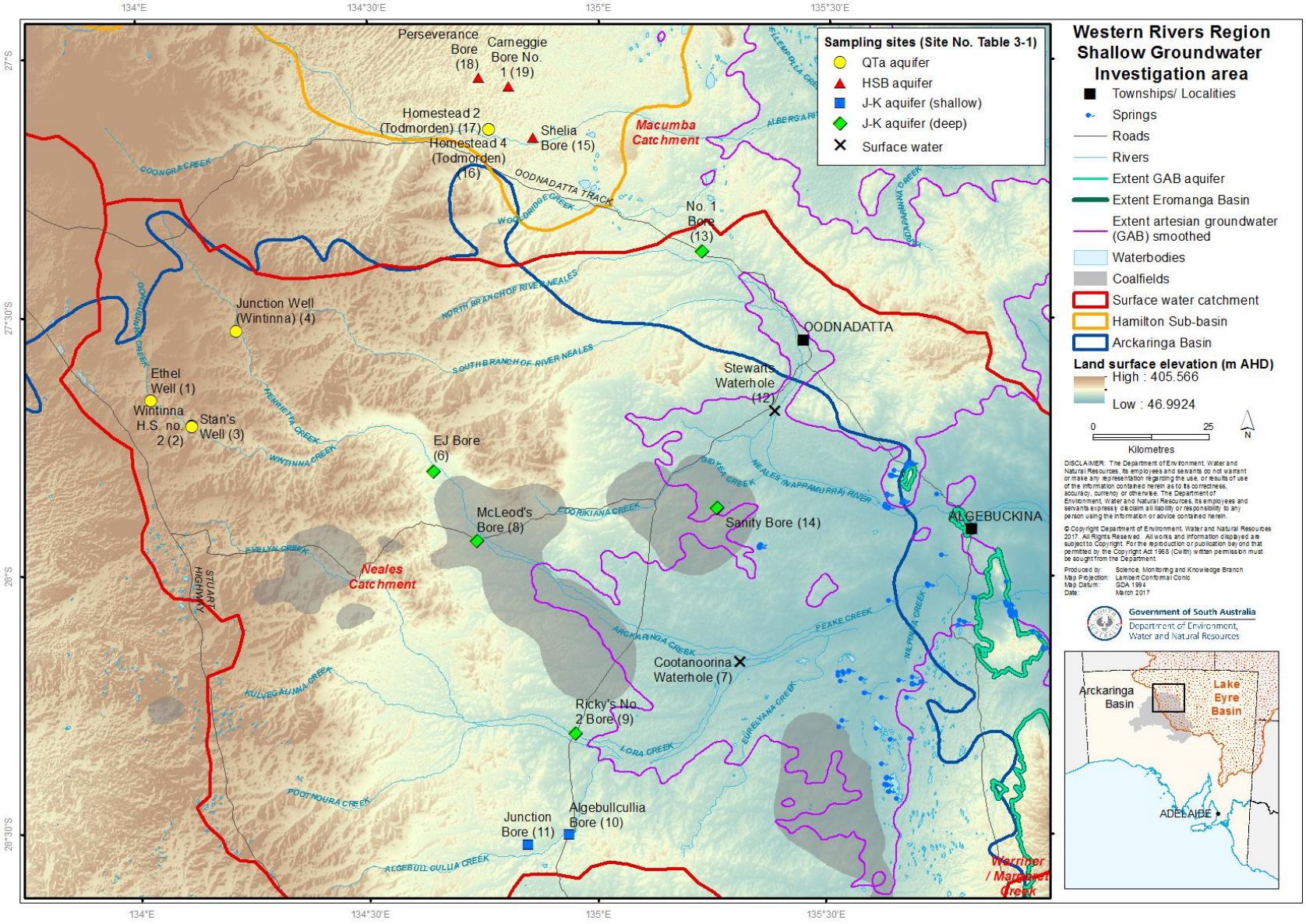

Figure 4-1: Hydrochemistry sampling sites

Table 4-3: Major ions, trace elements, total dissolved carbon and water quality

Unit no.	Site/Well name	Aquifer	Temp	Field pH	EC	Field Alk. $CaCO_3$	ORP	NH_4-N	NO_x-N	NO_2-N	PO_4-P	F^-	Cl^-	Br^-	NO_3^-
			°C		µc/cm	mg/L	mV	mg/L	mg/L	mg/L	mg/L	mg/L	mg/L	mg/L	mg/L
584000453	Algebullcullia Bore	J-K	26.3	6.68	6456	154	-64.8	0.38	0.052	0.006	0.007	0.8	1443	3.9	0.23
584000056	Junction Bore	J-K	33.1	6.79	6955	164	-55.2	0.22	0.092	0.032	0.005	0.6	1362	3.7	0.1
584100011	Ricky No. 2 Bore	J-K	28.8	6.6	7009	138	-56.2	0.25	0.047	<0.005	<0.005	0.6	2159	6.6	<0.05
	Cootanoorina Waterhole	-	21.2	6.76	133	20	190.5	0.20	2.1	0.83	0.14	0.27	27	<0.05	9.5
584200008	EJ Bore	J-K	31.1	6.77	6912	131	-73.8	0.34	0.050	0.007	<0.005	0.8	1359	3.4	0.09
584200004	McLeod Bore	J-K	28.9	6.83	7013	142	-67.1	0.26	0.051	<0.005	<0.005	1.3	1394	3.2	0.30
594300020	No. 1 Bore	J-K	40.3	7.01	4662	138	-103.9	0.30	0.056	<0.005	<0.005	0.72	710	1.4	0.16
584300036	Homestead 4 (Todmorden)	QTa	26.9	7.27	2443	190	-32.3	0.074	11	0.009	0.011	1.6	296	0.73	39
584300029	Homestead 2 (Todmorden)	QTa	27.8	7.35	2098	194	-4.1	0.035	11	0.006	0.014	1.9	241	0.62	35
584300017	Perseverance Bore	HSB	29	7.1	5653	95	-18.3	0.035	22	<0.005	0.018	0.62	1067	2.9	96
584300015	Carnegie Bore No. 1	HSB	29.5	7.09	6080	74	-8.4	0.029	22	0.013	0.014	0.77	1128	3.0	100
584300006	Sheila Bore	HSB	28.3	7.24	7299	176	40.8	0.055	12	0.006	0.014	1.5	1248	3.0	59
	Stewart Waterhole	-	25.7	7.3	262	20	52.4	0.077	0.087	0.032	0.023	0.08	23	<0.05	<0.05
574200013	Junction Well (Wintinna)	QTa	26.2	7.06	1588	100	-45.9	0.036	14	<0.005	0.016	0.41	278	0.8	58
574200018	Ethel Well	QTa	23.8	7.24	3105	285	150.2	0.13	24	0.036	0.012	0.73	718	2.3	93
574200022	Stan Well	QTa	25.2	7.28	1509	260	113.5	7.9	1.5	4.7	0.036	13	0.010	0.016	0.37
574200002	Wintinna H.S. No. 2	QTa	25	7.48	955	254	99.7	8.0	1.0	4.6	0.037	6.1	0.007	0.023	0.66
594200043	Sanity Bore	J-K	34.9	7.37	4047	220	-96.6	0.23	0.02	0.01	0.008	<0.2	776	2.5	<0.2

J-K: J-K aquifer. HSB: Hamilton Sub-basin aquifer. QTa: Cenozoic alluvial aquifer

Name	SO_4^{2-} mg/L	TC mg/L	IC mg/L	TOC mg/L	TN mg/L	Ca mg/L	K mg/L	Mg mg/L	Na mg/L	S mg/L	B mg/L	Si mg/L	Sr mg/L	Zn mg/L	Li µg/L
Algebullcullia Bore	662	57	56	0.6	0.4	163	50	133	947	219	1.5	4.0	2.4	<0.25	187
Junction Bore	609	62	61	0.6	0.3	150	39	123	842	200	1.5	5.8	2.2	<0.1	168
Ricky No. 2 Bore	822	51	50	0.6	0.3	246	56	142	1220	264	1.3	5.3	4.1	<0.1	177
Cootanoorina Waterhole	13	23	9.5	14	3.3	9.0	9.3	5.1	18	2.9	<0.2	22	0.1	0.06	16.2
EJ Bore	886	52	51	0.5	0.6	234	44	127	778	255	1.2	6.4	3.7	<0.1	194
McLeod Bore	1032	50	49	0.9	0.6	297	51	144	881	334	1.4	4.4	4.6	<0.25	196.0
No. 1 Bore	317	56	56	0.1	0.4	68	23	29	574	98	0.8	8.8	1.2	<0.5	93
Homestead 4 (Todmorden)	385	64	63	0.5	10.5	82	11	23	379	119	2.1	28	0.9	0.22	16
Homestead 2 (Todmorden)	293	58	57	0.5	9.7	60	10	17	325	91	2.1	28	0.7	0.14	13
Perseverance Bore	752	31	31	0.2	24	208	44	78	782	242	1.4	33	2.1	<0.25	2.2
Carnegie Bore No. 1	915	22	21	0.7	25	252	49	94	793	295	1.4	31	4.3	<0.25	0.9
Shelia Bore	1493	38	37	0.7	15	419	21	99	987	478	3.6	28	5.8	<0.25	1.7
Stewart Waterhole	38	18	11	7.2	0.6	14	7.9	3.5	25	13	<0.2	6.7	0.1	0.15	4
Junction Well (Wintinna)	106	35	35	0.7	15	77	11	24	183	33	0.6	35	0.6	0.24	8
Ethel Well	220	72	71	1.5	24	107	19	57	477	66	1.4	25	1.3	0.11	17
Stan Well	224	55	53	1.4	12	97	7.9	32	186	57	0.7	35	0.8	0.08	4
Wintinna H.S. No. 2	111	54	53	1.0	6.5	64	5.6	21	126	36	0.5	35	0.6	0.22	3
Sanity Bore	459	53	52	0.5	0.2	106	26	41	547	139	0.8	6.6	1.4	0.34	NA

NA: Not analysed

Name	Al µg/L	Sc µg/L	V µg/L	Cr µg/L	Mn µg/L	Fe µg/L	Cu µg/L	Zn µg/L	As µg/L	Se µg/L	Rb µg/L	Sr µg/L	Mo µg/L	Ba µg/L	U µg/L
Algebullcullia Bore	12	<3	<1	<1	143	2229	<3	31	<1	<2	60	2305	<2	20	<0.3
Junction Bore	10	<3	<1	<1	172	498	<3	5	<1	<2	63	2075	<2	13	<0.3
Ricky No. 2 Bore	21	<3	<1	<1	275	2264	<3	22	<1	<2	81	4258	<2	23	<0.3
Cootanoorina Waterhole	6645	6.1	39.0	5.2	95.9	7276	11.4	64.8	1.5	<0.4	4.5	87.1	<0.4	260.4	0.48
EJ Bore	30	<3	<1	1	174	2290	<3	338	<1	<2	82	3649	3	25	<0.3
McLeod Bore	6	2	<0.4	<0.4	223	1552	3	132	<0.4	<0.8	80	4532	2.3	27.0	<0.1
No. 1 Bore	11	4	<1	<1	63	452	<3	44	<1	<2	51	1192	<2	44	<0.3
Homestead 4 (Todmorden)	<10	<5	43	3	5	106	8	238	<2	5	17	886	17	21	6.7
Homestead 2 (Todmorden)	<10	5	56	6	<5	<10	5	154	2	5	16	666	31	19	5.6
Perseverance Bore	16	6.9	28.6	24.2	1.8	192	1.0	92.2	0.8	14.1	59.8	1955	2.0	20.0	2.39
Carnegie Bore No. 1	3	7.4	33.3	24.1	8.1	26	<0.5	106.9	1.0	13.8	49.7	3990	3.3	20.1	1.50
Sheila Bore	3	8	38.4	6.6	9	22	<1	118	0.9	11.5	15	5729	17.3	20.0	9.9
Stewart Waterhole	449	<5	8	<2	121	937	<5	153	3	<4	<5	132	<4	181	<0.5
Junction Well (Wintinna)	<10	6	88	<2	<5	<10	<5	254	5	<4	19	591	<4	55	0.9
Ethel Well	<10	5	23	<2	6	<10	5	127	2	8	34	1275	<4	96	5.4
Stan Well	<10	6	54	<2	<5	<10	<5	84	3	<4	15	783	<4	72	4.3
Wintinna H.S. No. 2	<10	7	87	<2	<5	<10	<5	231	5	<4	9	527	<4	91	2.4
Sanity Bore	<0.1	NA	NA	<0.05	<0.1	0.8	<0.05	0.34	<0.05	<0.05	NA	1.4	NA	NA	NA

NA: Not analysed

4.1.1.2 Stable isotopes of water

The stable isotopes deuterium (δ^2H) and oxygen-18 ($\delta^{18}O$) were analysed to determine if there were variations in endogenic composition, either between groundwater types or between groundwater and local vegetation. Because these stable isotopes are prone to fractionation, either by some transport processes or during phase transitions, they are particularly useful in discriminating between waters with differing environmental histories. However, the transfer of water to the atmosphere by transpiration does not affect the isotopic composition of the remaining water (Gat, 1996) because water uptake by plant roots does not cause fractionation. Consequently, they are useful in studies where the water source for vegetation is a focus (Walker et al. 2001).

A comparison between the stable isotope ratios of xylem water with that of potential sources of water provides the basis for interpretation. Where values are analogous allowing for analytical error, an inference regarding water within the vegetation and a potential source is possible. Consequently, an ideal study will attempt to obtain stable isotope ratios for all conceivable water sources for the vegetation in question, including surface water, groundwater and soil water from various depths including the unsaturated zone and the capillary fringe above the water table (Walker et al. 2001). Unfortunately, during this study, no soils samples considered adequate for stable isotope analysis were obtainable, consequently, the proceeding discussions pertain only to the groundwater sampled as a potential source of water within the vegetation in question.

Mass balance calculations can indicate whether the stable isotope results from xylem water are a potential mix, by helping establish a maximum upper limit of groundwater contribution to a given sample. The formula used to calculate the maximum possible fraction of groundwater contribution to xylem water is as follows:

$$F_{gw} = \frac{(Y_m - Y_{sw})}{(Y_{gw} - Y_{sw})} \quad (1)$$

Where F_{gw} is the fraction of groundwater in the mixed source (xylem) sample, Y_m is the mixed sample, in this case, the xylem sample, Y_{sw} is the surface water endmember, and Y_{gw} is the groundwater endmember sample.

Stable isotope ratios from groundwater samples may also indicate unique hydrochemical characteristics. As in the case of major ion and trace metal data, similar stable isotope values of water can infer a similar evolutionary history with respect to the source water.

Comparison of stable isotope values to a Local Meteoric Water Line (LMWL) enables interpretation of the effects of evaporation or mixing on groundwater samples. The LMWL describes stable isotope values from precipitation collected from a single site or set of "local" sites (USGS, 2004). Groundwater that has evaporated or has mixed with evaporated water typically plots below the LMWL along lines that intersect the LMWL at the location of the original un-evaporated composition of the water (USGS, 2004).

For this investigation, the LMWL for Alice Springs was chosen (Crosbie et al. 2012; IAEA 2013) for comparison during analysis of water stable isotope results. Alice Springs was favoured over Woomera (the closest town to the study area with stable isotopes in precipitation recorded) because of a limited water stable isotope record at Woomera (Liu et al., 2010).

Stable isotope analysis was undertaken using a Laser Water Isotope Analyser V2 (Los Gatos Research, Inc., Mountain View, CA, USA) (UC Davis, 2016). Training course notes prepared by the International Atomic Energy Agency (IAEA) indicate that although there is a potential issue with using this instrumentation to analyse highly saline samples, modifying analysis and maintenance protocols can overcome such issues (IAEA, 2009). IAEA (2009) also indicate that the analysis of seawater samples should pose little problems and that it is brine samples that may require specialised procedures. All samples analysed during this investigation returned salinities ≤ 7000 mS/cm, which is well below seawater and brine salinities. Consequently, it is considered that analytical issues related to the salinity are minimal. Additionally UC Davis indicate that part of their protocol for highly saline samples is to increase the number of injection runs from six to ten in order to obtain an acceptably accurate average reading.

4.1.1.3 Stronium isotopes ($^{87}Sr/^{86}Sr$)

Shand et al. (2009) states that strontium (Sr) is a divalent ion that shows similar geochemical characteristics to calcium (Ca), while noting that the isotopic abundance may be variable in rocks due to the formation of ^{87}Sr by the decay of naturally occurring ^{87}Rb (Rubidium-87). Consequently the mineralogy and age (to allow for the decay of ^{87}Rb) of rocks within an aquifer are important controls on the variation of $^{87}Sr/^{86}Sr$. By extension, Shand et al. (2009) and Åberg et al. (1989) described differences in the variations in the ratio of $^{87}Sr/^{86}Sr$ in groundwater as a sum of atmospheric inputs, mineralogy along the flow path, mineral dissolution, ion exchange characteristics, and residence time. These attributes therefore make $^{87}Sr/^{86}Sr$ useful for the study of groundwater mixing or exchange between different sources. A useful means of discriminating between different processes such as mixing of groundwater with multiple $^{87}Sr/^{86}Sr$ signatures, evaporation, dilution, exchange or mineral precipitation is to plot $^{87}Sr/^{86}Sr$ data against the reciprocal of Sr^{2+} (Shand et al. 2009). Such a method allows for the identification of source groundwater, mixing trends as well as the influence of mineral precipitation or evaporation.

4.1.1.4 Radiocarbon (Carbon-14)

Radiocarbon (^{14}C) was analysed as a means of determining the apparent age of groundwater. Radiocarbon can be useful with respect to calculating the apparent age of groundwater because such isotopes will decay at a predictable rate into more stable isotopic forms. This rate of decay can be used to estimate the apparent age of groundwater as long as the initial value of the radioisotope within groundwater (the value at the point of recharge) is estimable.

As well as the basic mathematical methods used to calculate an age, methods are available to correct results for other influences on the ^{14}C value (given as percent modern carbon or pMC) of a given sample beyond the initial input value and the decay rate (for comprehensive reviews on the subject, refer to Phillips 2013; Plummer and Glynn 2013). These influences include water–rock interaction and paleo-environmental influences. However for this report, an age determination or correction calculations required to calculate an age have not been applied. Instead, the raw ^{14}C results were used to provide a relative indication of age differences between samples and to identify possible mixing. The hydrochemical processes that may affect such values and thus may provide a potential source of error, have not been considered because without knowing the hydrochemical history of the groundwater from such a complex system, there is a risk that a correction may introduce further error in the age calculation. It has been recognised that sampling of groundwater across large sections of an aquifer may provide water samples with varying origins and recharge history while dispersion and mixing in heterogeneous aquifers can lead to a large distribution of apparent groundwater age, even from wells screened across short intervals (Weismann et al., 2002; Jurgens et al., 2012). Furthermore with respect to ^{14}C, Aggarwal et al. (2014) argues that age determination for results ≤5 pMC is too difficult to undertake with any certainty. Consequently, a conservative approach of using uncorrected ^{14}C data was employed. Further work could involve evaluating the groundwater age distributions from the environmental tracer data using lumped parameter models (LPMs). LPMs provide a mathematical evaluation of transport based on simplified aquifer geometry and flow configurations taking into account hydrodynamic dispersion and mixing (Jurgens et al. 2012).

Table 4-4: Stable isotopes, $^{87}Sr/^{86}Sr$ and Radiocarbon results from groundwater samples

Sample ID	Aquifer	δD per mill VSMOW	$\delta^{18}O$ per mill VSMOW	$^{87}Sr/^{86}Sr$	2se (*1e-6)	$\Delta^{14}C$ ‰	pMC %
Algebullcullia Bore	J-K	-41.1	-4.94	0.712081	0.000003	-926.0	7.40
Junction Bore	J-K	-40.2	-4.81	0.711672	0.000003	-981.6	1.84
Ricky No. 2 Bore	J-K	-42.7	-5.41	0.712695	0.000003	-891.0	10.90
Cootanoorina Waterhole.	-	20.1	6.40	0.711450	0.000003		
EJ Bore	J-K	-43.4	-5.73	0.711628	0.000003	-875.1	12.49
McLeod Bore	J-K	-44.1	-5.76	0.713626	0.000003	-940.5	5.95
No. 1 Bore	J-K	-49.1	-6.70	0.714051	0.000003	-873.5	12.65
Homestead No 4 Bore	QTa	-50.3	-6.66	0.714058	0.000003	-209.6	79.04
Homestead No. 2 Bore	QTa	-50.0	-6.54	0.713825	0.000003	-240.7	75.93
Perseverance Bore	HSB	-39.9	-4.17	0.713533	0.000003	-645.9	35.41
Carnegie Bore No. 1	HSB	-39.9	-4.14	0.713413	0.000003	-595.0	40.50
Sheila Bore	HSB	-43.3	-5.40	0.713297	0.000003	-259.3	74.07
Stewart Waterhole	-	15.4	1.15	0.712952	0.000003		
Junction Well (Wintinna).	QTa	-42.0	-6.01	0.712819	0.000003	-69.6	93.04
Ethel Well	QTa	-47.4	-6.98	0.712845	0.000003	-152.3	84.77
Stan Well	QTa	-39.6	-6.14	0.712081	0.000003	-25.6	97.44
Wintinna H.S. No. 2	QTa	-37.4	-6.33	0.711672	0.000003	-25.2	97.48

J-K: J-K aquifer. HSB: Hamilton Sub-basin aquifer. QTa: Cenozoic alluvial aquifer

4.1.2 Xylem water isotope chemistry

Twig samples from eight *E. coolabah*, four *E. camaldulensis,* and two *Acacia spp*. Trees were collected for stable isotope ratio determinations. The twig samples collected from healthy branches were approximately 20 cm long and 0.5–1 cm diameter. Sampling included removal of the outer bark in the field, samples cut to fit within the jar, and preserved in kerosene. A Laser Water Isotope Analyser determined ratio results for stable isotopes deuterium ($\delta^{2}H$) and Oxygen-18 ($\delta^{18}O$) after water extraction using the azeotropic method. Section 4.1.1.2 discusses data analysis methods.

With respect to the reliability of this method to provide an adequately accurate indication of the stable isotope composition of examined xylem water, Walker et al. (2001), notes that the largest source of error concerns the extraction of water from the sample material prior to analysis. Under-extraction of water using heat-based methods may lead to a negative bias because of isotopic fractionation during extraction. Walker et al (2001) reviewed test work designed to examine the efficacy of xylem-water extraction methodologies. Specifically, Walker et al (2001) cited a study by Thorburn et al. (1993) found that azeotopic methods that use kerosene (such as used during this study) or toluene give the most accurate extractions. Removal of green parts of the plant prior to storage in kerosene will mitigate other sources of error, notably mixing of evaporated water from these parts of the plant. Other variations, such as migration times of water from soil through the plant after recent rain or intra-canopy variations were either not relevant to this study due to the lack of any recent rainfall or were mitigated by collecting twigs from multiple sources of the plant.

The tree monitoring and sampling sites are summarised in Table 4-5 and the locations shown in Figure 4-2.

Table 4-5: Description of tree sampling sites

Site	Methods	Description
Stewart Waterhole (Neales River)	Sapflow monitoring Leaf and soil water potentials Soil, twig and surface water isotopes	*Eucalyptus coolabah* and lesser *E. camaldulensis* assemblage. This is approximately the most-downstream occurrence of *E. camaldulensis* (River Red Gum) in the Neales River catchment and has surface water monitoring at the waterhole. No monitoring bores are located in this area but saline seepage occurs at Stewart Waterhole indicating a relatively shallow water table.
Cootanoorina Waterhole (Lora / Arckaringa Creeks)	Sapflow monitoring Leaf and soil water potentials Soil, twig and surface water isotopes	*E. coolabah* dominant assemblage. Waterhole at the confluence of Lora and Arckaringa Creeks. Large, mature *E. coolabah* are common in this area and downstream the riparian tree assemblage thins out considerably. There is a surface water logger in Cootanoorina Waterhole but no nearby monitoring bores.
EJ Bore (Arckaringa Creek)	Sapflow monitoring Leaf and soil water potentials	*A. cambagei* and lesser *E. coolabah* assemblage near EJ Bore (Arckaringa Creek). This is typical mixed acacia dominant open woodland with occasional *E. coolabah* on channel bank positions. One of the dominant mature acacia species is *Acacia cambagei* (gidgee) and these occupy bank-top and floodplain positions. There is a surface water level bore installed here since 2013. This site is located immediately upstream of the Arckaringa coalfield.
Francis Camp Waterhole	Sapflow monitoring Leaf and soil water potentials	Mixed *E. coolabah* and *E. camaldulensis* assemblage. *E. camaldulensis* are dominant on the banks of the channel with some *E. coolabah* and more *E. coolabah* in floodplain positions. Non-instrumented mature acacias occur on outer floodplain channels. There is no surface water or groundwater monitoring near this site.
Wintinna Homestead (Wintinna Creek)	Sapflow monitoring Leaf water potentials Twig and groundwater isotopes	*E. camaldulensis* dominate the riparian tree assemblage with no *E. coolabah* observed. Other nearby large creeks can be *E. coolabah* dominant though Digby Giles (formerly Wintinna Station) 2015, pers. comm., March). There is no streamflow monitoring at this site but the homestead has wells with good quality (potable) unconfined groundwater approximately 10 m below the ground surface. This groundwater has sufficient yield to supply household and garden water and the base of the creek is likely to be 4–5 m below the level of the wells at the homestead.
Ethel Well (Wintinna Creek)	Leaf water potentials Twig and groundwater isotopes	*E. camaldulensis* dominant riparian tree assemblage similar to Wintinna Homestead site. No streamflow monitoring at this site but a nearby bore (Ethel Well) has good quality water from unconfined groundwater also around 10 m below ground level. Located upstream of Wintinna Homestead site.
Junction Well (Wintinna Creek)	Twig and groundwater isotopes	Mixed *E. camaldulensis* and *E. coolabah* riparian woodland with nearby bore with low salinity groundwater approximately 10–20 m below ground level; located upstream of Ethel Well site.
Algebullcullia Bore (Lora Creek)	Twig and groundwater isotopes	Very open *E. coolabah woodland and Acacia spp.* lined drainage channel. No streamflow monitoring but GAB bore located nearby with groundwater recorded between 15–45 m below ground level. Lora Creek is a minor tributary of the Neales River catchment.
Junction Bore (Lora Creek)	Twig and groundwater isotopes	Very open *E. coolabah woodland* lined drainage channel. No streamflow monitoring but GAB bore located nearby with groundwater recorded between 27–48 m below ground level.

Site	Methods	Description
Todmorden HS (Hamilton Creek)	Twig and groundwater isotopes	*Acacia aneura (*?) with emergent *E. coolabah l.* No streamflow monitoring but Homestead bore nearby, groundwater at unknown depth.
Sheila Bore (Hamilton Creek)	Twig and groundwater isotopes	*Acacia spp*. (*A. aneura*?) shrub land in drainage channels downstream of Todmorden Homestead. Sheila Bore has groundwater between 15–25 m below ground level with moderately high salinity recorded (7299 μS/cm)

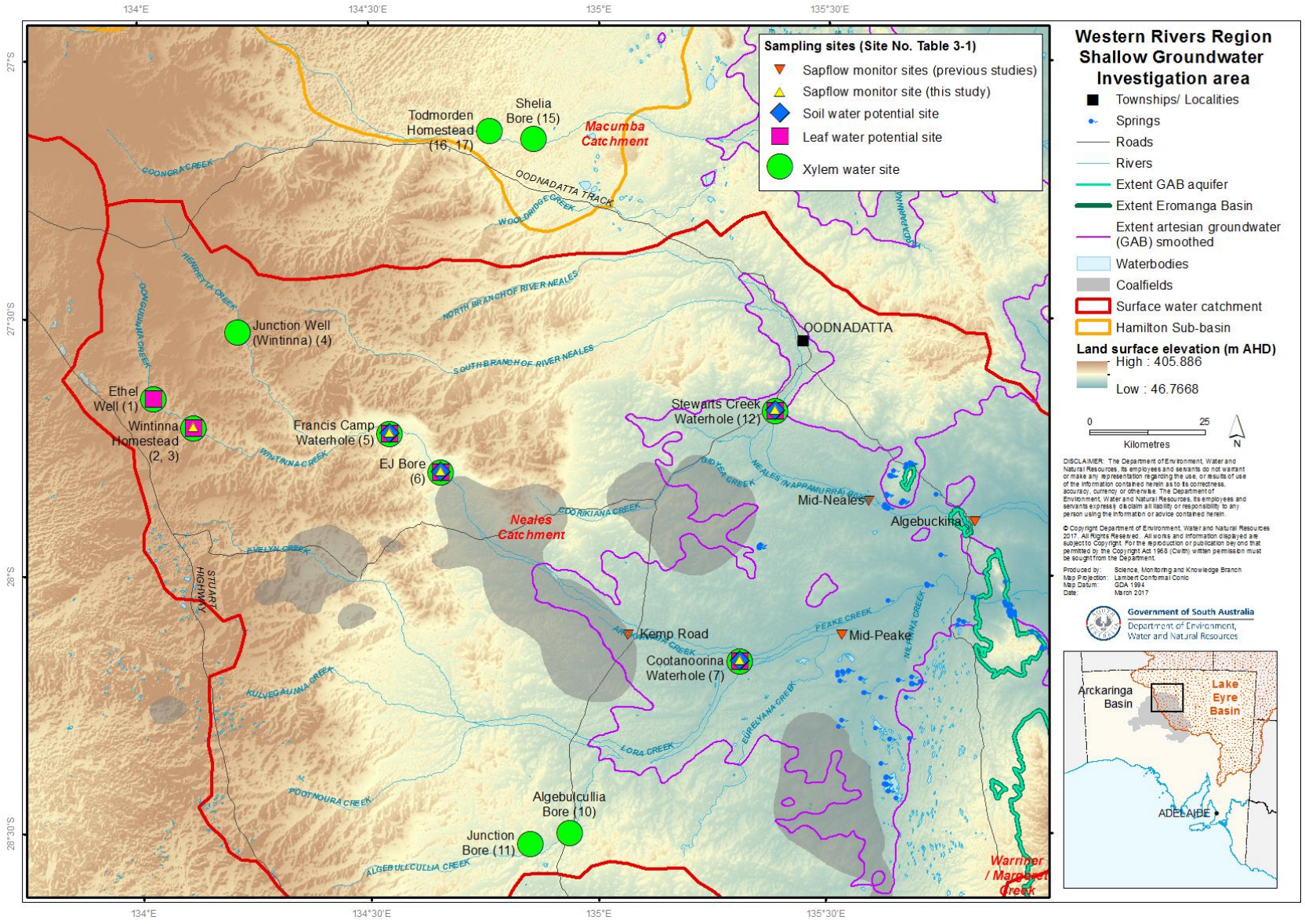

Figure 4-2: Tree and soil sampling sites The underlying image is a digital elevation model of the catchment and the tan polygons are the locations of coal deposits in the underlying Arckaringa Basin.

4.2 Results

4.2.1 Groundwater chemistry

Major ion concentrations in groundwater samples from different aquifers varied notably when their proportional distribution relative to one another was examined using a Piper diagram and scatter plots. Additionally, isotopic strontium ($^{87}Sr/^{86}Sr$) and radiocarbon (^{14}C) also proved beneficial with respect to defining different groundwater groupings based on aquifer type.

In total, three hydrochemical classifications for groundwater that relate to the source aquifer were developed:

1. GAB (J-K) aquifer
2. Hamilton Sub-basin (HSB) aquifer
3. Cenozoic alluvial (QTa) aquifers

In the case of the J-K aquifer, samples from shallow wells (screened <50 mbgs) were initially examined separately from samples collected from deeper wells. The reason for this was that groundwater collected from shallower wells is more likely to be directly accessible to riparian vegetation and is therefore of particular interest to this study.

4.2.1.1 J-K aquifer

Groundwater from the J-K aquifer is brackish, with EC varying between 4662 µS/cm (No. 1 Bore) and 7013 µS/cm (McLeod Bore). Salinity levels are comparable to groundwater from the HSB aquifer, but more saline than water from the QTa aquifer Figure 4-3A). pH for the most part suggest groundwater from the J-K aquifer is slightly acidic to neutral, varying from 6.6 (Ricky No. 2 Bore) and 7.01 (No. 1 Bore) (Figure 4-3A and Figure 4-3B); the only outlier is Sanity Bore (7.38). Redox condition are reducing, with field oxidation/ reduction potential (ORP) measurements reported between -55.2 mV (Junction Bore) and -103.9 mV (No. 1 Bore) (Figure 4-3B).

Proportional major ion hydrochemistry of J-K aquifer groundwater samples can be described as predominantly $Na^+ + Cl^- + (Ca^{2+} + SO_4^{2-})$ (Figure 4-4). There appears to be no significant difference in major ion or trace metal hydrochemistry between J-K aquifer groundwater collected from shallow bores (screened less than 50 mbgs) and deeper parts of the J-K aquifer, however, of some note is that samples from No. 1 Bore and Sanity Bore, which are located on the margins or within the artesian zone of the J-K aquifer display a small variance within this general proportional description. In these two cases, there appears to be a slightly higher proportional concentration of HCO_3^- and slightly lower proportional concentration of Cl^- and SO_4^{2-} than other results (Figure 4-4).

Using Cl^- as a conservative element, Mg^{2+}, K^+ and Na^+ all appear to be predominantly conserved and sourced from marine aerosols (Figure 4-3C, Figure 4-3D and Figure 4-5A). In contrast, SO_4^{2-} and Ca^{2+} are all elevated with respect to average seawater concentrations (Figure 4-5B and Figure 4-5C) and when compared to one another, the proportional relationship and near 1:1 trend suggests that the dissolution of gypsum is an important control (Figure 4-5D). Additionally, the lack of correlation between alkalinity and either Cl^- or Ca^{2+} suggests that for the most part, groundwater alkalinity in the J-K aquifer within the study area is independent of marine aerosol input or water-rock interactions with calcite (Figure 4-6A and Figure 4-6B). The only exceptions to the previous statement are groundwater samples from the two most easterly wells previously discussed, No. 1 Bore and Sanity Bore. Ratios of Ca^{2+} and alkalinity concentrations in groundwater from these wells suggest that calcite dissolution may be influential. In support of the notion that the dominant influence on salinity is input from marine aerosols is that Br^-: Cl^- ratios are typically above the seawater ratio of 1.5×10^{-3}, suggesting no influence from evaporate dissolution (Figure 4-6C).

With respect to trace elements, nitrogen oxides (NO_x-N) and Si concentrations are low compared to the QTa and HSB aquifers, with concentrations typically less than 0.1 mg/L NO_x-N Figure 4-6D) and 10 mg/L Si respectively (Figure 4-7A). In contrast, Li (Figure 4-7B), Mn and Fe (Table 4-3) concentrations are elevated compared to groundwater concentrations from the QTa and HSB aquifers, with concentrations typically greater than 90 µg/L (Li), 8 µg/L (Fe) and 60 µg/L (Mn) respectively.

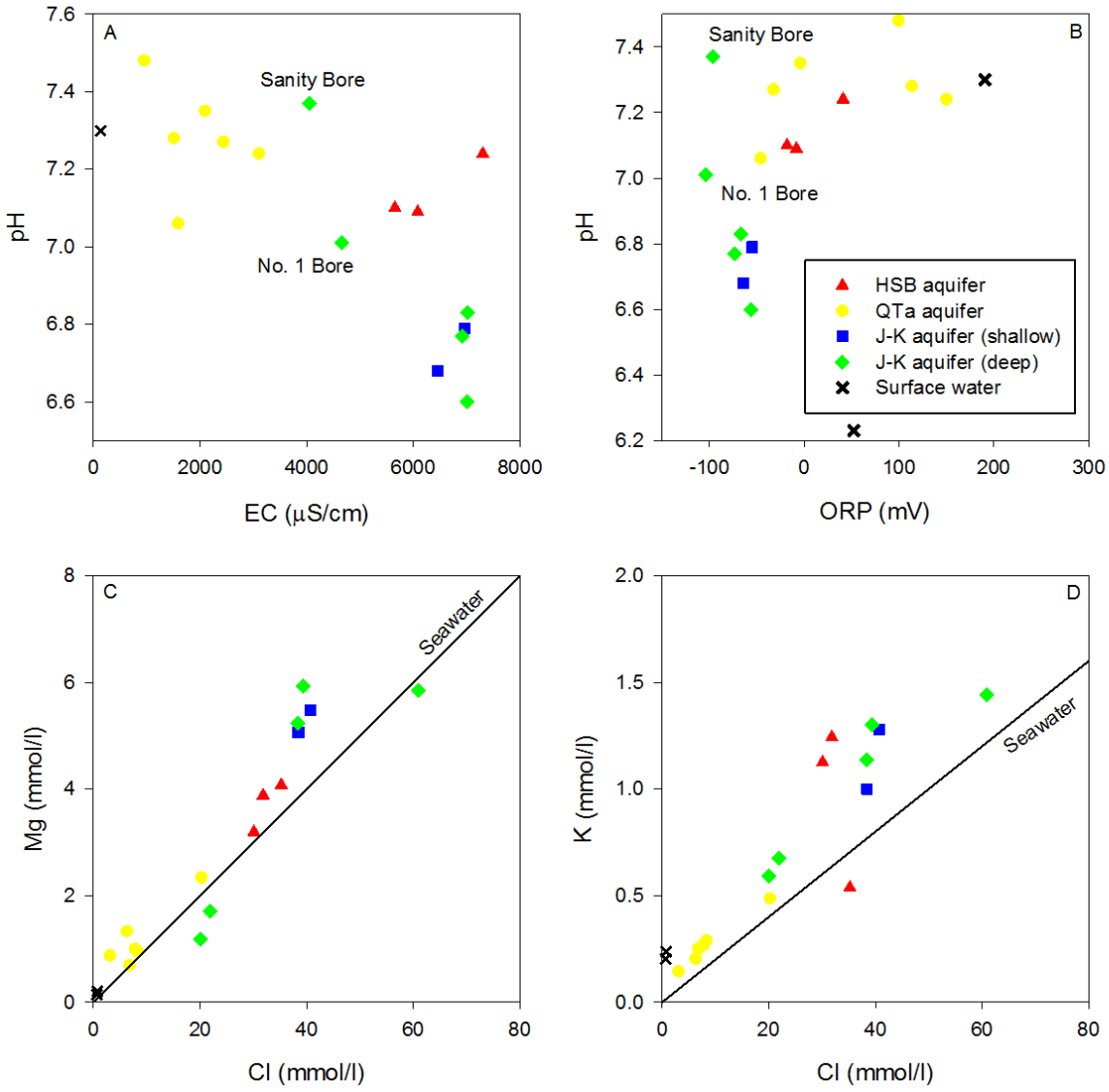

Figure 4-3: Scatter plots of A) EC (µS/cm) vs pH, B) pH vs ORP, C) Cl- (mmol/l) vs Mg (mmol/l) and D) Cl- (mmol/l) vs K+ (mmol/l). Note: Seawater lines indicate the average concentration of the given analyte expected in seawater. A correlation between results and this line indicate that the likely source of the analyte in question are marine-derived aerosols.

Within the study area, stable isotopes results from J-K aquifer groundwater cover a relatively wide range compared to other groundwater types; $\delta^{2}H$ range between -40.17‰ (Junction Bore) and -49.1‰ (No. 1 Bore) and $\delta^{18}O$ range between -4.81‰ (Junction Bore, Mt Barry) and -6.7‰ (No. 1 Bore) (Figure 4-8). It is notable that groundwater collected from the shallow J-K aquifer bores are slightly more enriched than those collected from deeper bores.

Isotopic strontium ($^{87}Sr/^{86}Sr$) ratios from J-K aquifer groundwater show a large variance compared to groundwater from other aquifers (Figure 4-9). $^{87}Sr/^{86}Sr$ ratios vary between 0.7115 (EJ Bore) and 0.7137 (Sanity Bore). Variations in $^{87}Sr/^{86}Sr$ ratios appear to correlate with two broad spatial areas. J-K groundwater with ratios less than 0.7127 come from areas near and south of Arckaringa Creek (Ricky No. 2, EJ, McLeod, Algebullcullia, and Junction Bores.). In contrast, J-K aquifer groundwater with ratios greater-than 0.7127 come from the northeast portion of the study area (No. 1 Bore and Sanity Bore). Additionally, when compared to the reciprocal of strontium (1/Sr), the difference between these two groups suggest that mineral (calcite) dissolution may have influenced Sr hydrochemistry in No. 1 Bore and Sanity Bore samples in comparison to the others. This compares favourably with previously discussed comparisons of Ca^{2+} and alkalinity concentrations in groundwater from these two wells and the potential contribution of calcite dissolution to hydrochemistry.

All radiocarbon results from J-K aquifer groundwater are low compared to samples from other aquifers (Figure 4-10). ^{14}C varied between 1.84 pMC (Junction Bore Mt Barry) and 12.65 pMC (No. 1 Bore). These results indicate that groundwater within the J-K aquifer is relatively old compared to groundwater from other aquifers.

4.2.1.2 Hamilton Sub-basin (HSB)

Groundwater from the HSB aquifer is brackish, with EC varying from 5653 µS/cm (Perseverance Bore) to 7299 µS/cm (Sheila Bore) (Figure 4-3A). Salinity is comparable to groundwater from the J-K aquifer, but more saline than water from the QTa aquifer. pH is neutral to slightly alkaline, varying between 7.09 (Carnegie Bore No. 1) and 7.24 (Sheila Bore) (Figure 4-3A and Figure 4-3B). Redox condition are slight reducing to oxidising, with field ORP measurements reported between -18.3 mV (Perseverance Bore) and 40.8 mV (Sheila Bore) (Figure 4-3B).

Proportional major ion hydrochemistry of HSB aquifer groundwater samples can be described as predominantly $Na^+ + Cl^- + (Ca^{2+} + SO_4^{2-})$ (Figure 4-4) and is therefore similar to results from the J-K aquifer, particularly those results from the non-artesian part of the J-K aquifer.

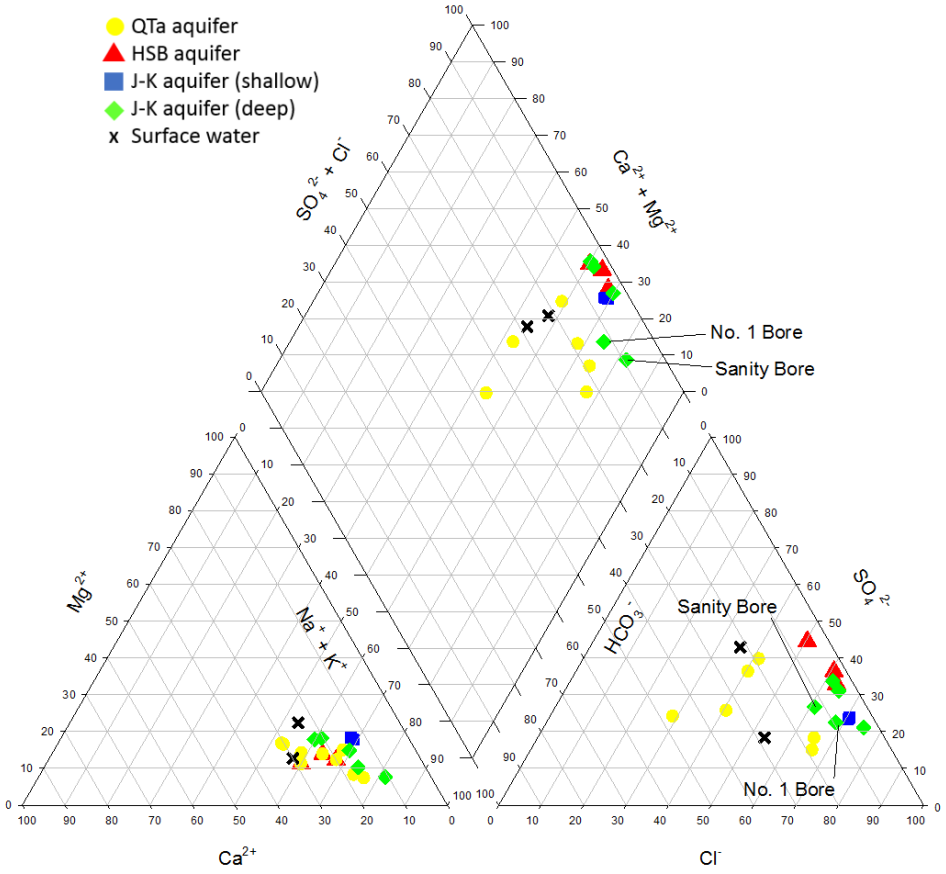

Figure 4-4: Piper diagram displaying major ion results from the area of investigation

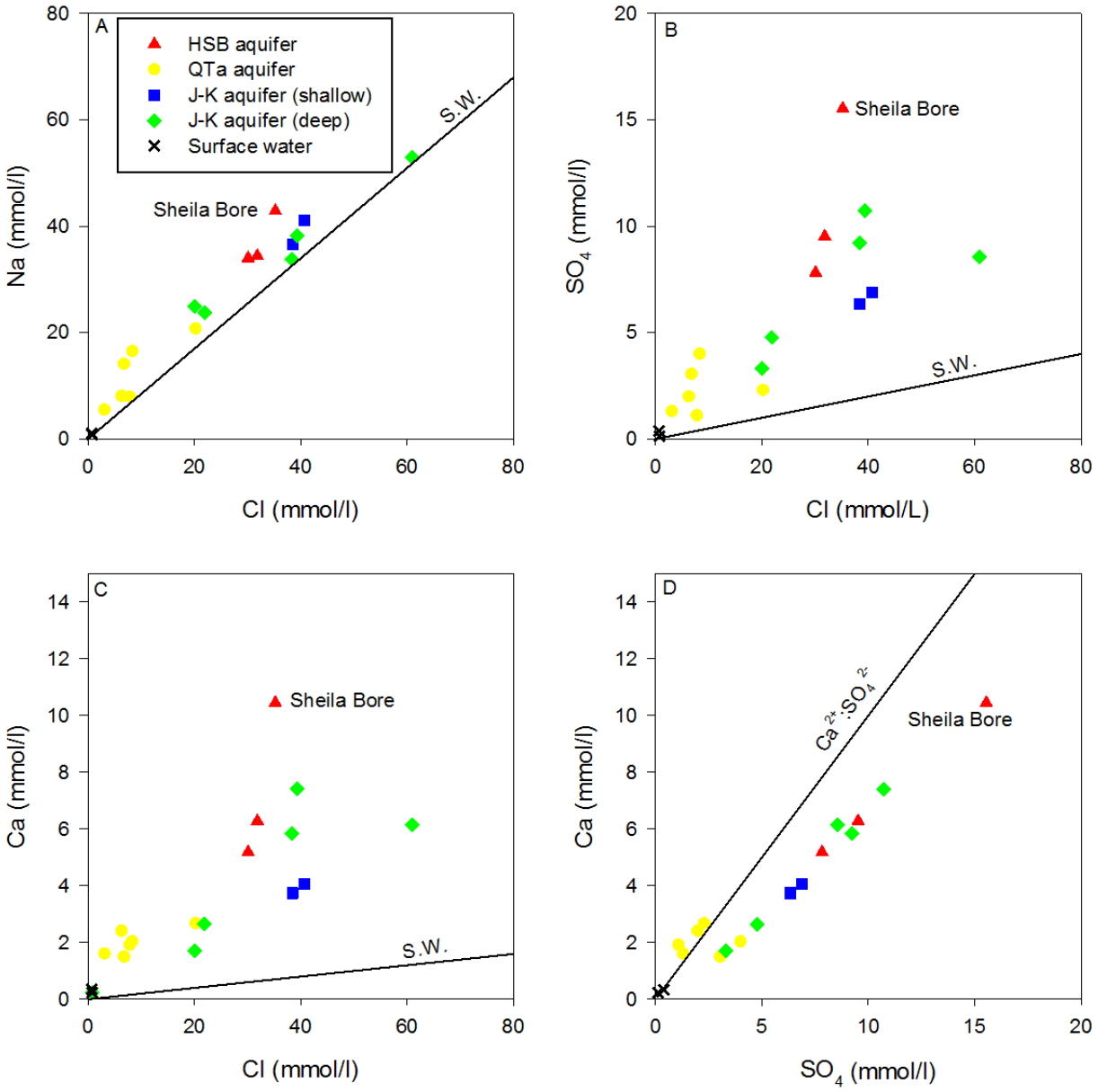

Figure 4-5: Scatter plots of A) Cl^- (mmol/l) vs Na^+, B) Cl^- (mmol/l) vs SO_4^{2-}, C) Cl^-(mmol/l) vs Ca^{2+} (mmol/l) and D) SO_4^{2-} (mmol/l) vs Ca^{2+} (mmol/l). Note: Seawater lines indicate the average concentration of the given analyte expected in seawater. A correlation between results and this line indicate that the likely source of the analyte in question are marine-derived aerosols.

Using Cl^- as a conserved element, Mg^{2+} and Na^+ appear to be predominantly conserved and sourced from marine aerosols (Figure 4-3A and Figure 4-5A). In contrast, SO_4^{2-} (Figure 4-5B) and Ca^{2+} (Figure 4-5C) concentrations are all elevated with respect to average seawater concentrations. A comparison of Ca^{2+} and SO_4^{2-} concentrations indicates that like the J-K aquifer, dissolution of gypsum is an important control on the concentrations of these ions in the HSB aquifer (Figure 4-5D). In contrast, concentrations of K^+ (Figure 4-3D) and HCO_3^- (Figure 4-6A) appear to be independent of salinity increases and therefore marine aerosols are unlikely to be the predominant source. Additionally, the lack of correlation between alkalinity and Ca^{2+} suggests that for the most part, alkalinity in the HSB aquifer groundwater within the study area is independent of water–rock interactions with calcite (Figure 4-6B). Similar to groundwater results from the J-K aquifer, Br^-: Cl^- ratios are typically above the seawater ratio of 1.5×10^{-3}, suggesting no influence from halite dissolution (Figure 4-6C).

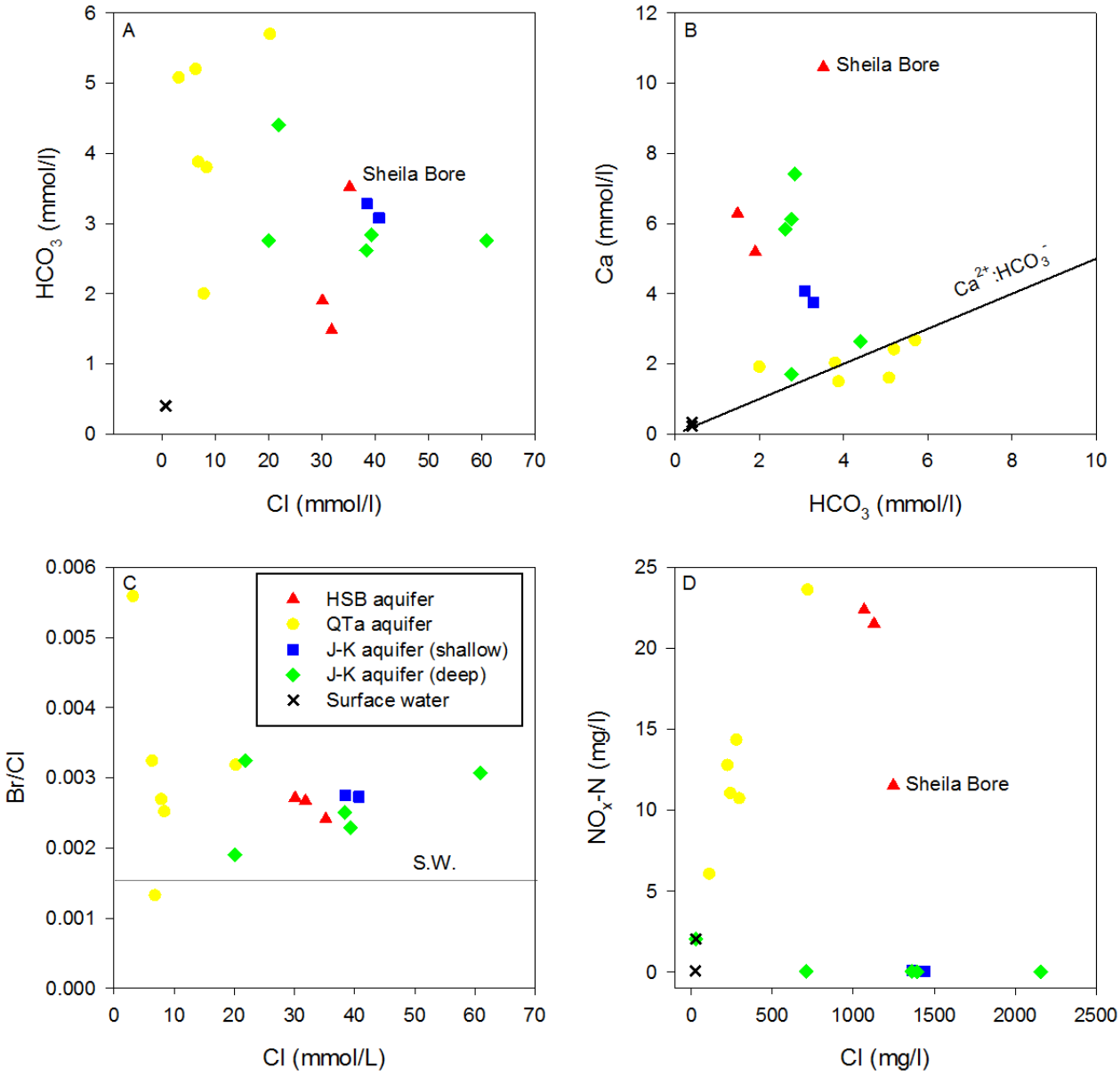

Figure 4-6: Scatter plots of A) Cl^- (mmol/l) vs HCO_3^-, B) HCO_3^- vs Ca^{2+} (mmol/l), C) Cl^- mmol/l vs Br^-/Cl^- and D) Cl^- (mmol/l) vs NO_x-N (mmol/l)

With respect to trace elements, NO_x-N (Figure 4-6D), V, U (Table 4-3) and Si (Figure 4-7A) concentrations are elevated compared to the J-K aquifer but comparable to the QTa aquifer. NO_x-N varies from 12 mg/L (Sheila Bore) to 22 mg/L (Perseverance and Carnegie Bore No. 1), V varies between 28.6 µg/L (Perseverance Bore) to 38.4 µg/L (Sheila Bore), U ranges between 1.5 µg/L (Carnegie Bore No. 1) and 9.9 µg/L (Sheila Bore) and Si varies from 27.9 mg/L (Sheila Bore) and 33.2 mg/L (Perseverance Bore). Additionally the trace elements Cr and Se were also found to be elevated when compare to groundwater from other aquifers (Table 4-1). Cr varied between 6.6 µg/L (Sheila Bore) and 24.2 µg/L (Perseverance Bore) and Se varied between 11.5 µg/L (Sheila Bore) and 14.1 µg/L (Perseverance Bore).

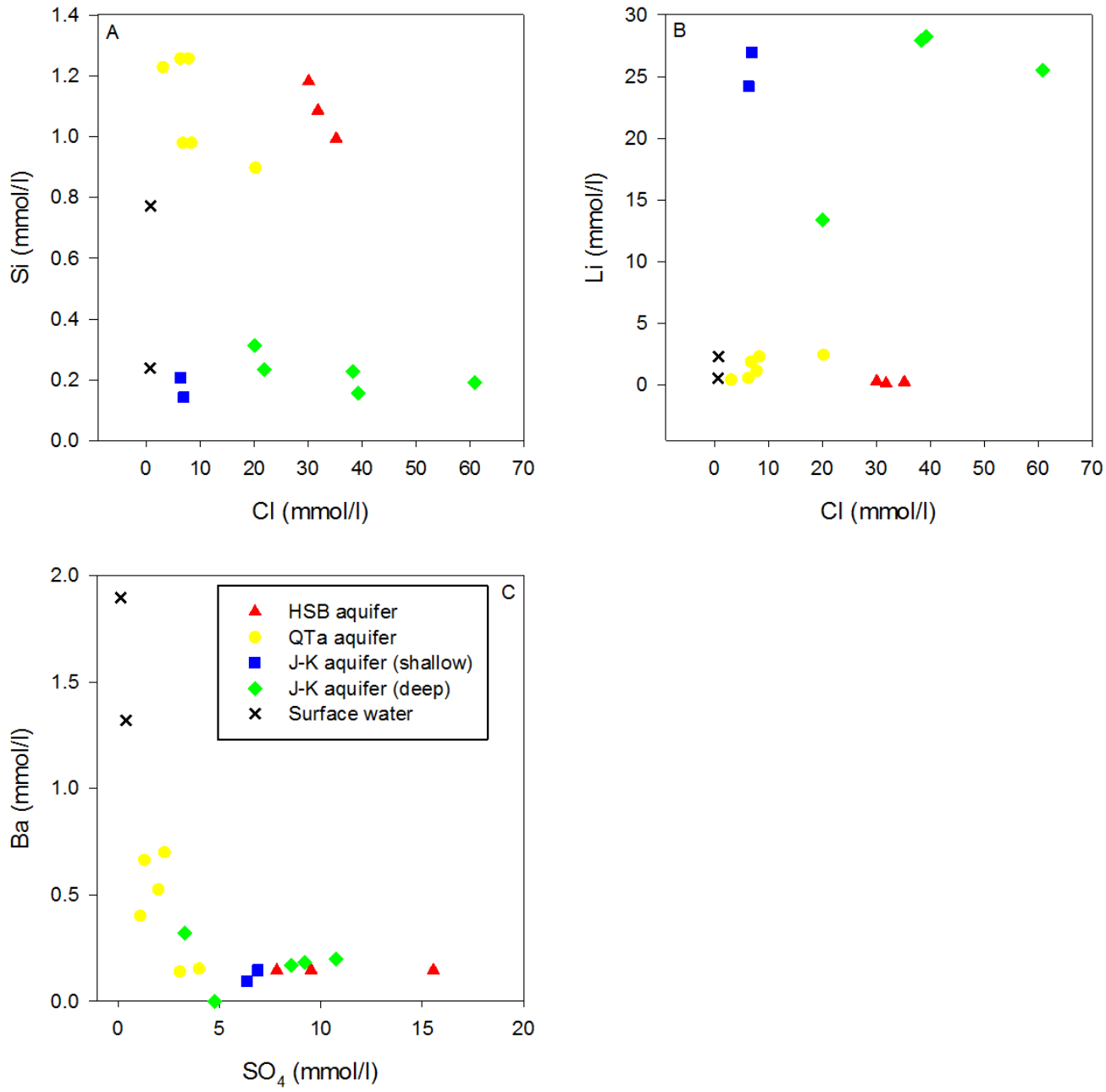

Figure 4-7: Scatter plots of: A) Cl^- (mmol/l) vs Si (mmol/l), B) Cl^- (mmol/l) vs Li (mmol/l) and C) SO_4^{2-} vs Ba (mmol/l)

Stable isotopes of HSB aquifer groundwater are relatively enriched compared to other groundwater types, but are most comparable to groundwater samples from the shallow portions of the J-K aquifer (Figure 4-8). δ^2H ranges between -39.87‰ (Perseverance Bore) and -43.35‰ (Sheila Bore) and $\delta^{18}O$ results range between -4.14‰ (Carnegie Bore No. 1) and -5.4‰ (Sheila Bore).

Isotopic strontium ($^{87}Sr/^{86}Sr$) ratios from HSB aquifer groundwater show only a small variance compared to groundwater samples from other aquifers, with ratios ranging between 0.7134 (Sheila Bore) and 0.7138 (Perseverance Bore) (Figure 4-9). These values are also relatively elevated when compared to other results. Similarly, the 1/Sr values also display a small variance of between 0.17 (Sheila Bore) and 0.47 (Perseverance Bore). Such small variations suggest that groundwater from the HSB aquifer may represent a type group. We note that $^{87}Sr/^{86}Sr$ ratios of the HSB aquifer are similar to those found from QTa aquifer as well as No. 1 Bore and Sanity Bore within the J-K aquifer.

^{14}C results from HSB aquifer groundwater are lower than or comparable to results from QTa aquifer groundwater but are more enriched than J-K aquifer groundwater samples (Figure 4-10). ^{14}C varied between 35.41 pMC (Perseverance Bore) and 74.07 pMC (Sheila Bore). These results indicate that groundwater within the HSB aquifer is generally older than those from the QTa aquifer but younger than groundwater from the J-K aquifer. Of note is the result from Sheila Bore, which is comparable to the older samples from the QTa aquifer groundwater. Of the three bores completed in the HSB aquifer that were sampled, Sheila Bore is located closest to a drainage channel (Alberga River), consequently the younger apparent age at Sheila Bore compared to the other HSB bores may be attributable to connectivity between the QTa and the HSB aquifers in the vicinity of Sheila Bore.

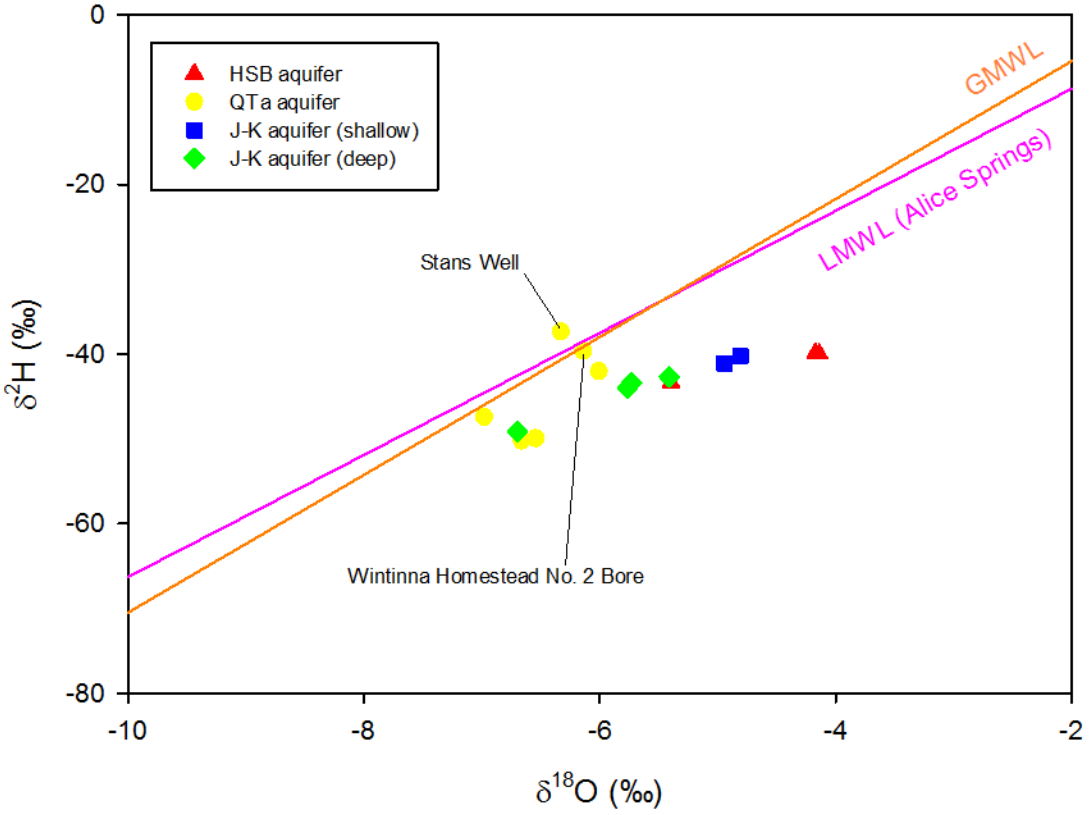

Figure 4-8: Stable isotopes δ^2H vs $\delta^{18}O$ from groundwater samples only

4.2.1.3 Cenozoic alluvial (QTa) aquifer

Groundwater from the QTa aquifer is fresh to brackish, with EC varying from 955 µS/cm (Stan Well) to 3105 µS/cm (Ethel Well) (Figure 4-3A). Groundwater salinity is typically lower than that found in the HSB and J-K aquifers. pH is slightly alkaline, varying between 7.06 (Junction Well and 7.48 (Wintinna H.S. No. 2 Bore) (Figure 4-3A and Figure 4-3B). Redox conditions are slightly reducing to oxidising, ranging between -32.3 mV (Homestead 4) and 150.2 mV (Ethel Well) (Figure 4-3B).

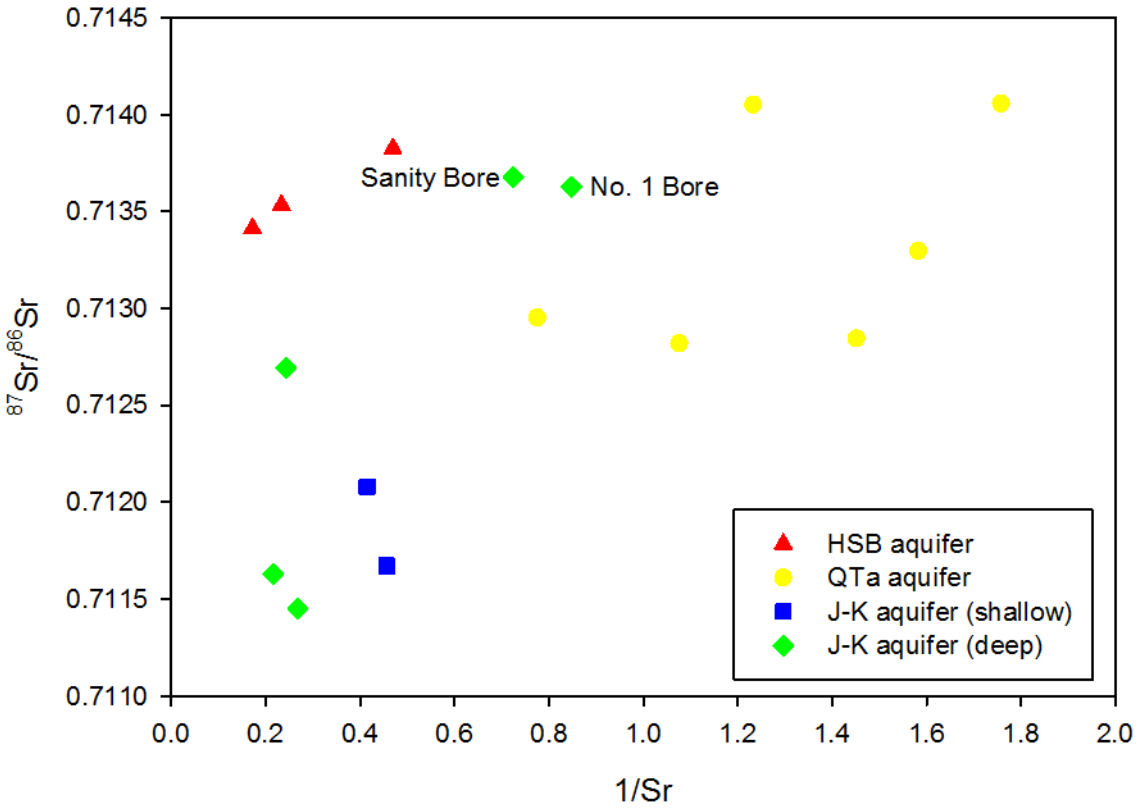

Figure 4-9: $^{87}Sr/^{86}Sr$ vs 1/Sr

Proportional major ion hydrochemistry of QTa aquifer can be described as $Na^+ + SO_4^{2-} + Cl^- + Ca^{2+} + HCO_3^-$, although there appears to be a relatively large proportional variation in anion concentration compared to groundwater from other aquifers (Figure 4-4). Proportional Cl^- concentrations vary between 50% and 85%, SO_4^{2-} varies between 30% and 75% and HCO_3^- varies between 15% and 50%. Proportional cation concentrations are comparable to groundwater from the J-K and HSB aquifers.

Using Cl^- as a conserved element, Mg^{2+} (Figure 4-3A), K^+ (Figure 4-3B) and Na^+ (Figure 4-5C) appear to be predominantly conserved and sourced from marine aerosols. In contrast, SO_4^{2-} (Figure 4-5B) and Ca^{2+} (Figure 4-5C) concentrations are all elevated with respect to average seawater concentrations. A comparison of Ca^{2+} and SO_4^{2-} concentrations indicates that like concentrations in the J-K and HSB aquifers, the dissolution of gypsum is an important control on the concentrations of these ions (Figure 4-5D). In contrast HCO_3^- appears to be independent of salinity increases as described by Cl^- and therefore marine aerosols are unlikely to be the predominant source (Figure 4-6A). Comparison between Ca^{2+} and HCO_3^- suggests that an important factor to concentrations in the QTa aquifer is the dissolution of calcite (Figure 4-6B). Similar to results from the J-K and HSB aquifers, Br^-: Cl^- ratios are typically above the seawater ratio of 1.5×10^{-3}, suggesting no influence from evaporate mineral dissolution (Figure 4-6C).

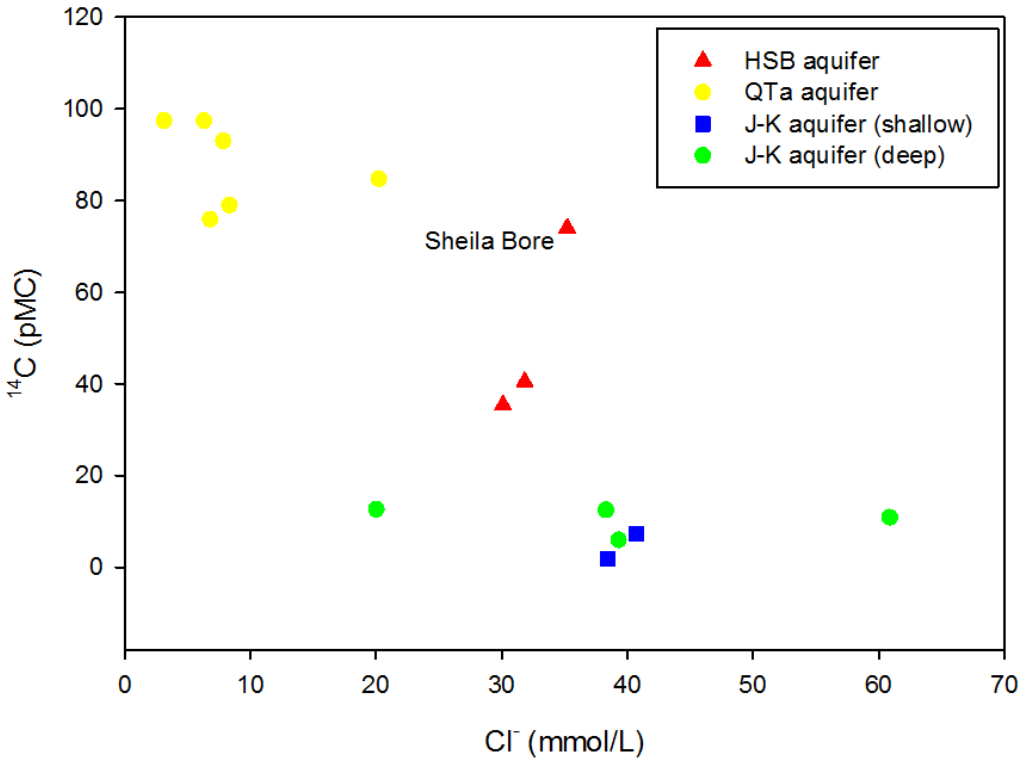

Figure 4-10: ^{14}C (pMC) vs Cl- (mmol/L)

With respect to trace elements NO_x-N, V, U, and Si, concentrations are elevated compared to the J-K aquifer and comparable to the HSB aquifer. NO_x-N varies from 6.1 mg/L (Wintinna H.S. No. 2) and 24 mg/L (Ethel Well) (Figure 4-6D), V varies between 23 µg/L (Ethel Well) and 88 µg/L (Junction Well Wintinna), U varies between 0.9 mg/L (Junction Well) and 6.7 mg/L (Homestead No. 4 Bore) and Si varies from 27.5 mg/L (Homestead No. 2 Bore and Homestead No. 4 Bore) and 35.3 mg/L (Junction Well and Stan Well) (Figure 4-7A). In addition, wells in the vicinity of Wintinna Creek have elevated concentrations of Ba in comparison to other locations, ranging between 55 µg/L (Junction Well) and 96 µg/L (Ethel Well) (Figure 4-7C). Finally, Ethel Well and Homestead Bores No. 2 and No. 4 near the Alberga River have elevated concentrations of Se (8 mg/L, 5 mg/L and 5mg/L respectively), which is similar to groundwater from the HSB aquifer.

Stable isotopes from the QTa aquifer groundwater samples are relatively depleted compared to other groundwater types, but are most comparable to groundwater samples collected from the deeper portions of the J-K aquifer. δ^2H ranges between -37.35‰ (Wintinna H.S. No. 2 Bore) and -50.25‰ (Homestead No. 4 Bore, Todmorden Station) and $\delta^{18}O$ ranges between -6.0‰ (Junction Well) and -6.98‰ (Ethel Well). Additionally, stable isotope results from Homestead No. 2, Homestead No. 4, and Ethel Well appear to plot closer to the average meteoric water lines than other results influenced by evaporation. This suggests that at these two locations, there has not been significant post-rainfall alteration of the stable isotope signature of water before infiltration to the watertable.

Isotopic strontium ($^{87}Sr/^{86}Sr$) ratios from QTa aquifer groundwater vary between 0.7128 (Stan Well) and 0.7141 (Homestead No. 2 Bore) (Figure 4-9). This variation in $^{87}Sr/^{86}Sr$ ratios is similar to those observed for the HSB aquifer as well as the No. 1 Bore and Sanity Bore samples from the J-K aquifer. In contrast is the relatively wide variance in 1/Sr values from the QTa aquifer, which range from 0.78 (Ethel Well) to 1.78 (Homestead No. 2 Bore). Of interest is that increases in 1/Sr values within the QTa aquifer correspond spatially, with low values found in the most-easterly samples and high values found in the most-westerly samples.

The only exception is the 1/Sr value from Homestead No. 4 Bore, which has a value of 1.23. Given this bore is less than 10 m distant from Homestead No. 2 Bore, this potentially highlights the natural variation inherent in groundwater. In suggesting this, it appears that both bores supply water to the homestead; however it is not clear at this time whether the bore usage is equal. The variation of 1/Sr values in QTa aquifer compares favourably with previously discussed comparisons of Ca^{2+} and alkalinity concentrations and the potential contribution of calcite dissolution to hydrochemistry. The correlation between 1/Sr and the spatial distribution of sampled wells may also indicate that calcite dissolution generally occurs progressively down the groundwater flow path.

^{14}C results from QTa aquifer groundwater are generally more modern than groundwater from either the HSB or the J-K aquifers (Figure 4-10). ^{14}C results varied between 75.93 pMC (Homestead No. 4) and 97.48 pMC (Wintinna H.S. No. 2 Bore). These results indicate that groundwater within the QTa aquifer is relatively young compared to groundwater from other aquifers.

4.2.2 Xyelm water chemistry

4.2.2.1 Stable isotopes of groundwater, surface water and xylem water

Although there are variations in the stable isotope ratios of water interpretable between various groundwater types, such variations are sufficiently small when compared to those observed with surface water and xylem water samples that groundwater might be considered as a single grouping for the purposes of determining the source of xylem water. Consequently, for the purposes of this section, we discuss groundwater results as a single group. Additionally, a general comparison between surface water results from Cootanoorina and Stewart Waterholes with all results is made.

Notably, the majority of xylem-water stable isotope results show some displacement away from the Global Meteoric Water Line (GMWL) and Local Meteoric Water Line (LMWL) average, suggesting that this water has undergone evaporative enrichment at some point.

4.2.2.2 Hamilton Sub-basin

Samples included one *E. coolabah* and one *Acacia spp.* sample sourced near the Homestead wells (Todmorden) and one *E. coolabah* sample sourced near Sheila Bore. All xylem stable isotopes from this area are enriched compared to the groundwater samples from the same area (Figure 4-11). δ^2H ratios for the E. coolabah vary between -12.88‰ (Sheila Bore site) and -19.38‰ (Homestead wells site, Todmorden) and $\delta^{18}O$ values vary between -1.20‰ (Homestead wells site, Todmorden) and 0.99‰ (Sheila Bore site). The xylem water stable isotopes results from the acacia sample collected from the Homestead Bore (Todmorden) site was particularly enriched with a δ^2H of 0.66‰ and a $\delta^{18}O$ value of 1.51‰. This compares to groundwater results that vary between -39.87‰ (Perseverance Bore) and -39.95‰ (Carnegie Bore No. 1) for δ^2H and -4.14‰ (EJ Bore) and -5.40‰ (Sheila Bore) for $\delta^{18}O$. Notably, stable isotope results from vegetation samples are reasonably comparable to surface water results.

4.2.2.3 Waterholes

As well as water samples collected from each waterhole, two *E. coolabah* samples and one *E. camaldulensis* sample were also collected from near the Stewart Waterhole and one *E. coolabah* sample was collected from near the Cootanoorina Waterhole. With respect to the Stewart Waterhole site, stable isotope results from the *E. camaldulensis* sample are very similar at this scale to the results from the waterhole sample (Figure 4-11). The *E. camaldulensis* sample returned a δ^2H value of 7.88‰ and a $\delta^{18}O$ value -0.79‰ compared to the waterhole sample that returned 15.37‰ δ^2H and 1.15‰ $\delta^{18}O$. The *E. coolabah* results from the Stewart Waterhole were variable, ranging from -7.90‰ to 3.54‰ for δ^2H and from -0.79‰ to 0.79‰ for $\delta^{18}O$. In keeping with the comparison between xylem and surface water results at this location, is that the xylem results here show the least evaporative influence of all the xylem waters collected during this investigation. This complements the results from surface water, which plot in close vicinity to the LMWL.

In contrast, stable isotope results from the Cootanoorina waterhole *E. coolabah* sample appears notably depleted compared to the surface water result; a δ^2H value of -13.82‰ and $\delta^{18}O$ value -1.04‰ were obtained; in comparison to the waterhole result of 20.12‰ δ^2H and 6.40‰ $\delta^{18}O$.

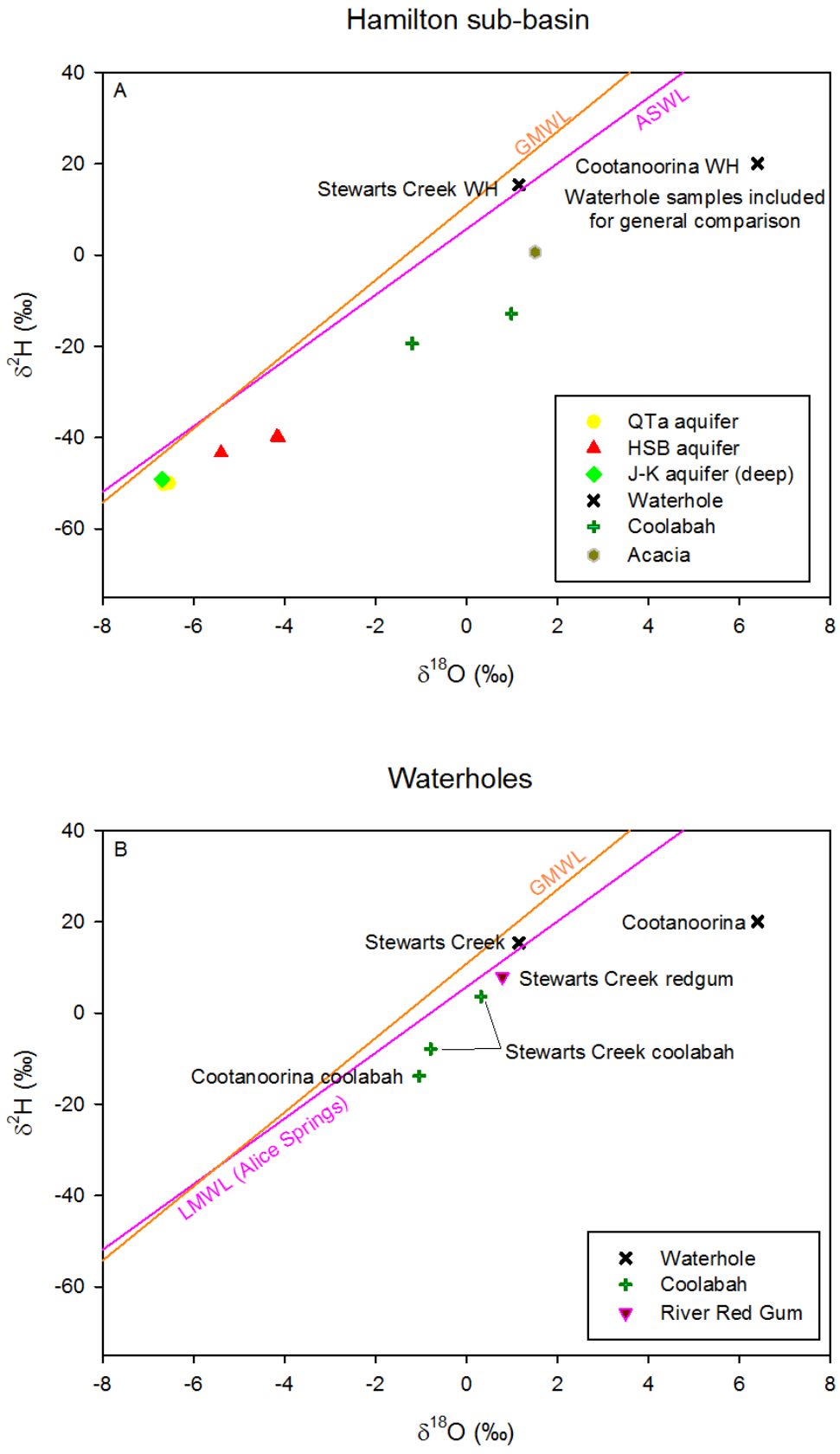

Figure 4-11: Stable isotope results for vegetation and groundwater samples from the a) Hamilton Sub-basin region and b) Stewart and Cootanoorina Waterholes

4.2.2.4 Lora Creek

Samples included one acacia sample and two *E. coolabah* samples sourced near Algebullcullia Bore and Junction Bore in the Lora Creek region. Stable isotope s of water from the acacia and *E. coolabah* are enriched compared to the nearby bore samples (Figure 4-12). The *E. coolabah* samples from near Algebullcullia Bore returned a δ^2H value of -35.23‰ and a $\delta^{18}O$ value -2.14‰ whereas the sample from near Junction Bore retuned values of -17.66‰ δ^2H and -0.02‰ $\delta^{18}O$. The Junction Bore acacia sample retuned a result comparable to the Junction Bore *E. coolabah*, which had a δ^2H value of -10.24‰ and a $\delta^{18}O$ value of 0.69‰. This compares to groundwater stable isotope values of -41.06‰ δ^2H and -4.94‰ $\delta^{18}O$ (Algebullcullia Bore) and -40.17‰ δ^2H and -4.81‰ $\delta^{18}O$ (Junction Bore).

The result for the *E. coolabah* sampled appear depleted when compared to the most depleted result from a surface water sample. This was collected from Stewart Waterhole, which returned values of 15.37‰ δ^2H and 1.15‰ $\delta^{18}O$. The results from the Junction Bore area are closer in value to the waterhole result than the groundwater results.

4.2.2.5 Wintinna and Arckaringa Creeks

Three E. camaldulensis samples, collected near the Junction Well, Ethel Well, and Stan Well sites and one E. coolabah sample collected from near the Junction Well site were analysed. All xylem water stable isotope results from this area are enriched compared to the groundwater samples from the same area (Figure 4-12). δ^2H ratios for E. camaldulensis vary between -20.32‰ (Ethel Well site) and -32.68‰ (Junction Well site) and $\delta^{18}O$ values vary between -1.95‰ (Ethel Well site) and -3.83‰ (Junction Well site). This compares to groundwater results that vary between -37.35‰ (Wintinna H.S. No. 2 Bore) and -47.41‰ (Ethel Well) for δ^2H and -5.73‰ (EJ Bore) and -6.98‰ (Ethel Well) for $\delta^{18}O$.

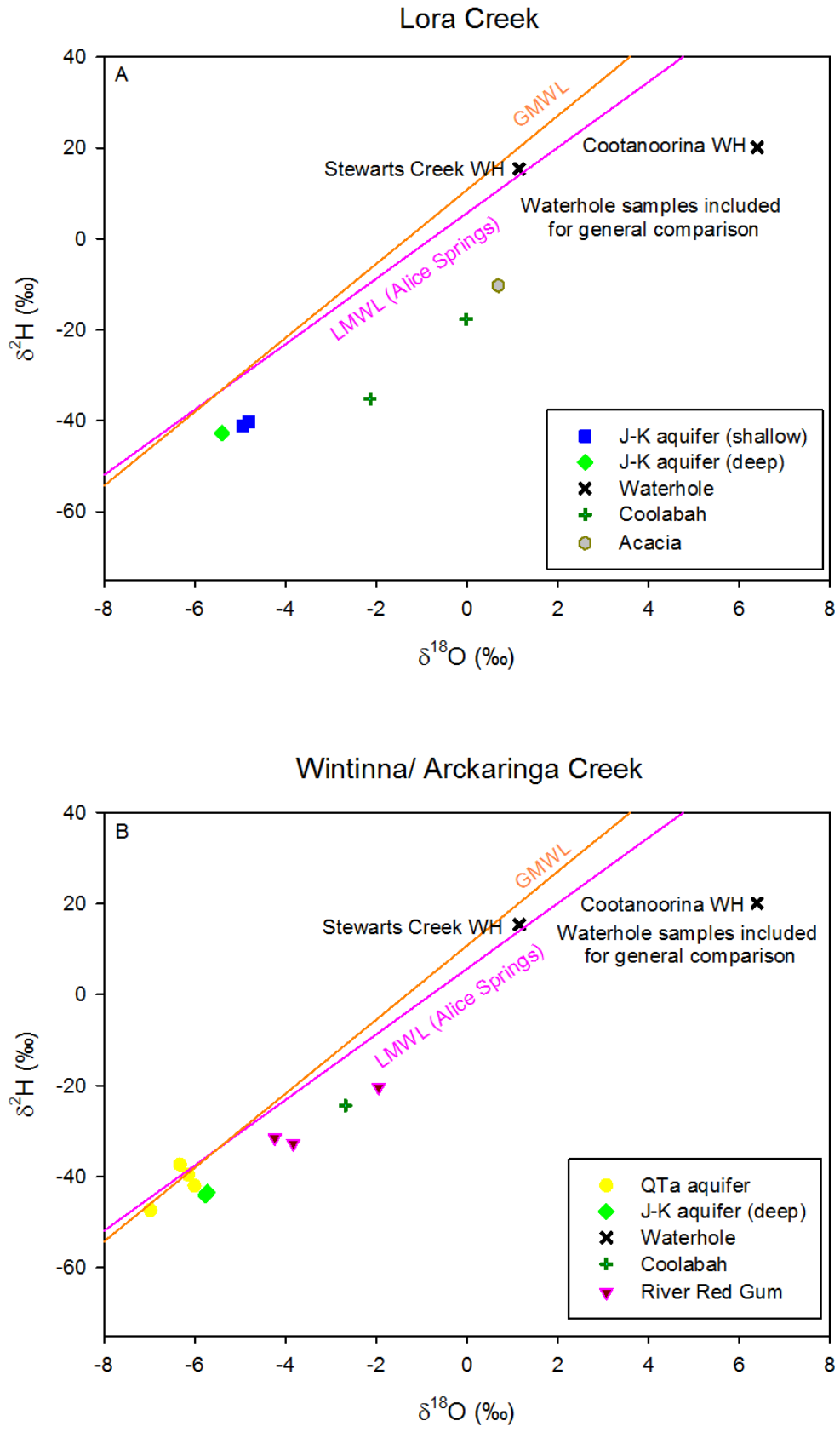

Figure 4-12: Stable isotope results for vegetation and groundwater samples from the a) Lora Creek and b) Wintinna and Arckaringa Creek regions

5 Leaf and soil matric water potentials – Method and results

5.1 Methodology

In order to draw water from the soil to the leaves, a tree must lower the leaf water potential to a point that is lower than the water potential of the soil. Measurements of leaf water potential (LWP) taken before dawn, when trees are not actively transpiring, are indicative of the water potential of the soil from which the trees are extracting water (i.e. the wettest part of the soil containing roots) as leaf water potentials are assumed to equilibrate over night with that of the soil (Eamus et al 2006). Ideally, measurement of soil water potentials occurs at different depths and by matching the pre-dawn LWP with the closest soil water potential, this infers the depth of soil from which the tree is taking its water. Without soil water sampling at depths, it can be assumed that the higher the tree's pre-dawn LWP is the more likely it is to be accessing water from a highly saturated source (e.g. groundwater or bank storage). Conversely lower LWP indicate that the tree is the less likely it is to be using groundwater or it is using groundwater but the groundwater is saline.

At each site, the field sampling aim was to collect three pre-dawn, morning and midday leaf water potential measurements from three trees growing on the channel banks, as well as three trees on the floodplain. Sampling from three tree species occurred where multiple canopy species were present. However, logistical constraints prevented the application of this design at all sites; in particular:

- Distances and road conditions between sites required long travel times between sites, therefore reducing the times during which trees could be measured
- The volume of nitrogen gas taken into the field restricted the total number of measurements.

Pre-dawn measurements occurred between 4.15 am and 6.30 am, morning measurements occurred between 8 am and 9.30 am and midday measurements occurred between 11 am and 3.30 pm. The large travel times between sites resulted is a wide range in times recorded as midday measurements.

Table 5-1 presents the number and species of trees and measurements collected and Figure 4-2 provides the location of sampled trees.

A 1505D model pressure chamber (PMS Instruments, n b 10 MPa capacity) was used to collect LWP measurements. A volume reducer in the cylinder to reduce the gas consumed was used in most cases except where samples were too large. In most cases, five minutes would elapse between sample collection and LPW measurement, but where there was a delay due to travel distances between collection and analysis, and then the samples were stored in sealed foil bags.

The percentage of canopy present was recorded for each tree using the Bushland Condition Monitoring Method (Croft et al., 2005) as an indicator of tree health.

Hand auguring restricted the collection of soil samples for soil matric potential by limiting the sampling depth and increasing the time required to collect samples. However, we collected near-surface samples at all leaf water potential sample sites except the Wintinna sites, which were too gravelly for the auger to penetrate. Table 5-2 and Figure 4-2 describe and display sampling locations respectively. Where surface water was present, (Stewart and Cootanoorina Waterholes) the level of the hole was surveyed relative to the water's surface using a dumpy level.

Samples consisted of approximately 200–400 mg of soil that was stored in double snap lock plastic bags.

Table 5-1: Summary of leaf water potential sampling results

					Pre-dawn			Morning			Midday		
Site (site no.)	Tree	Position	Species[1]	% canopy present	Mean LWP MPa	S.D.	n	Mean LWP MPa	S.D.	n	Mean LWP MPa	S.D.	n
Cootanoorina Waterhole (7)	CFC1	Floodplain	Coolabah	95	-3.09	0.12	3	-4.40	0.43	3	-3.69	0.08	3
	CFC2	Floodplain	Coolabah	95	-3.12	0.11	3	-3.86	0.42	3	-3.45	0.13	3
	CFC3	Floodplain	Coolabah	90	-3.19	0.06	3	-3.88	0.17	3	-3.75	0.24	3
	CBC1	Bank	Coolabah	75	-1.27	0.03	3	-3.11	0.21	3	-2.97	0.23	3
	CBC2	Bank	Coolabah	80	-1.29	0.04	3	-2.73	0.30	3	-3.16	0.10	3
	CBC3	Bank	Coolabah	80	-1.10	0.09	3	-2.42	0.20	3	-3.21	0.17	3
	CBS1	Bank	River Cooba	98	-0.84	0.08	2			0			0
	CBS2	Bank	River Cooba	85	-1.61	0.79	2	-2.65	0.08	2			0
EJ Bore (6) (Arckaringa Creek)	ACC1	Bank	Coolabah	65	-3.63	-0.06	3			0	-4.10	0.36	3
	ACC2	Bank	Coolabah	80	-3.45	-0.15	3			0	-3.71	0.12	3
	ACG1	Bank	Gidgee	90	-4.53	-0.08	3			0	-4.73	0.06	3
	ACG2	Bank	Gidgee	90	-4.48	-0.10	3			0	-4.77	0.07	3
Francis Camp Waterhole (5)	FCR1	Bank	Red Gum	70	-3.93	0.04	3			0	-4.2	0.13	3
	FCR2	Bank	Red Gum	75	-2.61	0.08	3			0	-3.3	0.22	3
	FCR3	Bank	Red Gum	85	-2.53	0.06	3			0	-3.1	0.10	3
	FCC1	Bank	Coolabah	65	-3.47	0.15	3			0	-3.54	0.25	3
	FCC2	Bank	Coolabah	90	-2.80	0.10	3			0	-3.2	0.21	3
	FFC1	Floodplain	Coolabah	85	-2.43	0.08	3			0	-2.95	0.16	3
	FFC2	Floodplain	Coolabah	60	-1.93	0.13	4			0	-2.7	0.25	3
Stewart Waterhole (12)	SFC1	Floodplain	Coolabah	80	-1.35	0.13	3			0	-3.13	0.32	3
	SCC2	Bank	Coolabah	95	-1.06	0.08	3	-3.33	0.04	2	-2.98	0.19	3
	SCC3	Bank	Coolabah	80	-1.09	0.05	3	-2.60	0.32	3	-3.76	0.19	3
	SCR1	Bank	Red Gum	55	-0.87	0.04	3	-1.84	0.36	3	-2.45	0.44	3
	SCR2	Bank	Red Gum	90	-0.51	0.09	3			0	-3.17	0.10	3
	SCR3	Bank	Red Gum	49	-0.50	0.05	3			0	-2.70	0.27	3
Wintinna HS (2)	WFR1	Floodplain	Red Gum	95	-2.33	0.18	2			0	-3.23	0.08	3
	WCR2	Bank	Red Gum	85	-2.17	0.13	3			0	-2.72	0.31	3
	WCR3	Bank	Red Gum	75	-2.45	0.07	2			0			0
Ethel Well	ECR1	Bank	Red Gum	90	-1.77	0.05	2			0	-3.21	0.23	3
	ECR2	Bank	Red Gum	90	-2.00	0.07	2			0	-3.07	0.58	3
	EFR3	Floodplain	Red Gum	65	-3.06	0.08	2			0	-3.72	0.24	3

[1]Coolabah (*Eucalyptus coolabah*), River Red Gum (*E. camaldulensis ssp. ovata*), River Cooba (*Acacia stenophylla*, Gidgee (*A. cambagei*)

Soil matric potentials were determined from a subsample of the core placed into a plastic cup and measured via dew point generation in a water activity meter (Decagon Aqua Link 4TE). This instrument performs multiple measurements automatically on each sample until stability of dew point and equilibration of temperature are reached. Measurements are stored internally until a set is completed and matric potential values are calculated by the Aqua Link software. Sequence integrity was cross checked with simultaneously hand noted values. Calibration verification is undertaken prior to, during and post analyses.

Soil water potential is a combination of soil matric potential (how tightly water is held in the soil, or soil dryness) and the osmotic potential (saltiness). Soil osmotic potential was not considered likely to contribute significantly to the overall soil water potential at these sites and therefore was not measured, although it is known to be a factor further down in the catchment (Costelloe et. al 2008. Instead matric potential was used as a surrogate for total water potential, given that the matric potential is likely to be a close match to the total water potential.

Table 5-2: Description of soil matric potential sampling sites

Site	Location	Hole depth (m)*	Details
Cootanoorina Waterhole	Floodplain	0.7	Between the two trees sampled for LWP and sapflow monitoring (CFC1 and CFC2); note that solid rock (Bulldog Shale) was encountered at 0.7m depth; this site was approximately 200 m from the waterhole
	Channel base	1.15	In the lowest point of the channel approximately 10 m downstream of the waterhole near tree CBC3; top of hole surveyed at 0.15 m above the level of the water surface
EJ Bore (Arckaringa Creek)	Top of bank	0.7	Top of bank next to trees ACC1 and ACG1, approximately 1 m from the edge of the bank
	Channel base	1.0	In lowest point of the channel below trees ACC1 and ACG1, channel approximately 1 m deep
Francis Camp	Top of bank	1.5	Top of bank next to trees FCR1 and FCC1, approximately 3 m from the edge of the bank
	Channel base	0.7	In lowest point of the channel near vehicle track crossing, channel approximately 3–4 m deep
Stewart Waterhole	Mid-bank	1.4	In a side channel below the elevation of the floodplain and top of bank, approximately 5 m from the water's edge; top of hole surveyed at 0.73 m above the level of the water's surface

*Below ground surface

5.2 Results

5.2.1 Water potentials

Results for all leaf water potential (LWP) measurements are given in Table 5-1 and pre-dawn and midday results summarised in Figure 5-1.

5.2.1.1 Comparison between sites and locations

At the time of sampling, Stewart Waterhole was full and Cootanoorina Waterhole held some water; all other sites were dry. Pre-dawn LWPs for the *E. camaldulensis* at Stewart Waterhole were the highest recorded in the sampling trip (between -0.50 and -0.87 MPa) compared with *E. camaldulensis* at dry sites where pre-dawn LWPs were ranged from -1.77 to as low as -3.93 MPa (Figure 5-1:). Similarly, *E. coolabah* on the bank at Stewart Waterhole and in the base of the channel at Cootanoorina Waterhole (CCC3) had the highest pre-dawn LWPs (-1.06 and -1.10). *E. coolabah* growing slightly further from the edge of the waterholes (Stewart floodplain, tree SFC1, approximately 20m from the bank, and Cootanoorina bank, trees CCC1 and CCC2) had slightly lower pre-dawn LWP between -1.27 and -1.35 MPa. *E. coolabah* growing at dry channel (EJ Bore) and floodplain sites had lower pre-dawn LWPs (-1.93 to -3.63 MPa).

At Cootanoorina Waterhole, the floodplain *E. coolabah* were located approximately 200 m from the channel bank. These had much lower pre-dawn LWPs (-3.09 to -3.19 MPa) than *E. coolabah* growing on the channel bank (-1.10 to -1.29). Soil coring near the floodplain *E. coolabah* found Bulldog Shale at approximately 1 m depth. If any shallow or perched groundwater is present near the waterhole, it appears unlikely to extend onto the floodplain.

At Francis Camp Waterhole, the two floodplain *E. coolabah* were growing approximately 100 m from the channel bank and had slightly higher pre-dawn LWPs than the two channel-bank *E. coolabah* but more measurements would be required to determine if this was a significant difference. At this site, the floodplain trees are also very sparse and they may have been able to access more soil water from rainfall two weeks prior to field sampling. There may also be an effect of the soil near the bank top being drier (i.e. due to the additional evaporative surface of the mostly bare vertical bank).

At Wintinna Homestead, there was little difference between the pre-dawn LWPs, with all trees growing close to the main channel and at similar elevations. At nearby Ethel Well however the tree growing on the floodplain was at slightly higher elevation than the other trees and some distance (30 m) from the main channel and had noticeably lower pre-dawn LWP than the trees close to the bank, which had similar but slightly lower pre-dawn LWP to Wintinna homestead.

Midday LWPs did not show clear trends between sites or species (Figure 5-1:), although the wide variation inherent within the collection times for the midday measurements may have contributed. However differences between pre-dawn and midday LWPs (calculated as midday – pre-dawn) display the influence of water availability, with trees that had higher pre-dawn LWPs (e.g. Stewart Waterhole and Cootanoorina Waterhole bank) having larger differences between pre-dawn and midday LWP (Figure 5-2). In contrast, *Acacia cambagei*s at the EJ Bore site had the lowest pre-dawn LWPs and very little difference in midday LWP (lower left hand side of graphs) and are therefore likely to be using very little water. The *E. camaldulensis* growing on the top of the bank at Francis Camp showed the lowest pre-dawn LWP and lowest difference with midday LWP (Figure 5-2 top). During the day a tree must be able to lower its LWP compared with pre-dawn LWP in order to draw water from the soil to the canopy and the trees with low pre-dawn LWP and little difference between pre-dawn and midday LWP may be under greatest water stress.

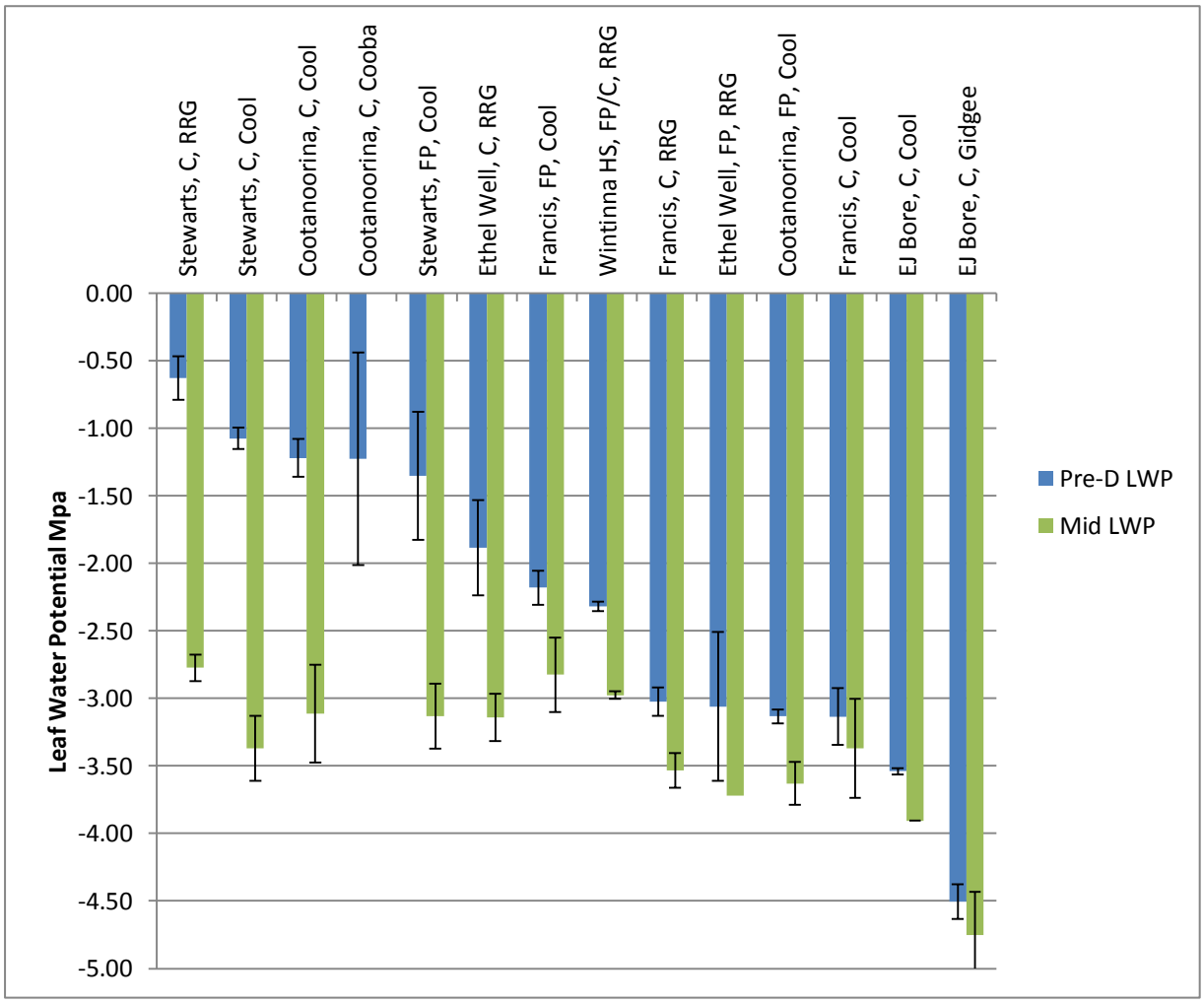

Figure 5-1: Mean average leaf water potentials (LWP) for each site, position and species pre-dawn (Pre-D) and midday (Mid), error bars showing standard deviation **HS = Homestead, FP = floodplain, C = channel, RRG = River Red Gum (*E. camaldulensis*), Cool = Coolabah (*E. coolabah*), Gidgee (*Acacia cambagei*), Cooba = River Cooba (*A. stenophylla*)**

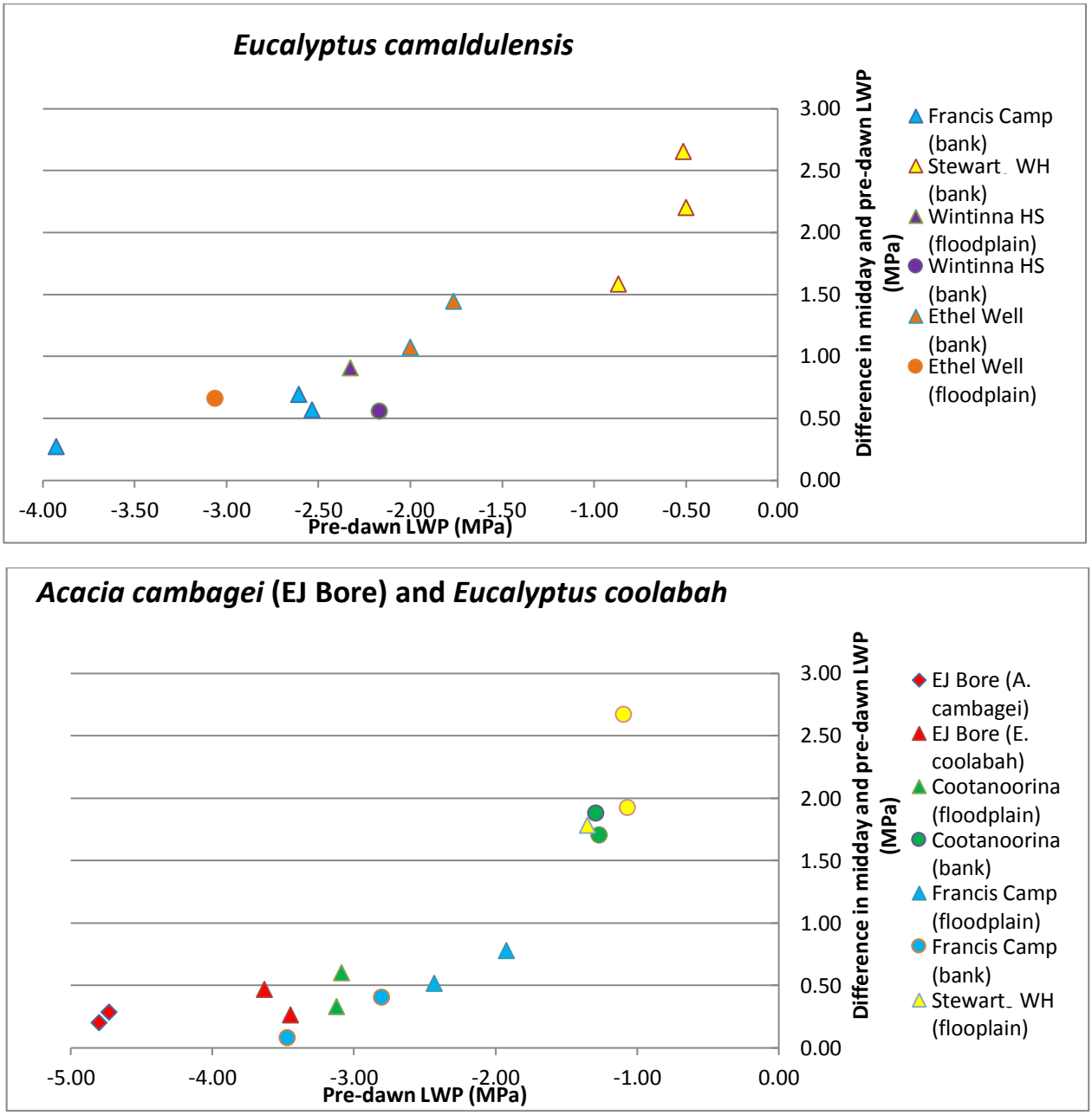

Figure 5-2: Difference between pre-dawn and midday LWPs (y axis) and pre-dawn LWP (x axis) for *E. camaldulensis* (River Red Gum) (top) and *A. cambagei* (Gidgee) at EJ Bore and all *E. coolabah* (Coolabah) (bottom)

It was noted in the field that at both sites where surface water was present (Stewart and Cootanoorina Waterholes), the soil was not saturated despite soil holes being located close to the water's edge (5 m and 10 m respectively) and extending below the elevation of the surface water. This indicates a lack of connection between shallow groundwater and these waterholes at the same elevation as the surface water in the very near vicinity. The soil in the profiles consisted of sandy clays and clayey sands.

Figure 5-3 compares soil matric potentials at different depths with mean average pre-dawn leaf water potentials. Cootanoorina Waterhole was the only site where the tree pre-dawn LWP and soil matric potentials at the same location overlap, with soils between 0.5 m and 1 m having corresponding matric potentials.

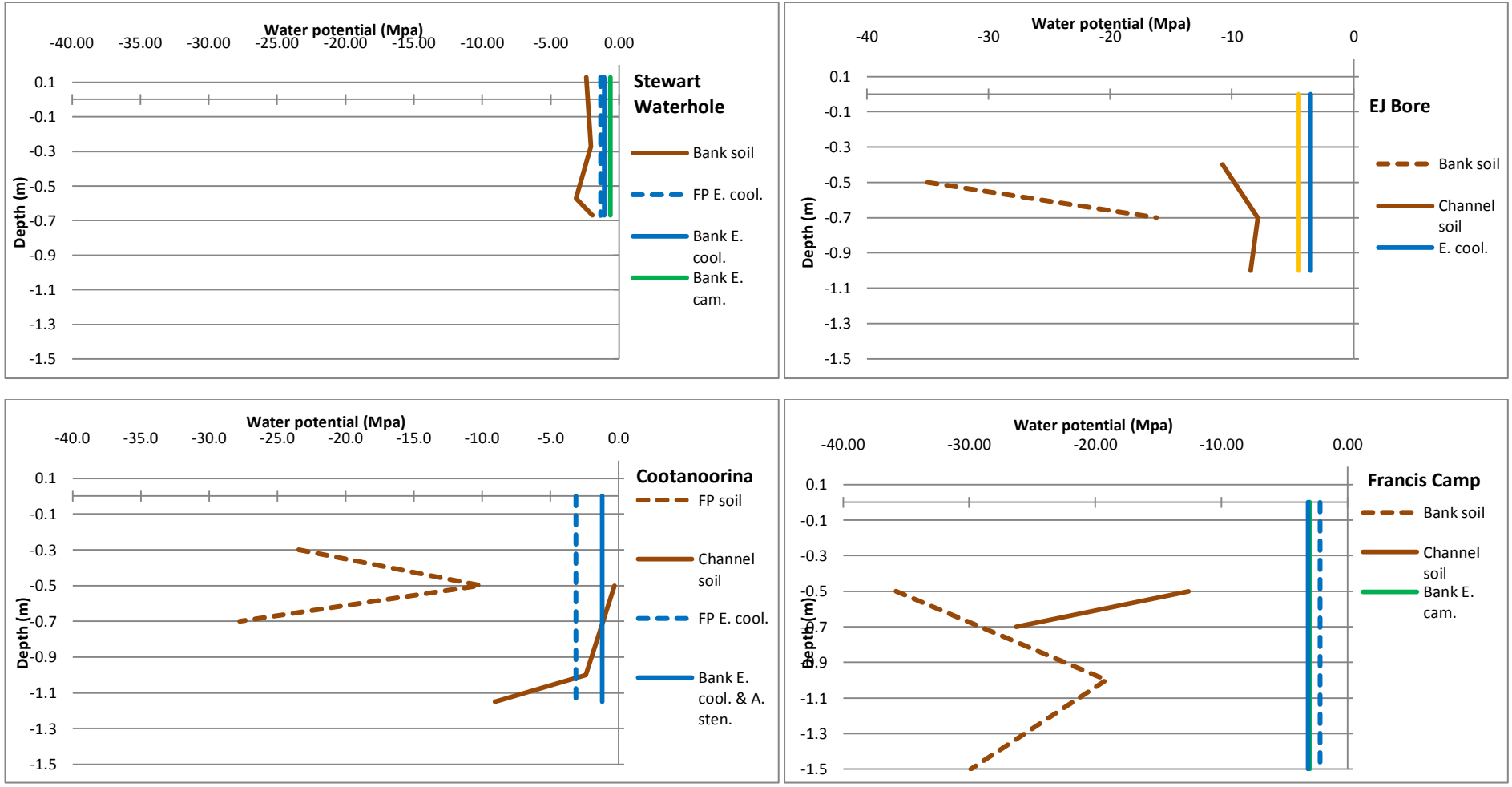

Figure 5-3: Soil matric potentials at measured depths and mean average pre-dawn leaf water potentials at four sites

Note: for sites Stewart Waterhole bank and Cootanoorina Waterhole channel the soil depth is relative to the surface water level (where water level = 0) and at all other sites it is relative to the soil surface: FP = floodplain, E. cam = *E. camaldulensis,* E. cool. = *E. coolabah*; A. cam. = *A. cambagei*, A. sten = *A. stenophylla;* tree water potentials are the mean average for a given species and location, with the mean for each tree calculated from one to three leaf measurements

At Cootanoorina Waterhole, the channel soil had much higher matric potentials than the floodplain soil sample (210 m away from the waterhole) except at the floodplain depth of 0.5 m, which had a similar matric potential to the channel sample at 1.15 m. Soil sampling at Arckaringa and Francis Camp occurred from the base of the channel and top of the bank. In these cases, the bank soil was drier (lower matric potential) than the channel soil profile. At Francis Camp, the trees growing below the elevation of the bank top (FCR2, FCR3, and FCC2) had higher pre-dawn LWPs than those growing on the bank top.

5.2.1.2 Leaf water potentials and tree health

The majority (77%) of trees were measured as being in healthy (≥90% canopy present) to moderately healthy (≥75%–89.99% canopy present) condition. Tree health did not show any correlation with pre-dawn LWPs (Figure 5-4). Two *E. camaldulensis* that were recorded as having the poorest tree health had the highest and third highest pre-dawn LWPs. These trees were located on the channel bank of Stewart Waterhole and may experience wider fluctuations in soil water availability if relying on bank storage (due to fluctuations in surface water levels) which could account for their poorer health.

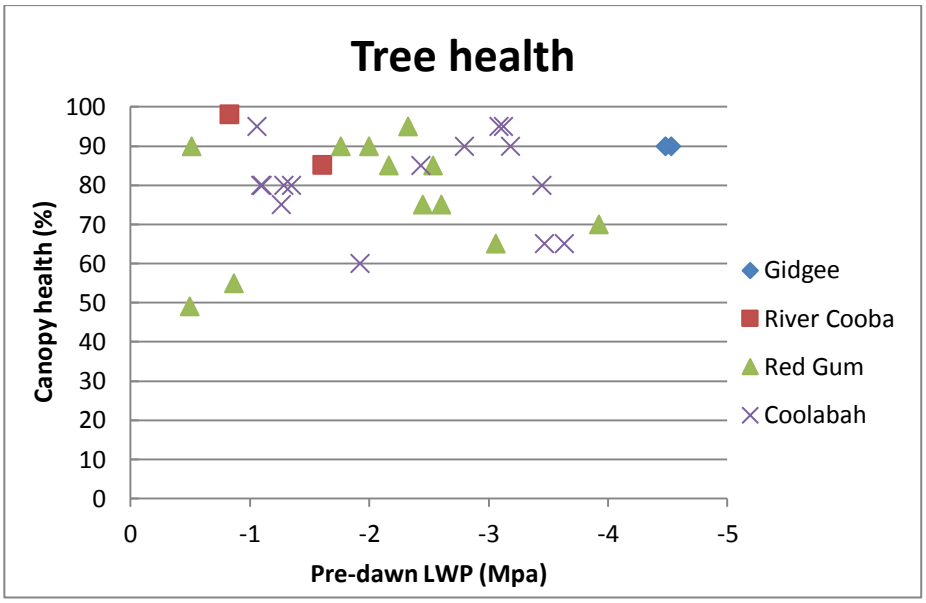

Figure 5-4: Tree health (% canopy present) vs mean pre-dawn LWP for each tree

6 Sapflow – Method and results

6.1 Methodology

Eleven heat-pulse sapflow meters (SFM1, ICT International) were installed in the Neales River catchment at five sites in March 2015 (Figure 4-2). Four sites were located in the Arckaringa sub-catchment and supplemented data collected at another Arckaringa site in 2013–14. The fifth site was located on the Neales River and supplemented data collected from two other Neales sites in 2013–14. The sapflow meters were installed into a selection of *Eucalyptus coolabah, E. camaldulensis* and *Acacia cambagei* at five sites (Table 4-1, Figure 4-2). Mature trees in relatively good health were chosen for the instrumentation. The instruments were installed between 0.5–1.5 m above the ground and on the southern side of the main stem of the tree. Although, the results from previous studies (e.g. Costelloe 2014; Costelloe 2015) suggest that circumferential variations in sapflow rates are significant, only a single meter was installed in each tree to maximize the number of sites.

The sapflow loggers comprised eight newly purchased units from DEWNR and three undamaged, functioning units from the Finke flood out site (The University of Melbourne) (Figure 4-2).

Data on riparian tree sapflow fluxes were first collected in the Neales River catchment between May 2013 and August 2014 and these results are reported in Ryu et al. (2014) and Costelloe (2014). During 2014–15, data were also collected from *E. coolabah* located in the Finke River flood out near the South Australian and Northern Territory border (Costelloe 2015) and from the South Australian reaches of the Diamantina River (latter as part of an unrelated project). The purpose of these field campaigns was to measure baseline data on riparian-floodplain tree transpiration rates in arid zone river reaches. The data collected from these field campaigns is presented and discussed in this report.

This report describes the data extracted from the loggers for the period March–November 2015 in the Neales River catchment and analyses the results in the context of earlier studies of riparian tree transpiration patterns in the Neales, Finke and Diamantina River catchments.

The new monitoring sites were:

1. Stewart Waterhole: Sapflow loggers were installed into a mature *E. camaldulensis* located below the bank top (dominant position of *E. camaldulensis* at this location) and in a mature *E. coolabah* located on the floodplain near the channel.
2. Cootanoorina Waterhole: sapflow loggers were installed into two mature *E. coolabah* located on the floodplain within a couple of hundred metres of the waterhole.
3. EJ Bore (Arckaringa Creek) sapflow loggers were installed into a mature *E. coolabah* located on the bank top of one of the larger channels (dominant position of *E. coolabah* at this location) and in a mature *A. cambagei* (gidgee) located immediately next to the *E. coolabah* and underneath its canopy (a common position for *A. cambagei* in this reach).
4. Francis Camp (Arckaringa Creek): sapflow loggers were installed into a mature *E. camaldulensis* located below the bank top (dominant position of *E. camaldulensis* at this location) and in a mature *E. coolabah* located on the bank-top and a second mature *E. coolabah* on the floodplain near the channel.
5. Wintinna Homestead: sapflow loggers were installed into a very large E. *camaldulensis* and a second smaller *E. camaldulensis* located near the edge of the channel.

6.1.1 Sapflow data collection

Raw temperature data ('Needle Temperature Mode') were recorded at a 30-minute time-step using a 30 J heat pulse, at a rate of three measurements per second, and a duration of 600 measurements after each pulse. These raw temperature data were converted to daily sapflow velocities using ICT proprietary software (Sapflow Tool) and information from one to two cores collected per tree to determine sapwood characteristics. The key measurements of each instrumented trees (Table 6-2) were used to determine sapwood dimensions (e.g. circumference at the sapflow logger, bark thickness, sapwood thickness) and thermal diffusivity (e.g. sapwood wet and dry core weight and dimensions).

6.1.2 Analysis

Splitting of the raw data files into smaller 60-70 Mb files (approximate maximum size raw data file that the software could handle) using the Sapflow Tool (v1.5 beta 1) occurred before being individually processed. The choice of using the beta version of the Sapflow Tool avoided previous problems encountered using the 2015 version of this software that centred on large files causing the software to crash. ICT International recommended using the new beta version to solve this problem. Most files from the current project contained occasional extreme and erroneous data values that hindered visualisation of the data in the software. The Sapflow Tool provides a filter function that can potentially be used to remove extreme values (i.e. choose to remove temperatures >100 and <0 °C). This was attempted but the beta Sapflow Tool version became unstable when the filtered data was processed. Consequently, an alternative method of removing outlier data that uses daily means calculated from raw data before outlier removal was employed. When processing the raw data to daily mean sapflow fluxes, default Sensor properties were used with the exception of 'Wood properties' used where the measured values of tree circumference, bark thickness and sapwood thickness collected from field and core measurements (Table 6-2). In addition, the analysis requires an estimate of thermal diffusivity that required the advanced calculation option of the software. This required calculation of the mean data on sapwood core wet and dry weights and volume from the cores collected from each sampled tree (Table 6-2). Mean daily sapflow fluxes (volumes) are reported in $cm^3\ d^{-1}$ in the accompanying data file and as a per unit area measure (in units of $cm\ d^{-1}$ and $kg\ m^{-2}\ d^{-1}$) by dividing the tree sapflow flux by the sapwood area of the tree.

6.1.3 Study period

The sapflow loggers were installed in trees within the Neales River catchment in March 2015. During the period of operation, the Neales River received below average rainfall in most months (Appendix A). Only two periods of streamflow were recorded by DEWNR stage loggers in the catchment (at Stewart and Algebuckina Waterholes) with flow peaks on 15 June and 5 November at Algebuckina and 16 June and 6 November at Stewart. Both these flows were small and did not connect between upper and lower reaches.

6.1.4 Upscaling

Area–population data are required to convert sapflow fluxes to unit area evapotranspiration estimates. Quadrat data were collected in November 2015 and involved measuring the circumference of all target species within the quadrat (Table 6-1). Where trees were distributed with relative uniformity, 100 m x 100 m quadrats were measured, whereas at sites with thin riparian zones, 200 m x 50 m or 500 m x 20 m quadrats were measured with the long axis running parallel to the bank.

Table 6-3 shows the areal-scaled evapotranspiration (ET) results for each site. These estimates used the quadrat data to determine the mean tree size and the sapwood core measurements. The latter were used to calculate the mean sapwood area of the mean tree, which was multiplied by the number of trees to derive a total sapwood area for the quadrat for a given species. The total sapwood area was multiplied by the mean sapflow flux per unit area to derive a total sapflow flux for the quadrant. This was then divided by the quadrat area to define an areal annual ET rate.

Table 6-1: Details of tree quadrats from Neales River sites

Site	Quadrat (species*)	Quadrat size (m)	No. stems	Mean circum. (m)	Sum tree area (m^2)	Sum sapwood (m^2)
Stewart WH	1 (r)	500x20	79	0.725	3.30	0.74
Stewart WH	1 (c)	500x20	88	0.753	3.97	1.26
Francis Camp WH	1 (r)	200x50	28	0.964	2.07	0.53
Francis Camp WH	1 (c)	200x50	120	0.925	8.16	2.01
Francis Camp WH	2 (c)	100x100	9	1.496	1.60	0.27
EJ Bore	1 (c)	100x100	6	1.560	1.16	0.20
EJ Bore	1 (a)	100x100	318	0.435	4.79	1.28
Cootanoorina WH	1 (c)	100x100	31	0.829	1.69	0.41
Cootanoorina WH	2 (c)	100x100	36	0.971	2.70	0.58
Wintinna Homestead	1 (r)	100x100	148	0.870	8.92	2.57
Wintinna Homestead	2 (r)	100x100	208	0.602	6.00	2.11

* species (c – *E. coolabah*, r – *E. camaldulensis*, a – *A. cambagei*), WH - waterhole

6.2 Results

Table 6-1 presents the quadrat results to provide an indication of the composition and density of trees at each site. Additionally, Table 6-3 presents the sapflow results. Results are first presented in summary, general behaviour of the different monitored species are then analysed before being discussed in terms of previous sapflow data collected in the Neales, Finke and Diamantina catchments.

Table 6-2: Details of trees instrumented with sapflow loggers within Neales River catchment in March 2015

Species	Name	Instrument	Location	Latitude	Longitude	Mean bark thickness (m)	Mean sapwood thickness (m)	Sapwood area (cm^2)	Wet sapwood (g)	Dry sapwood (g)	Wet diam. (m)	Sapwood volume
E. camaldulensis	Stewart red gum	SFM1F20P	Stewart Waterhole	-27.68368	135.38335	0.014	0.016	255.0	0.285	0.18	0.0055	0.36162
E. coolabah	Stewart coolabah	SFM1D102	Stewart Waterhole	-27.68413	135.38350	0.013	0.024	286.1	0.41	0.32	0.0054	0.52798
E. coolabah	Coot. coolabah 1	SFM1F10A	Cootanoorina Waterhole	-28.17518	135.31042	0.016	0.017	187.7	0.34	0.26	0.0053	0.36913
E. coolabah	Coot. coolabah 2	SFM1D10G	Cootanoorina Waterhole	-28.17515	135.31052	0.011	0.022	215.7	0.43	0.34	0.0053	0.47433
E. coolabah	Upper Arck. coolabah	SFM1F20B	EJ bore	-27.80297	134.65477	0.020	0.024	575.9	0.535	0.405	0.0054	0.53935
A. cambagei	Upper Arck. acacia	SFM1D10Q	EJ bore	-27.80297	134.65477	0.010	0.012	50.3	0.255	0.195	0.0054	0.26707
E. camaldulensis	Francis red gum	SFM1F20M	Francis Camp Waterhole	-27.72833	134.54422	0.016	0.024	313.0	0.475	0.325	0.0054	0.55767
E. coolabah	Francis coolabah 1	SFM1F20I	Francis Camp Waterhole	-27.72832	134.54413	0.020	0.023	313.6	0.47	0.35	0.0053	0.49749
E. coolabah	Francis coolabah 2	SFM1EC02	Francis Camp Waterhole	-27.72768	134.54433	0.033	0.019	303.3	0.28	0.255	0.0053	0.41191
E. camaldulensis	Wintinna red gum 1	SFM1F20I	Wintinna Creek near homestead	-27.71418	134.11903	0.025	0.018	633.5	0.315	0.215	0.0054	0.39403
E. camaldulensis	Wintinna red gum 2	SFM1F209	Wintinna Creek near homestead	-27.71410	134.11898	0.020	0.036	366.6	0.72	0.455	0.0053	0.78430

6.2.1 Scaled evapotranspiration results

The quadrat data (Table 6-1**Error! Reference source not found.**) illustrate the pattern of assemblage composition escribed in Table 4-5

These annual rates varied from 2–58 mm (Table 6-3) and were significantly less than the median annual rainfall over the catchment (Oodnadatta 147 mm, Bureau of Meteorology).

Table 6-3: Summary of mean per unit area sapflow-fluxes and leaf water potential from Neales River sites

Species	Position	Site	Mean daily unit area sapflow (kg m^{-2} d^{-1})	Annual ET rate over quadrat (mm)	Pre-dawn potential (MPa)	Midday potential (MPa)
E. camaldulensis	Bank	Stewart WH	730.6	28	-0.87	-2.45
E. coolabah	Floodplain	Stewart WH	178.5	28	-1.35	-3.13
E. coolabah	Floodplain 1	Cootanoorina WH	133.4	7	-3.09	-3.69
E. coolabah	Floodplain 2	Cootanoorina WH	800.7	10	-3.12	-3.45
E. coolabah	Bank top	EJ bore	-798.6	NA	-3.63	-4.1
A. cambagei	Bank top	EJ bore	-90.5	NA	-4.53	-4.73
E. camaldulensis	Bank	Francis Camp WH	127.6	12	-3.93	-4.2
E. coolabah	Bank top	Francis Camp WH	130.5	12	-3.47	-3.54
E. coolabah	Floodplain	Francis Camp WH	177.7	2	-2.43	-2.95
E. camaldulensis	Bank/channel 1	Wintinna HS	629.5	39	-2.17	-2.72
E. camaldulensis	Bank/channel 2	Wintinna HS	211.1	32	-2.33	-3.23

6.2.2 Sites

6.2.2.1 Stewart Waterhole results

The Stewart Waterhole sapflow loggers were only operational between June–August (*E. coolabah*) and March–September (*E. camaldulensis*) and showed significantly different mean sapflow rates per unit area. The *E. camaldulensis*, located just below the bank top, had a mean unit area sapflow of 728 kg m^{-2} d^{-1} compared to the *E. coolabah* located on the floodplain near the bank top with a mean unit area sapflow of 175 kg m^{-2} d^{-1}. The loggers were operational during the June 2015 flow event but did not show any response to this streamflow (Figure 6-1, Figure 6-2).

The two instrumented Stewart Waterhole trees showed the highest pre-dawn leaf potentials (-0.87 to -1.35 MPa) of all the trees surveyed and this is consistent with the trees accessing water from a readily available source (e.g. groundwater or bank storage supplied by water in the waterhole). The depth to groundwater is relatively shallow in this area, based on the occurrence of saline seeps of water entering the upstream end of the waterhole during a period of no flow in March 2002. However, the waterhole does dry out (e.g. observed in May 2013) suggesting that the water table must fluctuate enough to drop below the base of the waterhole during extended dry periods.

6.2.2.2 Wintinna Homestead results

The Wintinna loggers placed in *E. camaldulensis* were the most-upstream location of the logger sites. The loggers were operational from March to November 2015. Loggers were placed into a large mature tree and a younger tree on the edges of the Wintinna Creek channel system. The mature *E. camaldulensis* had a mean unit area sapflow of 630 kg m^{-2} d^{-1} compared to the younger *E. camaldulensis* with a mean sapflow of 211 kg m^{-2} d^{-1}. The younger tree showed greater fluctuations in daily sapflow but neither tree showed any response to a small streamflow event reported to occur in mid-2015 (F Lumb (Wintinna Station) 2015, pers. comm. November) (Figure 6-2). No streamflow occurred in the upper Arckaringa catchment in November 2015.

6.2.2.3 Francis Camp Waterhole results

The Francis Camp Waterhole is an ephemeral waterhole with a mix of *E. camaldulensis* and *E. coolabah* at bank top positions and *E. coolabah* in floodplain positions. Outer channels along the floodplain contained largely *acacia spp.* Three loggers were installed at this site; in bank top *E. camaldulensis* and *E. coolabah* and a floodplain *E. coolabah*. The loggers were operational from March to November 2015, except for the bank top *E. coolabah* (March to September 2015). The *E. camaldulensis* had a mean unit area sapflow of 128 kg m^{-2} d^{-1} while the bank top *E. coolabah* had a mean sapflow of 131 kg m^{-2} d^{-1} and the floodplain *E. coolabah* had a mean sapflow of 178 kg m^{-2} d^{-1}. The similarity in mean unit area sapflow-results for the bank top trees suggests that both species have similar transpiration rates when located in very similar morphological positions. The slightly higher sapflow rates of the floodplain *E. coolabah* possibly indicate a more abundant water source. The floodplain *E. coolabah* also showed a possible seasonal variation in sapflow fluxes, with the March and November fluxes being up to 30% greater than the winter sapflow fluxes. A seasonal signal is consistent with the trees having transpiration that is energy constrained rather than water constrained and would indicate a relatively stable and abundant water sources (either groundwater or deep soil water).

6.2.2.4 EJ Bore results

This location is approximately midway between Francis Camp Waterhole and Arckaringa homestead. The reach is *acacia spp.* -dominant with scattered mature *E. coolabah* growing beside shallow channels. A logger was installed in a mature *E. coolabah* and in an *A. cambagei* located next to, and under the canopy of, the instrumented *E. coolabah*. Both trees returned negative sapflow fluxes. The *E. coolabah* had a mean unit area sapflow of -799 kg m^{-2} d^{-1} while the *A. cambagei* had a mean unit area sapflow of -91 kg m^{-2} d^{-1}. This suggests either the logger needles were installed in the reverse order or that the trees were experiencing hydraulic lift (i.e. bringing soil water up from deeper levels and depositing it at shallower soil levels). In the latter case, the loggers may only be measuring sapflow from part of the root system implying that different sides of the tree connect to different parts of the root system. Given the extremely close proximity of the two trees (a common occurrence in this reach), the similarity in their flux direction is not surprising. The low sapflow rate of the *A. cambagei* was lower than data from other *Acacia spp.* measured at the Kempe Road site on Arckaringa Creek during 2013–14, which had mean unit area sapflows of 168-275 kg m^{-2} d^{-1}.

Both trees at this site exhibited a large negative response on 30 May (Figure 6-1), particularly the *A. cambagei*, and this is likely in response to rainfall and possible streamflow, as Mt Barry homestead measured 36 mm of rainfall on 29-30 May.

Similar to Francis Camp Waterhole, the soils at this site presented highly negative soil matrix potential values (< -7 MPa) indicating very dry conditions in the bank top position (up to 0.7 m depth) and in the channel (up to 1 m depth). These dry conditions are indicative of gravelly, free draining soils in combination with dry conditions in the preceding months (e.g. Mt Barry only measured 16 mm of rainfall from June to November).

6.2.2.5 Cootanoorina Waterhole results

Sapflow loggers were placed into two mature floodplain *E. coolabah* within a few hundred metres of Cootanoorina Waterhole. The two trees were of similar size and within 10–20 m of each other but showed quite different sapflow results (Figure 6-1). One had a mean unit area sapflow of 133 kg m^{-2} d^{-1} and low variability (very similar to the Francis Camp bank *E. coolabah*) while the second tree had a high and variable mean unit area sapflow of 801 kg m^{-2} d^{-1}. Both trees had similar leaf water potential results and so the differing sapflow results are surprising. The *E. coolabah* with the high sapflow rates also showed large reductions in rates coincident with most rainfall events in the study period. This could be either due to effects of rainfall on the sapflow logger or due to the tree briefly switching to shallow roots to take advantage of increased near surface soil moisture. The latter reason would imply that the high sapflow fluxes are from deeper roots accessing deeper soil moisture.

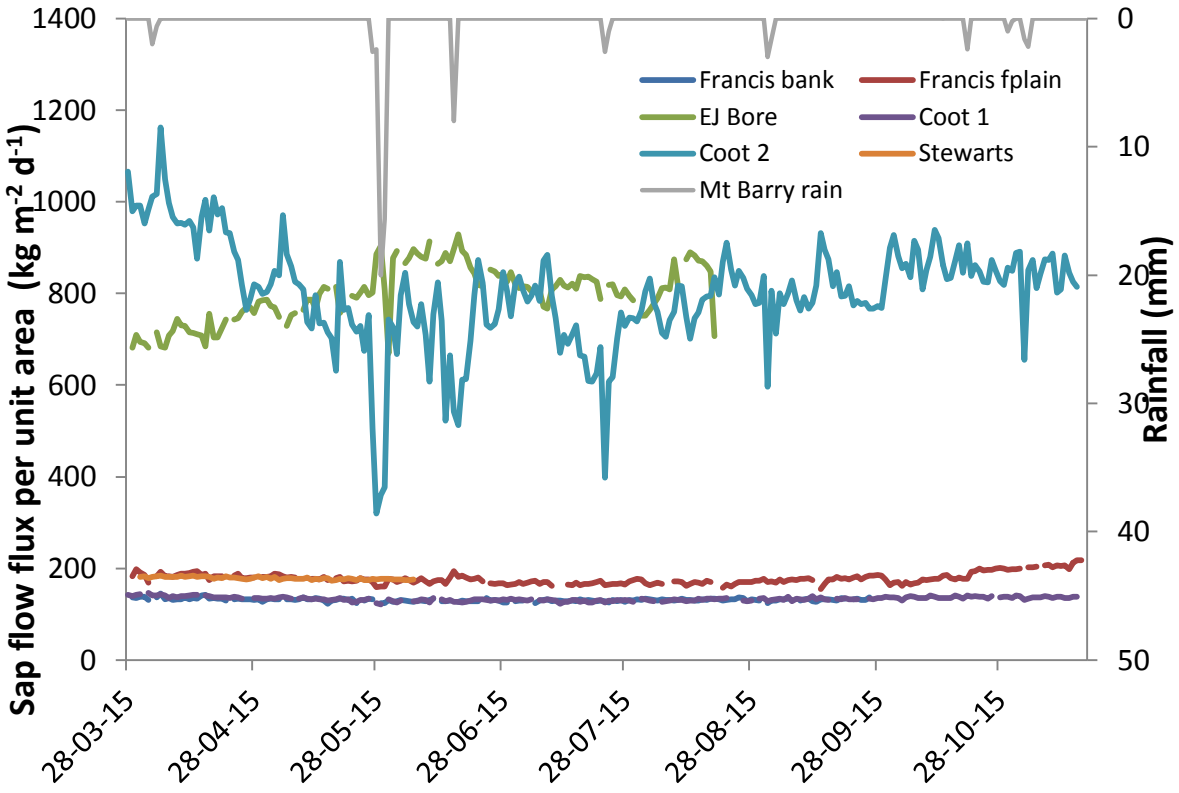

Figure 6-1: Mean per unit area sapflow fluxes for instrumented *E. coolabah* in the Neales River catchment, 2015

The auger hole between the trees intersected very dry soils in the top 0.7 m (<-10 MPa, Figure 5-3) and Bulldog Shale at approximately 1 m. The shallow depth to Bulldog Shale may explain the differences in sapflow between the trees as water availability in the Bulldog Shale may be very patchy (i.e. associated with heterogeneous fracture or weathering zones). Alternatively, the may find it difficult to extract water and there may be high circumferential variability due to different areas of the root system having varying access to soil moisture. Notably, a *E. coolabah* located downstream of Cootanoorina Waterhole, on the broad floodplain of Peake Creek had a brief three day record from 2013 (before logger damage by dingos) with relatively high sapflow results (mean of 358 kg m^{-2} d^{-1}) in an area known to have shallow depths to the Bulldog Shale (i.e. within 1 m).

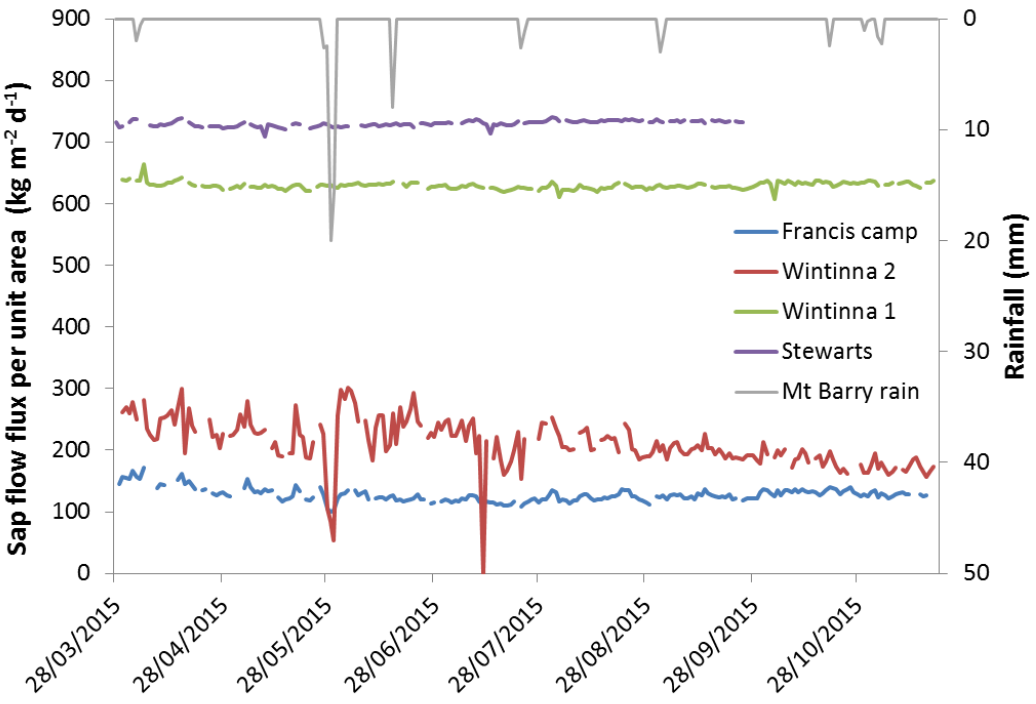

Figure 6-2: Sapflow results (per unit area of sapwood) for E. *camaldulensis* trees in the Neales River catchment.

6.2.3 Comparison to previous sapflow results

On a per unit area of sapwood basis, the results of the Neales River sites in 2015 were consistent with previous sapflow data collected in the Neales, Finke and Diamantina catchments (author's unpublished data) (Figure 6-3). However the results are also significantly lower than data from riparian/floodplain eucalypts reported by O'Grady et al. (2009) from the Ti-Tree Basin (200 km north of Alice Springs). O'Grady et al. (2009) reported on results from two short field campaigns (April and November) conducted on *E. vitrix* (closely related to *E. coolabah*) and *E. camaldulensis* that had access to groundwater (<7 m depth). The sapflow flux per unit area for *E. camaldulensis* in the Ti Tree Basin study were in the range of 4000–5000 kg m^{-2} d^{-1} while *E. vitrix* recorded rates between 2000–3000 kg m^{-2} d^{-1}. The *E. coolabah* measured in the Finke and Diamantina River sites (author's unpublished data) tended to have higher mean sapflow rates than observed in the Neales River catchment, although these sites experienced more substantial flow events during their instrumented periods.

The response of the Neales River catchment trees to rainfall and possible streamflow (see Figure 6-1 and Figure 6-2) was more subdued than shown by *E. coolabah* in the Finke and Diamantina catchments (Figure 6-3). The Finke River catchment trees typically showed a substantial response to the large flood event of January 2015 (inferred from rainfall data) that resulted in widespread inundation in the study site (Finke Flood out). The Diamantina *E. coolabah* sites were located between Birdsville and Goyder Lagoon and showed significant responses to sub-bank full flows in 2015. The timing of the responses was somewhat delayed relative to the onset of streamflow and suggests that the peak tree response was coincident with shallow groundwater recharge from the channel flow. In contrast, none of the monitored trees in the Neales catchment in 2015 displayed a clear response to streamflow events. The different Neales sites monitored in 2014 also only showed very modest responses to small sub-bank full flows. For instance, rainfall and sporadic streamflow events in February 2014 and a modest increase in sapflow within the *E. coolabah* from the hypersaline zone in the mid-Neales (Costelloe 2011) appeared to correlate. The Arckaringa Creek site did not experience streamflow in February 2014 but the *E. coolabah* displayed short-term decreases in sapflow following rainfall in February and April 2014. This response may be due to activation of shallower parts of the root system utilising the increases in near surface moisture following rainfall.

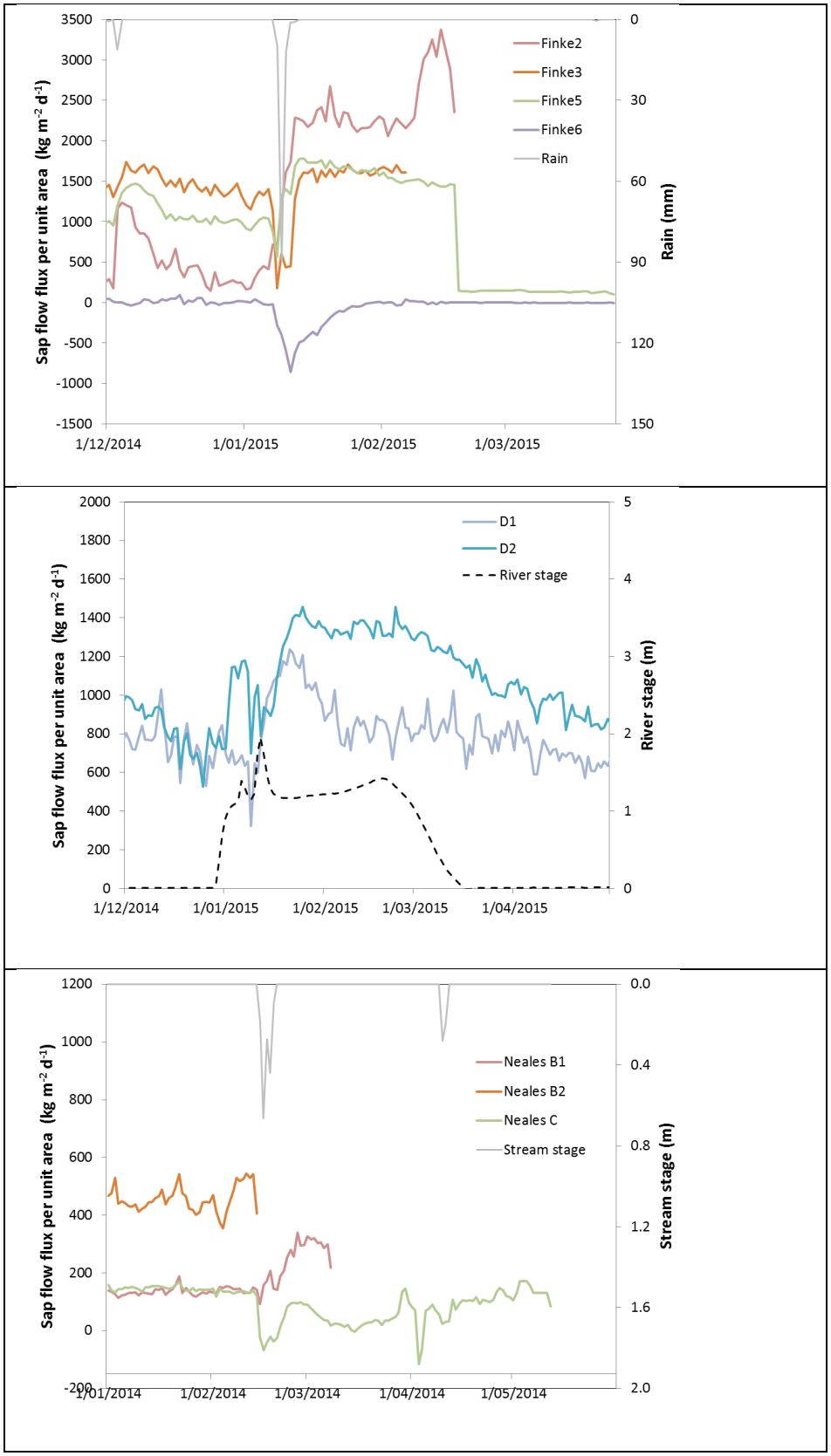

Figure 6-3: Daily sapflow flux per unit area for four *Eucalyptus coolabah* treesfrom previous studies in the Finke River flood out (top), Diamantina River catchment (middle) and Neales River catchment (bottom). Note different scales on the x and y axes.

7 Remote sensing GDE Index

7.1 Datasets and pre-processing

7.1.1 Study area

The study area is defined using an ESRI© ArcMap™ shapefile comprised the catchments of the Macumba River, Neales River and Warriner / Margaret Creek (Figure 7-1) totaling approximately 105 300 km^2.

7.1.2 AWAP daily precipitation data

The Australian Water Availability Program (AWAP) daily precipitation data were downloaded from the Bureau of Meteorology website from 1 January 1998 to 30 June 2015 (BOM, 2015a). This consists of a raster surface, for all of Australia each day (6390 rasters), of rainfall totals (mm) interpolated from the Bureau of Meteorology's station data using robust topography-resolving analysis methods at a resolution of 0.05° × 0.05° (approximately 5 km × 5 km) (Jones et al. 2009).

To reduce processing time of subsequent steps, pixels outside the study area were masked out (see example in Figure 7-2). The spatial reference properties of the data were changed to the projection of the NDVI data (from Geographic Coordinate System GCS_GDA_1994 to Projected Coordinate System GDA_1994_South_Australia_Lambert).

As there are relatively few rainfall stations within or in close proximity to the study area (Figure 7-2 inset), and some were not in use during all of the study period, there are occasional gaps in the data (i.e. pixels = NoData). These occur from 2008 onwards, particularly along the northeast edge of the study area.

To examine the extent of this issue, zonal statistics for each rainfall raster were calculated (area, min, max, range, mean and STD). Seventy percent of the rasters had no missing data (i.e. area = total size of the study area). The raster with the largest area of missing data was for 28 March 2014, with 55% of the pixels NoData. Of those rasters with missing data, 60% had a maximum value of 0 mm (i.e. no rain recorded in any of the other pixels), 13% had a maximum value over 5 mm and 2% had a maximum value over 25 mm. To prevent the analysis being limited by the NoData values, the NoData values were changed to the mean value of the other pixels for each raster.

Some rain (5.2 mm at Oodnadatta and 2.6 mm at Coober Pedy) fell a fortnight prior to the November sampling, however it was a very dry year leading up to the sampling. The mean daily rainfall for the study area is graphed in Appendix A.

7.1.3 MODIS NDVI data

This research used the NDVI data from the MODIS sensor. The MODIS instrument records data in 36 spectral bands ranging from 0.4 µm to 14.4 µm and in spatial resolutions ranging from 250 m to 1 km. The Terra and Aqua polar-orbiting satellites each carry a MODIS instrument and together image the entire Earth surface every 1 to 2 days. In addition to supplying the raw reflectance data, NASA produces several highly validated image products from MODIS data, including the MOD13Q1 vegetation indices product.

The Normalised Difference Vegetation Index (NDVI) is a useful tool for monitoring vegetation growth and death cycles (greenness and vigour). The NDVI is based on the contrast between the red (R) and near infra-red (NIR) reflectance. There is a large difference in R and NIR reflectance for photosynthesizing green vegetation, and a small difference for other cover types. The index is formulated so that strongly growing vegetation produces high NDVI values, up to 0.8, and dead vegetation or exposed dry soil produce lower NDVI values, approximately 0.1 to 0.2.

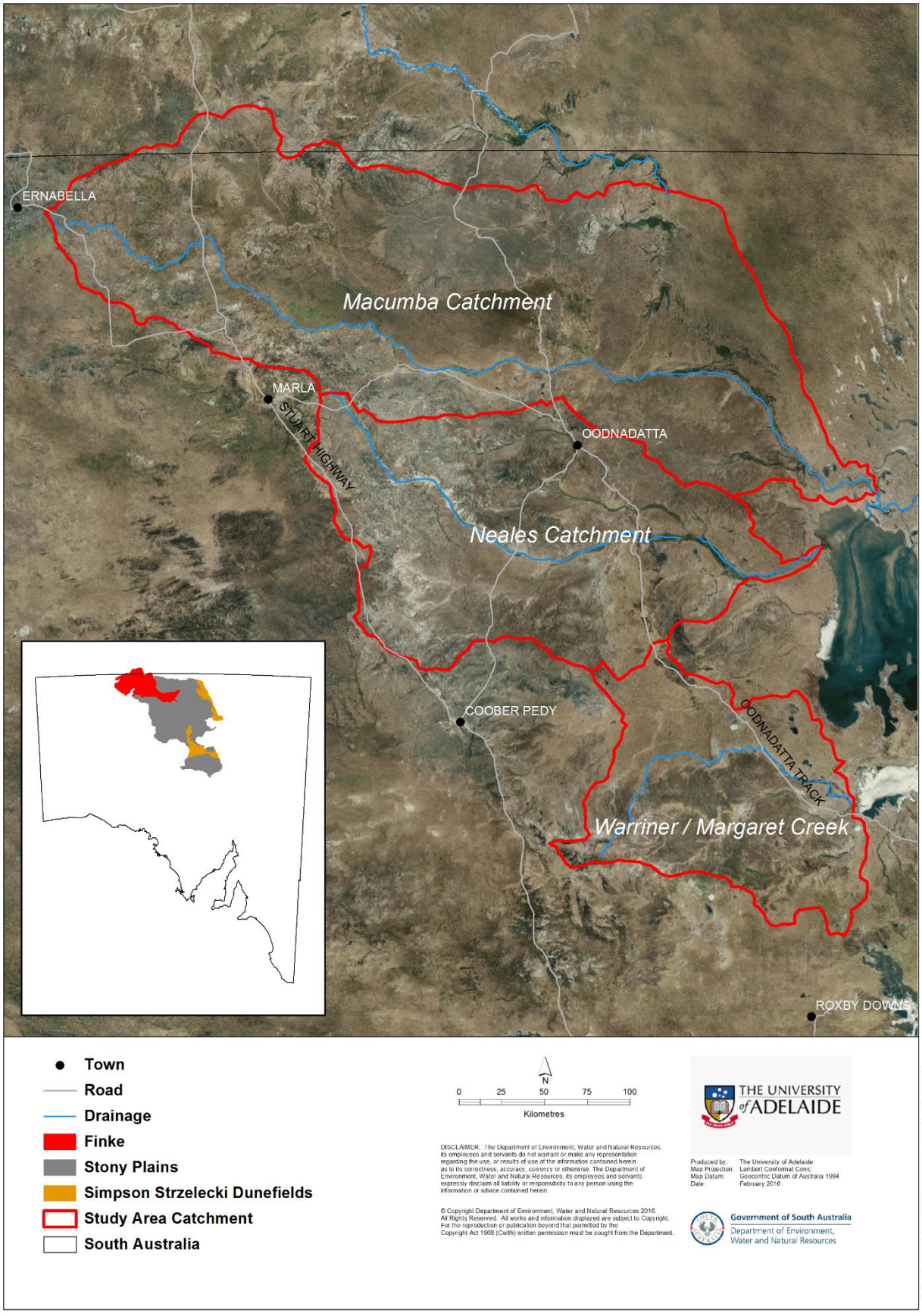

Figure 7-1: GDE Index study area

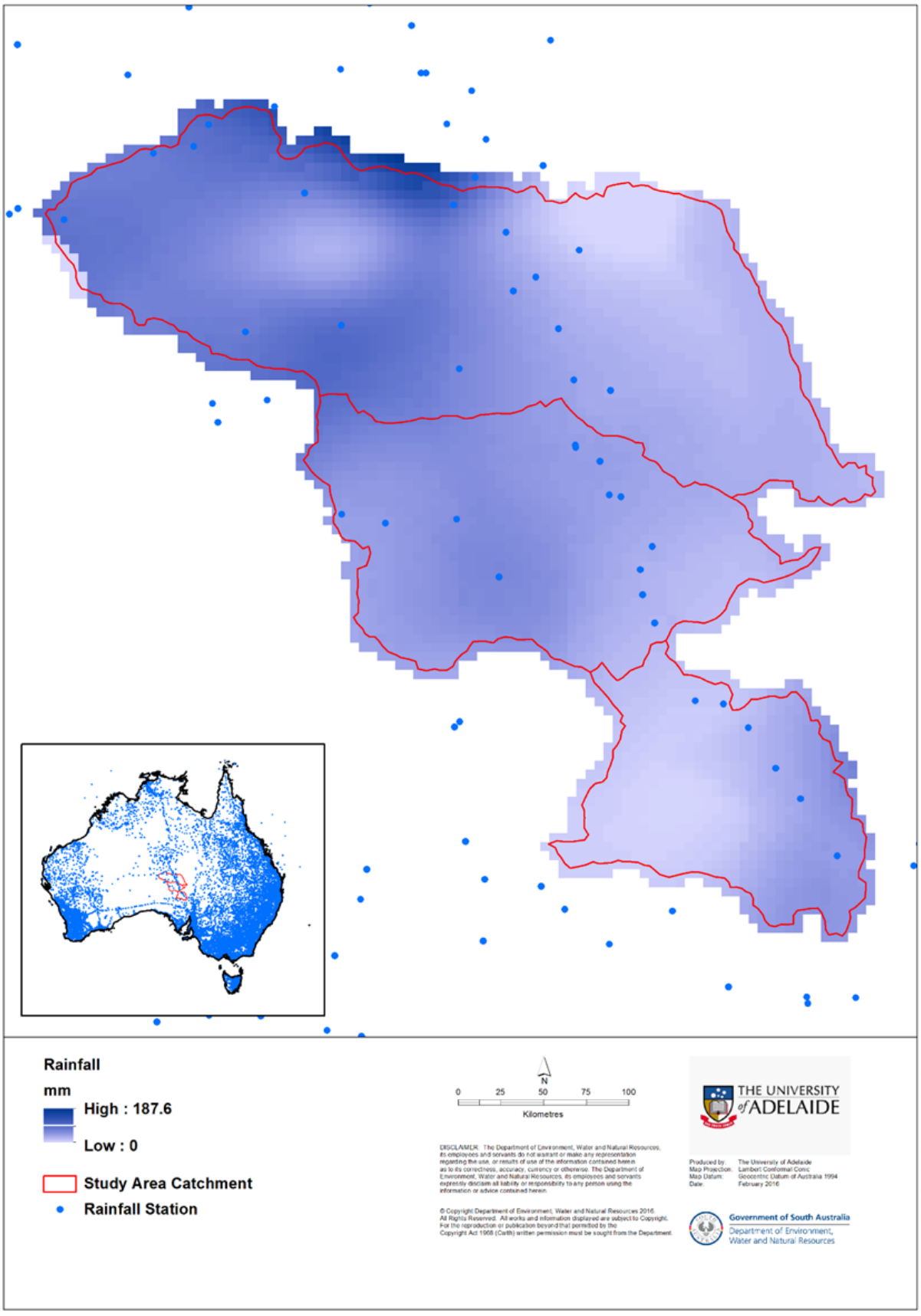

Figure 7-2: Example of an AWAP daily rainfall raster for the study area (11 February 2000)

This project used the MODIS MOD13Q1 version 005 NDVI product, which is available at 250 m resolution once every 16 days. The MOD13Q1 NDVI (henceforth referred to as MODIS NDVI) is a cloud-free composite product created from all MODIS images over a given area within a 16 day period, and prioritising retention of image elements (pixels) with no cloud-contamination and near to nadir (looking directly down) view angle.

Complete temporal coverage of MOD13Q1 NDVI was acquired from the start of the MODIS archive (18 February 2000) to 25 June 2015. In total 353 MOD13Q1 image dates were acquired and analysed in this project. The first date of each image composite, the 'image start day' is presented in Table 7-1.

Four MODIS scenes were required to cover the study area. Prior to analysis, all four scenes for each image date were mosaicked into 353 single images covering the whole study area. Due to the wide swath of MODIS, these mosaicked images covered much of Australia. To reduce processing time of future steps, pixels outside the study area were masked out (see example in Figure 7-3).

The mean NDVI for the study area for each composite is graphed in Appendix A.

Table 7-1: Image start day for all MODIS MOD13Q1 NDVI image composites analysed in this project

Image start day	Approx. date*	Year															
		00	01	02	03	04	05	06	07	08	09	10	11	12	13	14	15
1	1 Jan		x	x	x	x	x	x	x	x	x	x	x	x	x	x	x
17	17 Jan		x	x	x	x	x	x	x	x	x	x	x	x	x	x	x
33	2 Feb		x	x	x	x	x	x	x	x	x	x	x	x	x	x	x
49	18 Feb	x	x	x	x	x	x	x	x	x	x	x	x	x	x	x	x
65	6 Mar	x	x	x	x	x	x	x	x	x	x	x	x	x	x	x	x
81	22 Mar	x	x	x	x	x	x	x	x	x	x	x	x	x	x	x	x
97	7 Apr	x	x	x	x	x	x	x	x	x	x	x	x	x	x	x	x
113	23 Apr	x	x	x	x	x	x	x	x	x	x	x	x	x	x	x	x
129	9 May	x	x	x	x	x	x	x	x	x	x	x	x	x	x	x	x
145	25 May	x	x	x	x	x	x	x	x	x	x	x	x	x	x	x	x
161	10 Jun	x	x	x	x	x	x	x	x	x	x	x	x	x	x	x	x
177	26 Jun	x	x	x	x	x	x	x	x	x	x	x	x	x	x	x	
193	12 Jul	x	x	x	x	x	x	x	x	x	x	x	x	x	x	x	
209	28 Jul	x	x	x	x	x	x	x	x	x	x	x	x	x	x	x	
225	13 Aug	x	x	x	x	x	x	x	x	x	x	x	x	x	x	x	
241	29 Aug	x	x	x	x	x	x	x	x	x	x	x	x	x	x	x	
257	14 Sep	x	x	x	x	x	x	x	x	x	x	x	x	x	x	x	
273	30 Sep	x	x	x	x	x	x	x	x	x	x	x	x	x	x	x	
289	16 Oct	x	x	x	x	x	x	x	x	x	x	x	x	x	x	x	
305	1 Nov	x	x	x	x	x	x	x	x	x	x	x	x	x	x	x	
321	17 Nov	x	x	x	x	x	x	x	x	x	x	x	x	x	x	x	
337	3 Dec	x	x	x	x	x	x	x	x	x	x	x	x	x	x	x	
353	19 Dec	x	x	x	x	x	x	x	x	x	x	x	x	x	x	x	

*Image start date is listed as approximate to allow for the effect of leap years on post 29 February image start days

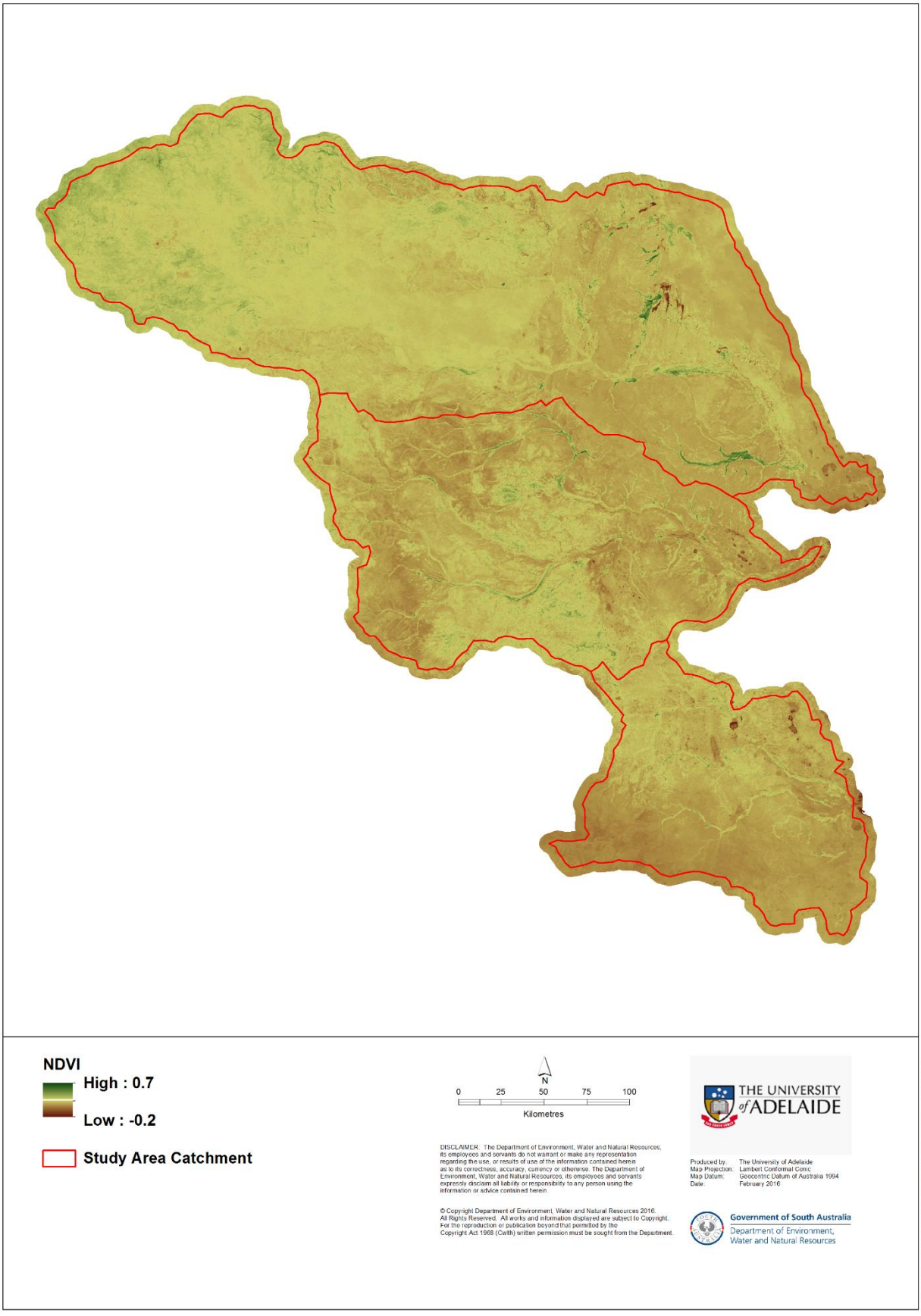

Figure 7-3: Example of a MODIS 16-day NDVI composite raster for the study area (18 February to 5 March 2000)

7.1.4 GDE Atlas of Australia data

The National Atlas of Groundwater Dependent Ecosystems (GDE Atlas) presents the current knowledge of groundwater dependent ecosystems across Australia. The Atlas was funded by the Australian Government through the National Water Commission's Raising National Water Standards Program. It was developed by the National Water Commission, SKM, CSIRO and the Bureau of Meteorology with input from every State and Territory as part of the Groundwater Action Plan (SKM, 2012).

It displays ecological and hydrogeological information on known groundwater dependent ecosystems and ecosystems that potentially use groundwater. The primary outputs of the GDE Atlas are a map of GDEs that rely on the subsurface presence of groundwater (vegetation), and a map of GDEs that rely on the surface expression of groundwater (springs and groundwater dependent rivers and wetlands).

The following shapefiles (a surface and subsurface file for each area), part or all of which fall within our study area, were downloaded from the Bureau of Meteorology's Atlas of Groundwater Dependent Ecosystems web site (BOM, 2015 b), merged into a surface and subsurface layer and clipped to the study area for a qualitative comparison with our GDE Index Tool outputs:

- Finke River
- Lake Frome
- Diamantina River
- Warburton

7.1.5 Field data

The shapefile of leaf water potential monitoring sites and the eastings and northings resulting from the water quality field survey (Section 5) were used to form a spatial link to the GDE Index data. GDE values were extracted for each well and tree location.

7.1.6 Water Observations from Space

Released in late 2014, Geoscience Australia's *Water Observations from Space* (WOfS) is the world's first continent-scale product of the presence of surface water derived from Landsat satellite imagery. WOfS covers the entire Australian continent at 25 m spatial resolution, providing information through time-series analysis (1987 to present) on where water is usually seen, such as in lakes and rivers, and where it is unusual, such as during flooding events (Mueller et al. 2016).

With a revisit rate of 16 days (23 times per year) and some observations affected by cloud, shadow or other quality issues, not all historical floods will have been observed by satellite. The algorithm (LC25-Water) developed for WOfS is designed to locate large areas of water (in general at least four Landsat pixels, i.e. approximately 50 m by 50 m or 0.25 ha), and as a result it may miss small water bodies (Mueller et al, 2016).

There are five summary composite datasets for all of Australia which are publically available online in map form (http://www.ga.gov.au/flood-study-web/#/search) through the Australian Flood Risk Information Portal:

1. Clear Observations – The number of times a pixel was successfully observed (i.e. not masked for clouds, shadows, etc.) over the period 1987 to present
2. Water Observations – The number of occasions on which water was detected over the period 1987 to present
3. Water Summary – The percentage of successful observations where a pixel was observed to be water (i.e. the ratio of Water Observations to Clear Observations as a percentage)
4. Confidence – The confidence (or probability) that a water observation in this location is correct. The Confidence Level assigned to each water observation is based on a statistical analysis of factors, including topographic position, elevation and slope, other independent satellite observations of water, topographic maps of water features, and the observation frequency. The confidence layer can be used to filter uncertain observations
5. Filtered Summary – The percentage of water observations filtered by confidence (the same data as Water Summary but with pixels with a confidence < 1 masked)

The Filtered Summary data was extracted for the study area.

7.2 GDE Index Tool methodology

7.2.1 GDE Index

The GDE Index depends on:

- Greenness threshold (derived from MODIS NDVI imagery), above which growth is considered likely to be reliant on access to water (either surface, soil or ground)
- Rainfall threshold within a defined short period, above which rainfall is considered to have been 'significant' enough to cause a green flush
- Dry-period duration, i.e. a period post significant rainfall after which soil moisture is expected to be depleted, and vegetation is expected to require access to groundwater to produce significant growth.

The GDE Index Tool is written in python script, using predominantly ArcGIS spatial analyst tools. All data are raster TIFFs. Before processing the user is prompted to enter the parameters to be used in that particular run or scenario:

- **NDVI_Threshold** (e.g. 0.2)
- **Rainfall_Days** - number of days of cumulative rainfall for a 'significant' rainfall event (e.g. 7)
- **Rainfall_Threshold** - cumulative rainfall (mm) threshold for a 'significant' rainfall event (e.g. 25)
- **Dry_Period** - dry period duration in days (e.g. 180)
- **Root_Directory -** the directory pathname where the data is stored (e.g. D:/MODIS_GDE_Index_in_LEB/Data)

The processing methodology is summarised in the following 10 steps (see Appendix B for more detail):

1. For each NDVI raster (353 rasters, i.e. one composite per 16 days).
   Is the NDVI pixel value >= the NDVI_ threshold? (e.g. is NDVI >= 0.2?)
   Yes = 1, No = 0. (1 = the greener pixels).
   Results in 353 output rasters (one per 16 days).

2. For each NDVI pixel location.
   How many times did the pixel location reach the NDVI_Threshold?
   Sum the outputs of Step 1.
   Results in one single output raster (**Number of green periods).**

3. For each rainfall raster (6,390 rasters, one per day).
   How much rain fell in the previous Rainfall_Days in each pixel location? (e.g. 7 days)
   E.g. Sum the rainfall rasters for the previous 7 days.
   Results in 6390 output rasters (one per day).

4. For each Step 3 raster (one per day).
   Is the Step 3 cumulative rainfall pixel >= Rainfall_Threshold? (e.g. >= 25 mm)
   Yes = 0 (i.e. a 'significant' rainfall event), No = 1. (1 = drier Rainfall_Days).
   Results in 6390 output rasters (one per day).

5. For each 16 day period (matching the NDVI composite dates).
   Were there any significant rainfall events either within the 16 days or in the preceding Dry_Period duration?
   For the range of dates in question, multiply the input rasters from Step 4.
   For each pixel location, if ANY raster value for these dates = 0 (i.e. a significant rainfall event) the output pixel will be 0, otherwise the result will be 1 (i.e. extended dry period).
   Results in 353 output rasters (one per 16 days).

6. For each Step 5 raster (one per 16 days).
   Resample the Step 5 data (5 km x 5 km cell size) to be the same cell size as the NDVI data (250 m x 250 m) and align (snap) to the NDVI data.
   Results in 353 output rasters (one per 16 days).

7. For each Step 6 pixel location.
   How many times was a pixel in an extended dry period (i.e. = 1)?
   Sum the outputs of Step 6.
   Results in one single output raster **(Number of dry periods)**.

8. For each 16 day composite period.
   I**s a pixel green and dry (i.e. persistent green)?**
   Yes (= 1) if Step 1 results = 1 (High NDVI) and Step 6 results = 1 (dry period); otherwise No (= 0).
   Results in 353 output rasters (one per 16 days).

9. For each Step 8 pixel location.
   How many times was a pixel persistent green?
   Sum the outputs from Step 8.
   Results in one single output raster. **(Number of dry and green periods).**

10. For each Step 9 pixel location.
    What percentage of times were the dry periods above the NDVI_Threshold?
    (Step 9 / Step 7) x 100.
    Results in one single output raster – The GDE Index for the parameters input (0 - 100%) **(GDE Index)**.

The index is calculated per pixel (i.e. for each image pixel in the study area); the design goal is to calculate the proportion of time the vegetation vigour (NDVI) of a pixel was due to access to groundwater, but not due to access to surface or soil water.

Frequent exceedance of the NDVI threshold value is deemed to be an indicator of vegetation permanency resulting from a ready access to water (either surface or ground) (Steps 1 and 2). Periods during which vegetation growth is due to 'significant' rainfall events are eliminated (Steps 3 to 8). The final GDE image index is an estimate of the proportion of time a given area exhibited vegetation vigour high enough that it was probably enabled by access to groundwater (Steps 7, 9 and 10).

In the example of parameters input above, the tool will calculate how often areas (individual pixel locations) have an NDVI value greater than 0.2 following 180 days (approximately 6 months) without a 'significant' rainfall event (defined as 25mm cumulative rainfall within any 7 day period). The GDE Index is expressed as the percentage of times a pixel remained above the NDVI threshold during extended dry periods. 0% = NDVI values were never above the NDVI threshold (0.2) in any extended dry period for that pixel; 100% = NDVI values were always above the NDVI threshold in every extended dry period. Outputs from Steps 2, 7, 9 and 10 of this scenario are presented in the results section.

7.2.2 Comparison with other datasets

7.2.2.1 GDE Atlas of Australia

An example of the final output from our GDE Index Tool was visually compared to the two GDE Atlas of Australia outputs; ecosystems that rely on the surface expression of groundwater (rivers, wetlands, springs) and ecosystems that rely on the subsurface presence of groundwater (vegetation).

7.2.2.2 Field data

The field data supplied was linked to the GDE Index data for visualisation and a short qualitative investigation. Time constraints did not allow a more quantitative or thorough investigation at this time.

7.2.2.3 Water Observations from Space

A brief examination of the Water Observations from Space Filtered Summary inundation data was undertaken for reference purposes.

7.3 Results

The GDE Index Tool allows the user to input any combination of parameters they wish to examine. This section presents the results of just one example of running the GDE Index Tool using a particular combination of parameters. A selection of other possible scenarios can be seen in Appendix C.

Next, a brief comparison of some field data with the GDE Index values for this scenario at the tree survey sites is undertaken. Finally, an evaluation of our GDE Index Tool outputs against the GDE Atlas of Australia (SKM, 2012) are presented.

7.3.1 The GDE Index

Examination of the daily rainfall data and temporal NDVI traces in Appendix A shows that during dry periods the mean NDVI for the study area as a whole is generally about 0.15. There is an obvious increase in NDVI post 'significant' rainfall, which peaks at 0.2 to 0.25 generally, then tapers off over the following 6 months if there are no other significant rainfall events.

Figure 7-4 shows the output from Step 2 of the GDE Index Tool. This is the number of times a pixel was above the NDVI threshold in the 353 NDVI composite images. In this case the threshold was set at 0.2. In approximately half of the study area the pixel values exceeded the threshold less than 35 times, and a further quarter of the area less than 100 times. It is worth noting that the Finke IBRA (Interim Biogeographic Regionalisation for Australia) in the northwest of the study area clearly has higher NDVI values in general than the rest of the study area, with some pixels above the 0.2 threshold in all 353 images (Figure 7-4). This is supported by Lawley et al. (2011) and Clarke et al. (2014). Figure C-1 in Appendix C shows the difference in Step 2 outputs between NDVI thresholds set at 0.2, 0.3 and 0.4.

An example of the output from Step 7, the number of dry periods, is displayed in Figure 7-5. This is the number of periods where there were no significant rainfall events within a defined period. For this example a 'significant' rainfall event was defined as 25 mm of rain falling within a 7 day period; the duration of a dry period was set at 180 days (6 months). Once again these parameters were chosen based on the data in Appendix A. The pixel values range from 28 dry periods to 205 dry periods (from a possible maximum of 353), with more dry periods generally in the south of the study area. Appendix C Figure C-2 also shows the output from Step 7 if the duration of the dry period is set to 120 days (4 months).

The number of times that an area was above the 0.2 NDVI threshold during dry periods (no significant rainfall events with 180 days) can be seen in Figure 7-6 (Step 9 output). The majority of higher values are in the Finke IBRA. The largest value is 179 periods (out of the possible 353). Outputs for 0.3 and 0.4 NDVI thresholds are included in Figure C-3 in Appendix C.

The final output (Step 10) is the GDE Index (Figure 7-7a). It presents the proportion of time a given area exhibited vegetation vigour (i.e. the percentage of dry periods which remained above the NDVI threshold). Areas mapped as light green to dark green are predicted to have low to high frequency access to groundwater or a steady supply of water stored in the unsaturated zone, respectively. The majority of the study area is predicted to have little access to groundwater. Within the Stony Plains IBRA the higher values generally follow the stream lines. The highest values are found at Dalhousie Springs in the far north of the study area (Figure 7-7b & c), with some pixels permanently above the NDVI threshold of 0.2 (i.e. GDE Index = 100). The Finke IBRA is showing high GDE Index values for this scenario (see Discussion section below). Other patches, particularly around the Simpson Strzelecki Dunefields IBRA show low potential for being GDEs, with pixel values generally below 5%. Outputs for 0.3 and 0.4 NDVI thresholds are included in Figure C-4 in Appendix C.

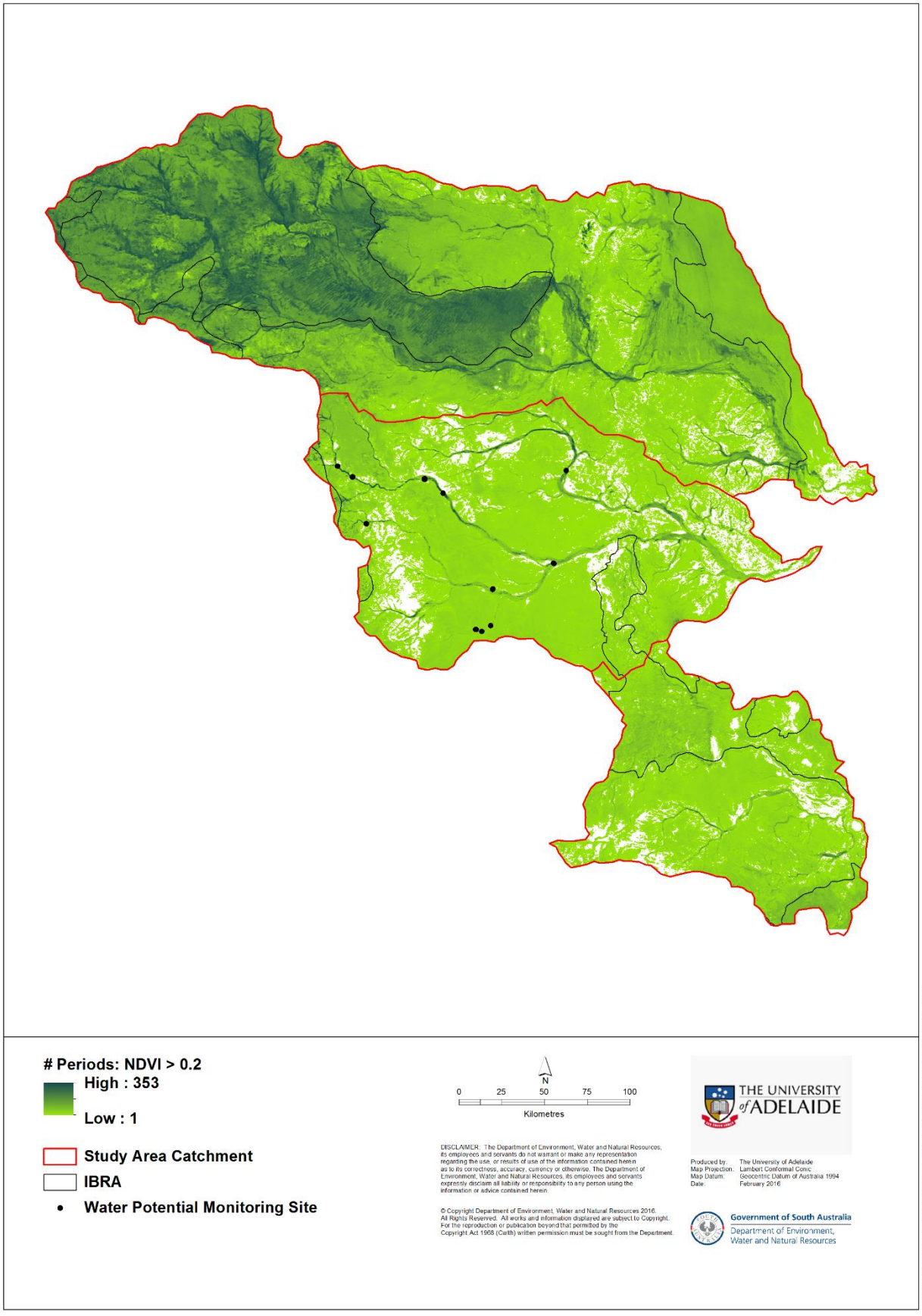

Figure 7-4: Step 2 output. Number of times above NDVI threshold of 0.2 in the 353 NDVI images.

Figure 7-5: Step 7 output. Number of dry periods, where a dry period is defined as 180 days with no 7 days > 25 mm rain (possible maximum = 353 periods, actual maximum = 205 periods, actual minimum = 28 periods).

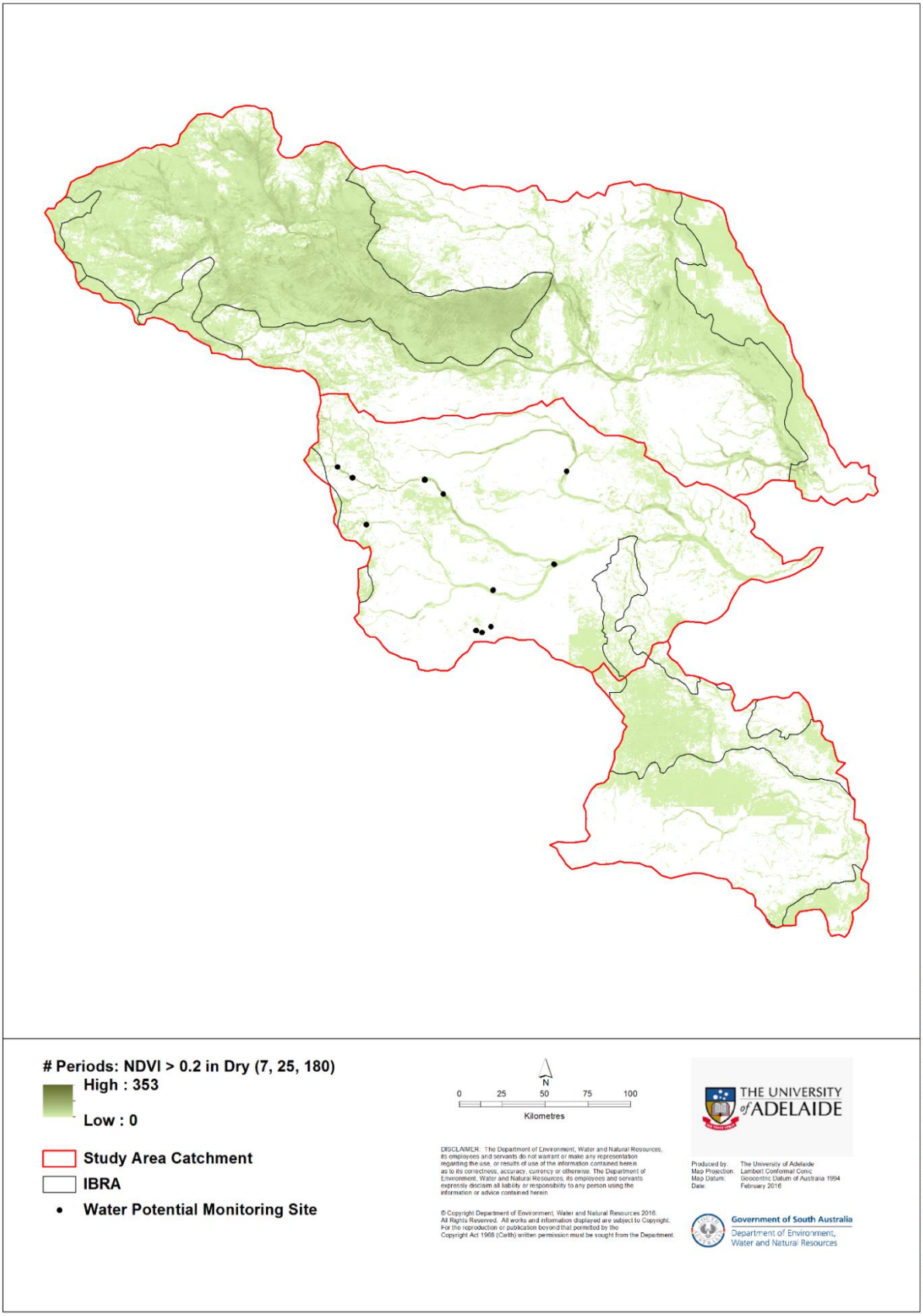

Figure 7-6: Step 9 output. Number of times green in dry periods, where green is defined as NDVI > 0.2 and a dry period is defined as 180 days with no 7 days > 25 mm rain.

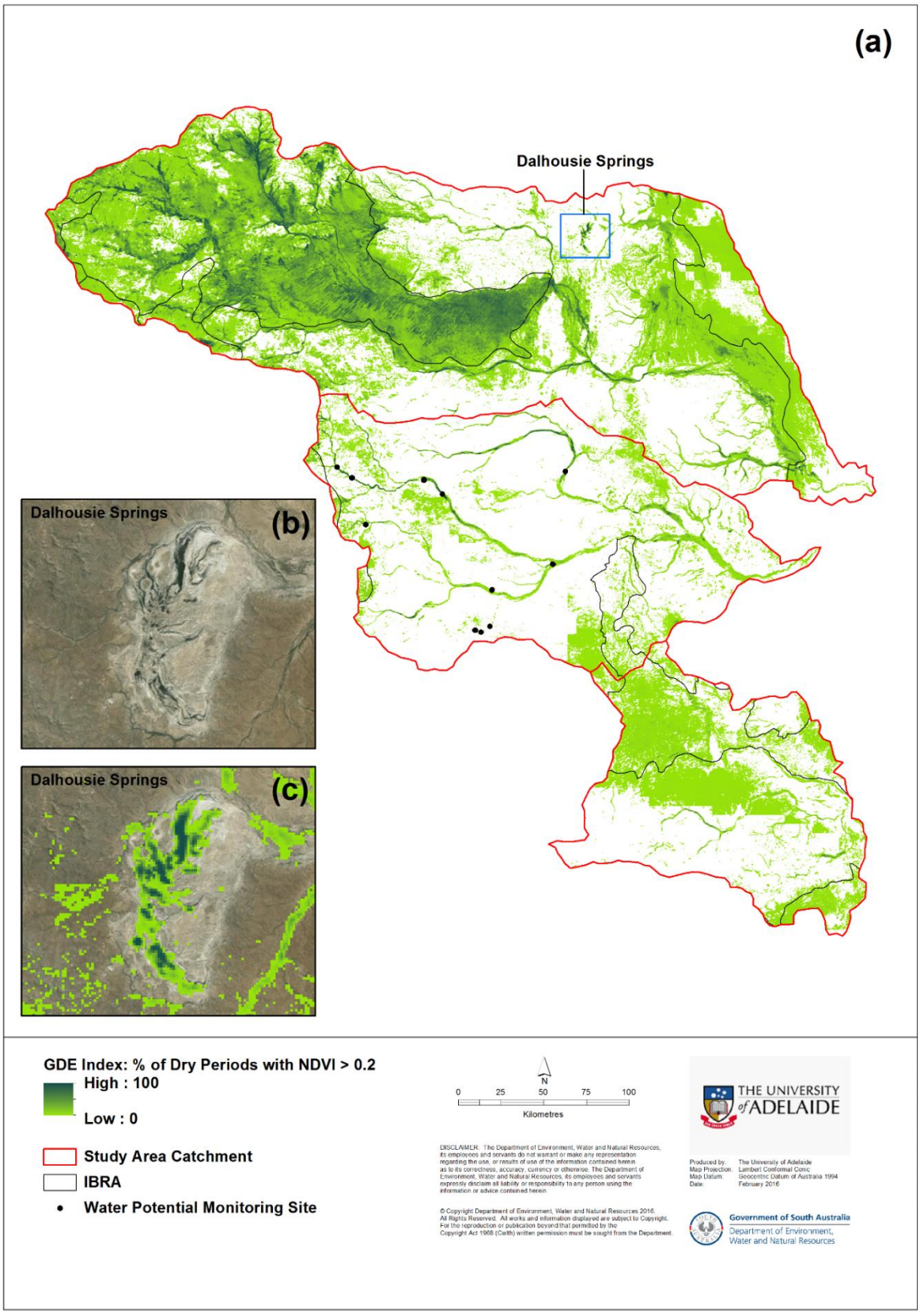

Figure 7-7: Step 10 output. (a) GDE Index, the percentage of dry periods which were green (0% to 100%), where a dry period is defined as 180 days with no 7 days > 25 mm rain and green is defined as NDVI > 0.2; (b and c) Dalhousie Springs enlargement.

7.3.2 Comparison with the GDE Atlas of Australia

The methodology applied in creating the National Atlas of Groundwater Dependent Ecosystems (GDE Atlas) is described briefly here. Full details are available in the methodology report (SKM, 2012).

7.3.2.1 GDE Atlas of Australia methodology

For all of Australia, MODIS data was used to assess changes in the rate of evapotranspiration (ET) over time, and Landsat data was analysed to map the vegetation greenness using spectral response. The combination of these layers allowed the creation of a single Inflow Dependence (ID) layer that inferred where landscapes might access water in addition to rainfall (i.e. water stored in the unsaturated zone, groundwater, or surface water). We then applied rules to determine the likelihood of this additional source of water being groundwater (SKM, 2012).

We divided Australia into eight areas of broadly similar hydrogeological, ecological, and climatic characteristics (work packages). A different set of rules was applied to each work package to identify potential groundwater interaction for mapped vegetation ecosystems (resulting in a map of ecosystems that rely on the subsurface presence of groundwater), and for mapped river, wetland and spring ecosystems (resulting in a map of GDEs that rely on the surface expression of groundwater).

7.3.2.2 Rules for identification of GDEs that rely on the surface and subsurface expression of groundwater for WP2

The majority of our study area falls within the Eastern Central Australia and the Nullarbor Plain Work Package 2 (WP2). A portion of the Finke IBRA section in the north-west is part of Work Package 7 (WP7). The GDE Atlas output for our study area, for ecosystems that rely on the surface expression of groundwater (rivers, wetlands, and springs), is shown in Figure 7-8; and the output for ecosystems that rely on the subsurface presence of groundwater (vegetation) in Figure 7-9.

7.3.2.2.1 Rules for identification of GDEs that rely on the SURFACE expression of groundwater for WP2

1. Areas with persistent surface water are likely to receive inputs from groundwater with the exception of waterbodies within the EHZ18 part of the Lake Eyre Basin.
2. Waterbodies are less likely to be groundwater fed, where cracking clay soils exist.
3. Waterbodies intersecting a known spring location are more likely to be GDEs
4. Areas with shallow watertables are more likely to receive inputs from groundwater.
5. Rivers flowing through fractured rock aquifers in the Adelaide Geosyncline (in EHZ33) and through the GAB aquifers are likely to receive groundwater inputs.

7.3.2.2.2 Rules for identification of GDEs that rely on the SUBSURFACE presence of groundwater for WP2

1. Vegetation growing in areas with shallow groundwater is more likely to be a GDE.
2. Vegetation type is an indicator of groundwater use.
3. Native vegetation that has a relatively high and constant ET in dry periods is more likely to be using groundwater.
4. Native vegetation surrounding a known spring location or a known GDE is more likely to be a GDE.
5. Vegetation growing in soil that has a low water storage capacity is more likely to be accessing groundwater than vegetation which grows in soil where more water is stored in the unsaturated zone.
6. Vegetation growing near river or wetlands GDEs is also likely to be using groundwater.
7. Vegetation growing in areas where cracking soil plains exist is more likely to rely on trapped surface water or water stored in the unsaturated zone than groundwater.

Visual comparison of our GDE Index scenario presented here (see Section 4.1 for the parameters used in this scenario) and the GDE Atlas of Australia show some differences (Figure 7-10 a, b, and c).

Figure 7-10 d shows this particular scenario of the GDE Index masked by the GDE of Australia outputs (both surface and subsurface). It clearly illustrates that the main differences occur in the Finke and Simpson Strzelecki Dunefields IBRA. Very few potential GDEs have been mapped in these areas in the GDE Atlas of Australia. Apart from the Finke IBRA, those areas mapped by using the GDE Index Tool and not the GDE Atlas are classified as areas of low GDE potential by the GDE Index Tool, with values generally below 5 (i.e. less than 5% of the dry periods remained above the NDVI threshold, using the parameters set for this scenario).

The majority of ecosystems that rely on the surface expression of groundwater (rivers, wetlands, and springs) identified in the GDE Atlas of Australia were also included in our GDE Index (Figure 7-10e). There are some low potential river and creek channels and some smaller patches of higher potential in the south which were not identified using the parameters set in this scenario.

Figure 7-10 f illustrates the areas mapped as reliant on subsurface groundwater (vegetation) which were not mapped with the parameters used in this GDE Index scenario. These include some large patches classified as low potential in the east and south, along with some smaller higher potential patches and tributaries of the larger stream channels in the middle section.

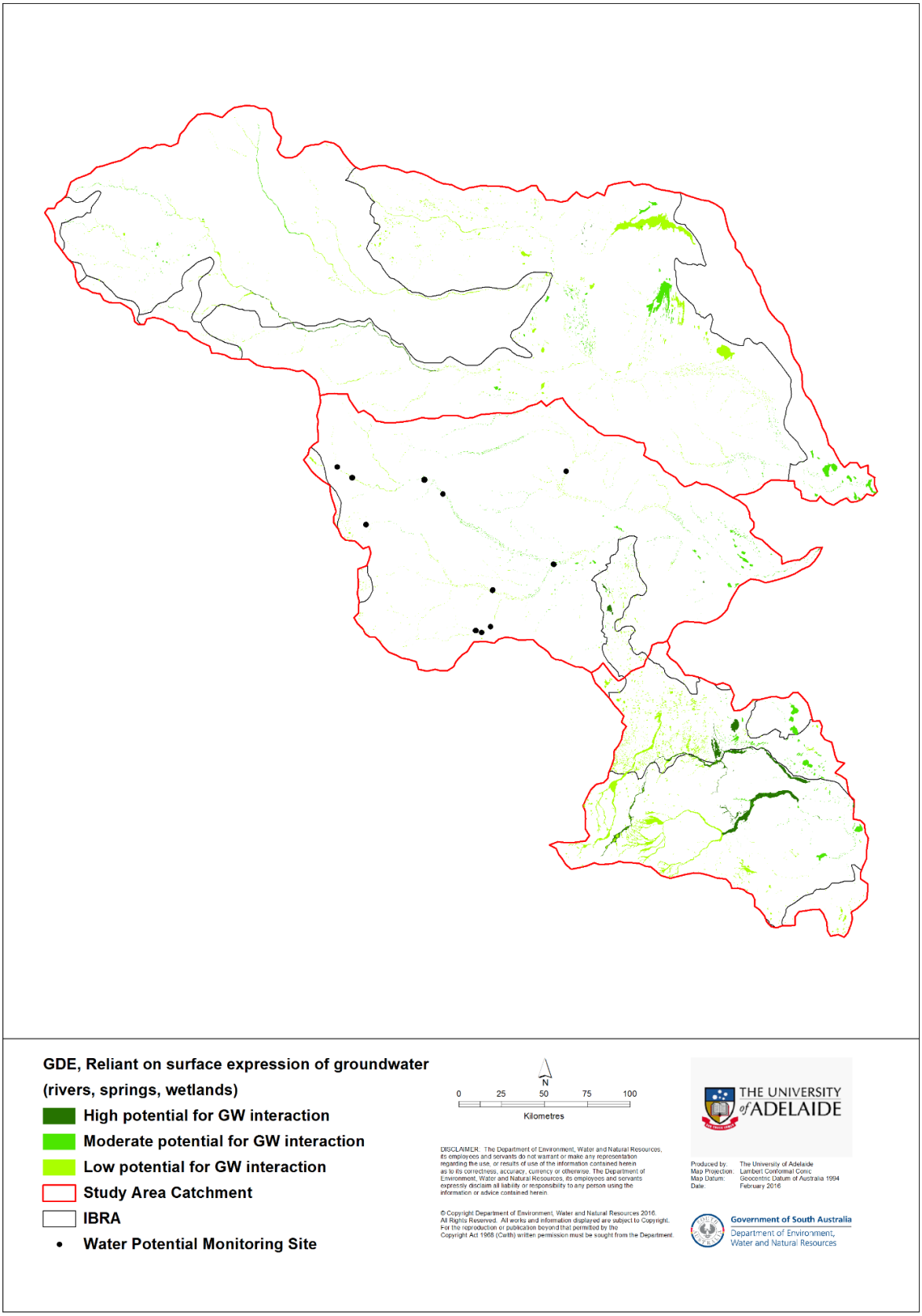

Figure 7-8: GDE Atlas of Australia: ecosystems that rely on the surface expression of groundwater (rivers, wetlands, and springs)

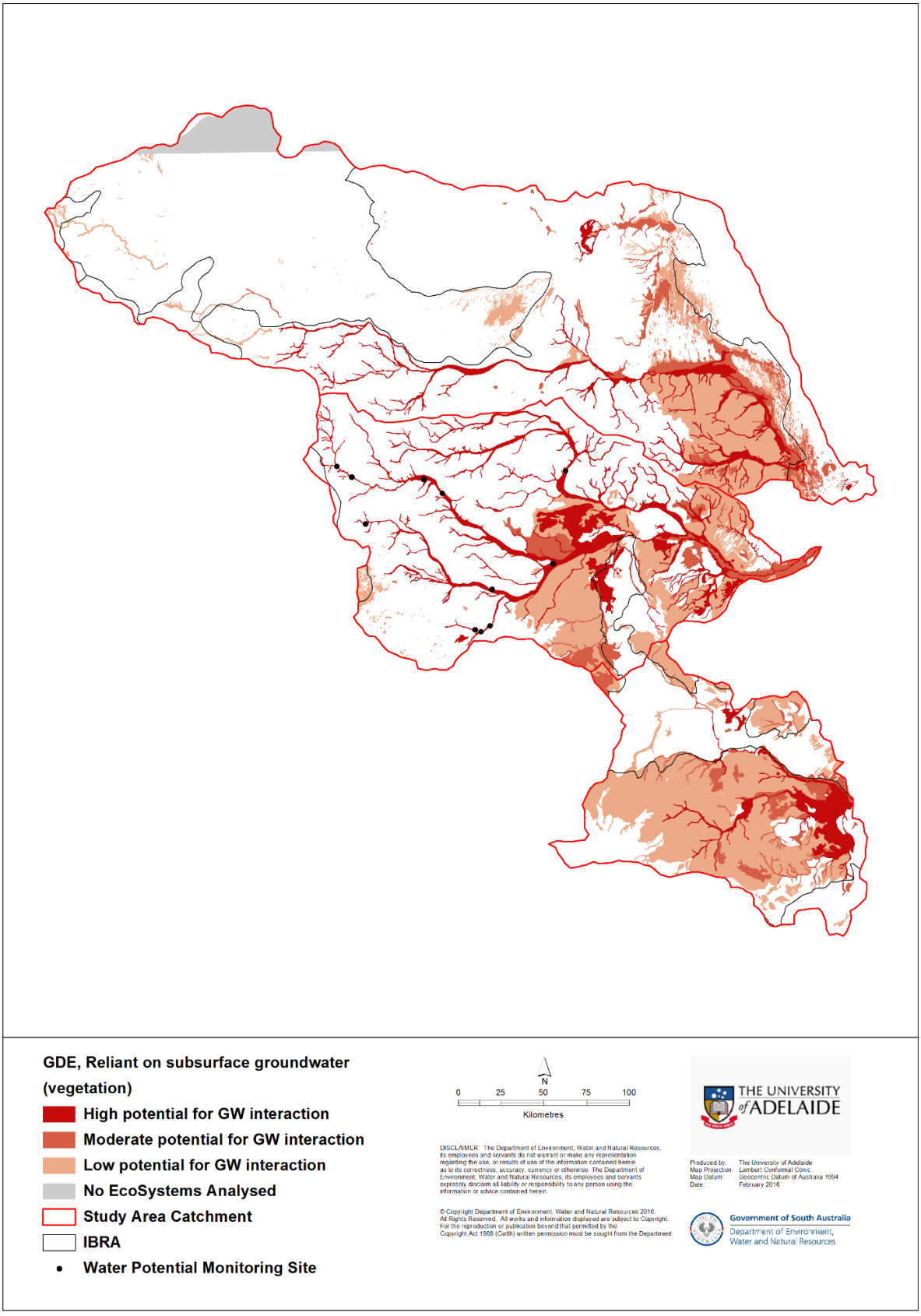

Figure 7-9: GDE Atlas of Australia: ecosystems that rely on the subsurface expression of groundwater (vegetation)

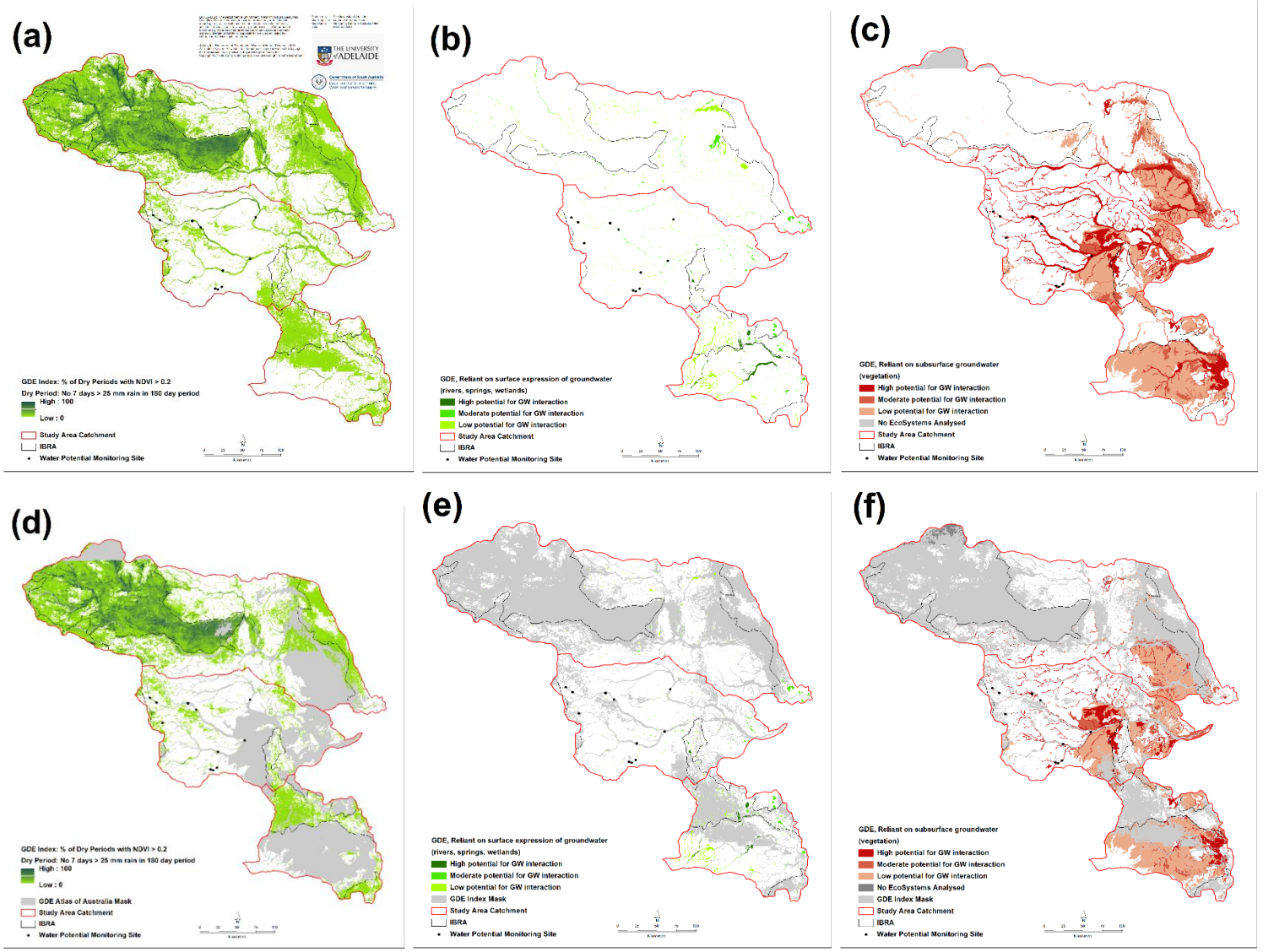

(a) GDE Index (b) GDE Atlas of Australia: Ecosystems that rely on the surface expression of groundwater (rivers, wetlands, springs) (c) GDE Atlas of Australia: ecosystems that rely on the subsurface presence of groundwater (vegetation) (d) GDE Index masked by the GDE Atlas of Australia (surface and subsurface) (e) GDE Atlas of Australia (surface) masked by the GDE Index (f) GDE Atlas of Australia (subsurface) masked by

Figure 7-10: Comparison of outputs from the GDE Index Tool and the GDE Atlas of Australia

7.3.3 Field data

7.3.3.1 Leaf water potential monitoring

Table 7-2 and Figure 7-11 shows the results of linking the GDE Index for one particular scenario to the LWP monitoring data as reported in Section5.2.1. Appendix D maps the monitoring sites at two scales, plus the GDE Index at the larger scale. These maps demonstrate that one 250 m MODIS pixel can cover many monitoring locations at a site. These maps also demonstrate that at each of the LWP monitoring locations, the field measurements tend to be clustered in larger zones with similar GDE Index values. The LWP samples did not adequately sample the variation in the area. Often a wider range of GDE Index values can be seen short distances from the monitoring locations (e.g. at Cootanoorina Waterhole values of 6.25 and 84.03 are only two pixels or 500 m apart (Appendix D-2).

All the monitoring locations were in areas identified by the GDE Index parameters for this scenario. Wintinna Homestead has the highest potential of being a GDE, with values above 90 (i.e. 90% of dry periods with NDVI > 0.2, where a dry period was defined as 180 days without a significant rainfall event, which in turn was defined as any 7-day period with cumulative rainfall over 25 mm), followed by a *E. coolabah* location on the bank at Francis Camp (FCC2) at 82.4 (Table 7-2 and Appendix D-6). The Ethel Well site recorded a GDE Index value of 67.6; while the majority of the locations at the EJ Bore, Cootanoorina Waterhole and Francis Camp Waterhole sites ranged from 30 to 50. None of the locations at Stewart Waterhole were above 6.3, along with three locations at Cootanoorina Waterhole and one at Francis Camp (see Section 5).

There are no obvious correlations or relationships between the GDE Index and either the pre-dawn (Figure 7-12a) or midday (Figure 7-12) leaf water potential reading, by either tree type or position (bank vs. floodplain). This is not surprising due to the 250 m resolution of the GDE Index data. Any particular pixel may contain a number of tree species and both bank and floodplain areas. Conversely, there is considerable localized variation in the GDE Index as shown by the large-scale maps in Appendix D which has not been sampled by on-ground leaf water potential measurements.

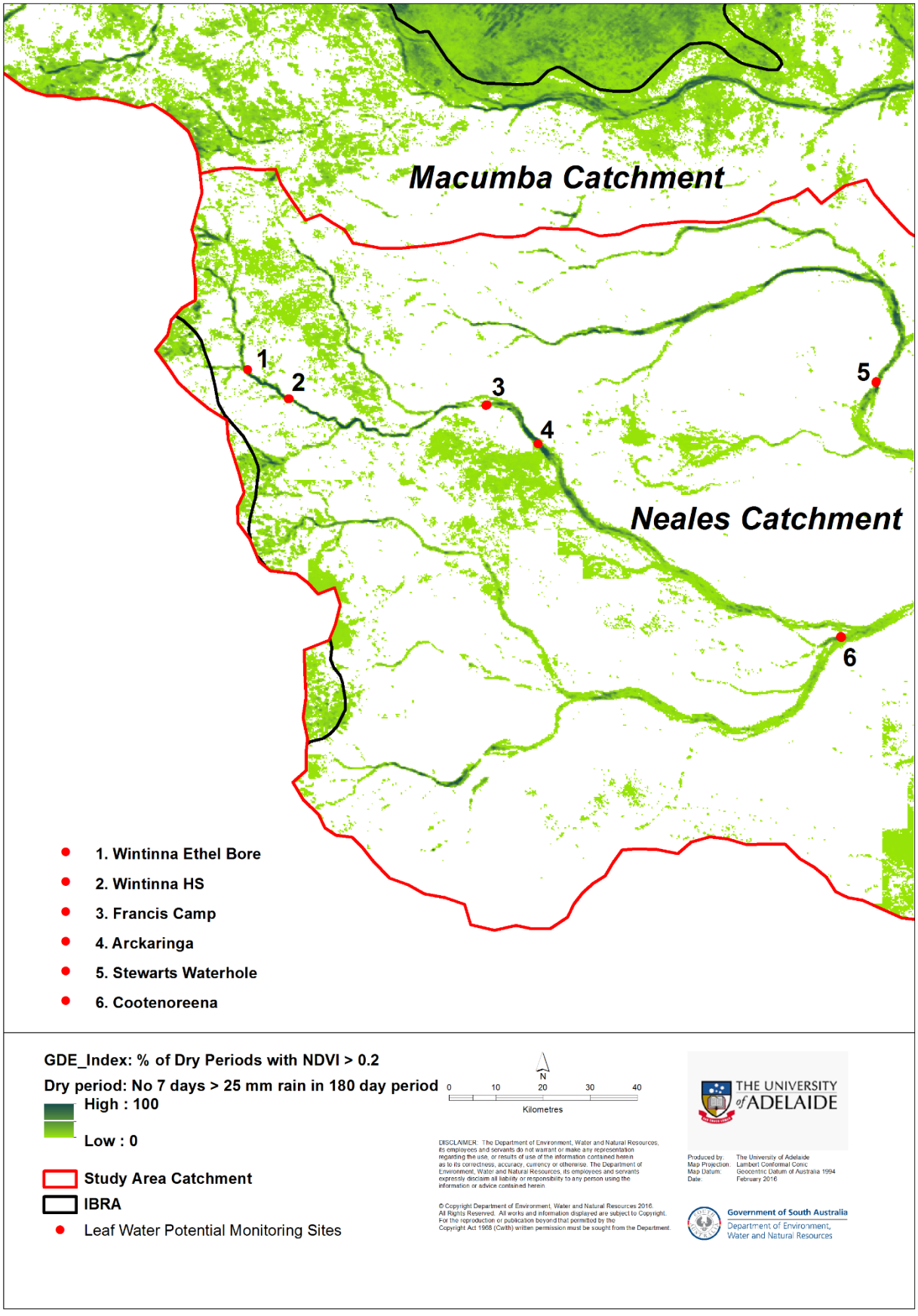

Figure 7-11: Leaf water potential monitoring sites in relation to GDE Index output scenario

Table 7-2: Summary of pre-dawn and midday leaf water potential sampling results with sample GDE Index values[1]

Site	Position	Species[2]	Tree	Mean pre-dawn LWP	Mean midday LWP	GDE Index[3]
EJ Bore	Bank	*E. cool.*	ACC1	-3.63	-4.10	46.6
EJ Bore	Bank	*E. cool.*	ACC2	-3.45	-3.71	42.6
EJ Bore	Bank	*A. cam.*	ACG1	-4.53	-4.73	46.6
EJ Bore	Bank	*A. cam*	ACG2	-4.48	-4.77	42.6
Cootanoorina WH	Bank	*E. cool.*	CCC1	-1.27	-2.97	6.3
Cootanoorina WH	Bank	*E. cool.*	CCC2	-1.29	-3.16	30.6
Cootanoorina WH	Bank	*E. cool.*	CCC3	-1.10	-3.21	22.9
Cootanoorina WH	Bank	*A. sten.*	CCS1	-0.84	NR	6.3
Cootanoorina WH	Bank	*A. sten.*	CCS2	-1.61	NR	6.3
Cootanoorina WH	Floodplain	*E. cool.*	CFC1	-3.09	-3.69	50.0
Cootanoorina WH	Floodplain	*E. cool.*	CFC2	-3.12	-3.45	50.0
Cootanoorina WH	Floodplain	*E. cool.*	CFC3	-3.19	-3.75	50.0
Francis Camp WH	Bank	*E. cool.*	FCC1	-3.47	-3.54	37.0
Francis Camp WH	Bank	*E. cool.*	FCC2	-2.80	-3.2	82.4
Francis Camp WH	Bank	*E. cam.*	FCR1	-3.93	-4.2	37.0
Francis Camp WH	Bank	*E. cam.*	FCR2	-2.61	-3.3	37.0
Francis Camp WH	Bank	*E. cam.*	FCR3	-2.53	-3.1	37.0
Francis Camp WH	Floodplain	*E. cool.*	FFC1	-2.43	-2.95	3.4
Francis Camp WH	Floodplain	*E. cool.*	FFC2	-1.93	-2.7	37.0
Stewart WH	Bank	*E. cool.*	SCC2	-1.06	-2.98	6.3
Stewart WH	Bank	*E. cool.*	SCC3	-1.09	-3.76	5.6
Stewart WH	Bank	*E. cam.*	SCR1	-0.87	-2.45	5.6
Stewart WH	Bank	*E. cam.*	SCR2	-0.51	-3.17	6.3
Stewart WH	Bank	*E. cam.*	SCR3	-0.50	-2.70	6.3
Stewart WH	Floodplain	*E. cam.*	SFC1	-1.35	-3.13	5.6
Wintinna HS	Bank	*E. cam.*	WCR2	-2.17	-2.72	93.6
Wintinna HS	Bank	*E. cam.*	WCR3	-2.45	NR	98.2
Wintinna HS	Floodplain	*E. cam.*	WFR1	-2.33	-3.23	93.6
Wintinna EB	Bank	*E. cam.*	ECR1	-1.77	-3.21	67.6
Wintinna EB	Bank	*E. cam.*	ECR2	-2.00	-3.07	67.6
Wintinna EB	Floodplain	*E. cam.*	EFR3	-3.06	-3.72	67.6

[1]Tree data based on results in Section 4.1.2 with GDE Index values added to sample locations

[2]E. cool. = *Eucalyptus coolabah*, E. cam. = *E camaldulensis*, A. cam. = *Acacia cambagei*, A. sten. = *A. stenophylla*

[3]Note: This GDE Index modelled % of dry periods with NDVI > 0.2, where a dry period was defined as 180 days without a significant rainfall event, which in turn was defined as any 7 day period with cumulative rainfall over 25 mm.

NR = not recorded

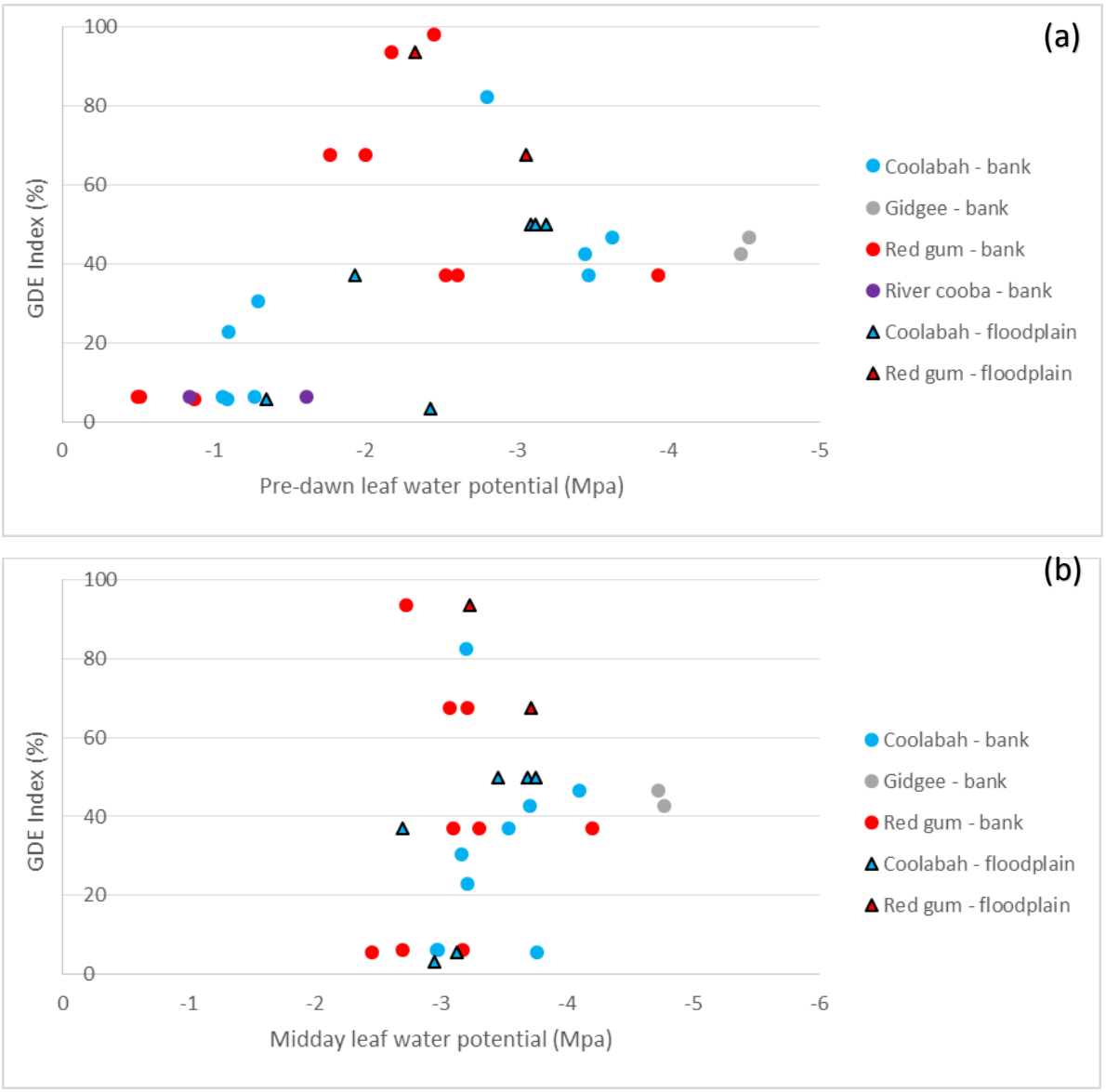

Figure 7-12: Relationship between GDE Index and (a) mean pre-dawn leaf water potential for each tree and (b) mean midday leaf water potential for each tree

7.3.3.2 Water quality

Water quality field sampling (Figure 7-13) is reported in Section 1. Table 7-3 shows the results of linking the GDE Index to the water sampling data. Four of the sites that coincided with wells that are completed within the J-K aquifer (Algebullcullia Bore, Junction Bore, Ricky No. 2 Bore and No. 1 Bore) were not identified as potential GDEs in this scenario (i.e. 0% of dry periods with NDVI > 0.2, where a dry period was defined as 180 days without a significant rainfall event, which in turn was defined as any 7-day period with cumulative rainfall over 25 mm). Six others had a GDE Index of less than 10 (EJ Bore, McLeod Bore, Sheila Bore, Stewart Waterhole, Stan Well and Wintinna H.S No 2 Bore). For the remaining sites the GDE Index values ranged from 11.2 to 40.3. In the case of EJ Bore and McLeod Bore, these wells were completed within the J-K aquifer at a depth greater than 50 mbgs. The remaining wells (Sheila Bore, Stan Well and Wintinna H.S No 2 Bore) are completed within the QTa aquifer.

At this time, no further spatial analysis has been carried out on this data.

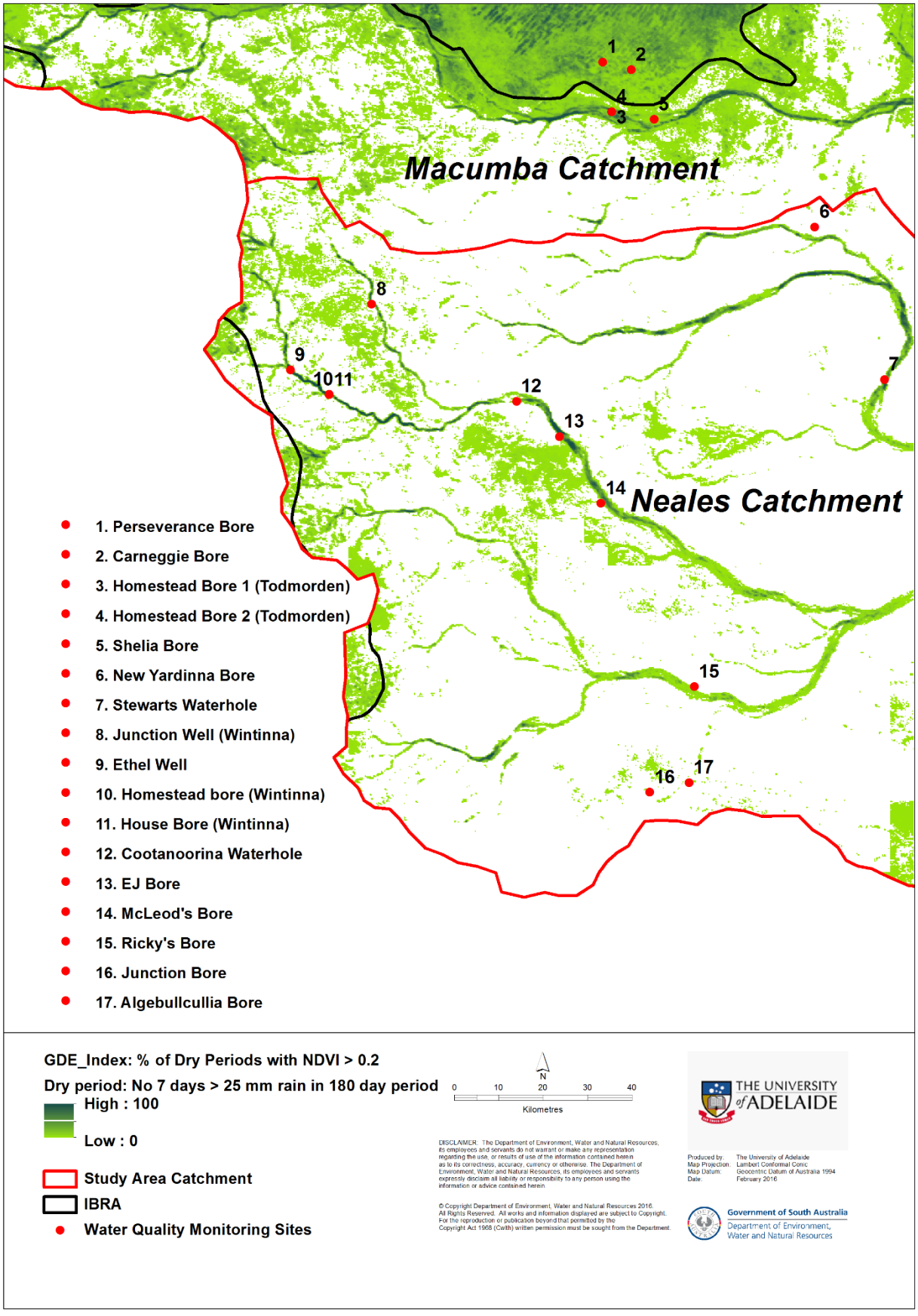

Figure 7-13: Water quality and hydrochemistry sampling sites

Table 7-3: Summary of water quality results with GDE Index values

Name	Type	Aquifer	Temp	EC	TDS	Depth to water (mbgs)	GDE Index
Algebullcullia Bore	Well	GAB	26.3	6456	4095	15.27	0.0
Junction Bore	Well	GAB	33.1	6955	3913	27.11	0.0
Ricky No. 2 Bore	Well	GAB	28.8	7009	5460	4.91	0.0
Cootanoorina Waterhole	Water-hole		23.6	146.6	98.15	-	37.0
EJ Bore	Well	GAB	31.1	6912	4017	32.95	0.7
McLeod Bore	Well	GAB	28.9	7013	4238	20.59	1.4
No. 1 Bore	Well	GAB	40.3	4662	2346.5	10	0
Homestead No. 4 Bore (Todmorden)	Well	QT	26.9	2443	1534	?	25.2
Homestead No. 2 Bore (Todmorden)	Well	QT	27.8	2098	1300	?	25.2
Perseverance Bore	Well	QT	29	5653	3412.5	33	18.4
Carnegie Bore	Well	QT	29.5	6080	3640	31	11.2
Sheila Bore	Well	QT	28.3	7299	4433	15.2	6.7
Stewart Waterhole	Water-hole		25.7	262	167.7	-	5.6
Junction Well (Wintinna)	Well	QT	26.2	1588	1007.5	6.9	40.3
Ethel Well	Well	QT	23.8	3105	2054	9	37.0
Stan Well	Well	QT	25.2	1509	975	8.1	9.1
Wintinna No. 2 Bore)	Well	QT	25	955	624	?	9.1

7.3.3.3 Water Observations from Space

The areas most frequently inundated are shown in the WOfS Filtered Summary data in Figure 7-14. A brief examination of this data revealed that 93.4 % of the study area had no inundation detected in clear Landsat observations. Almost 6.5 % of the area has been inundated in up to 10% of these observations, and a further 1% of the area between 10% and 20 % of times. Less than 0.02% of the study area has an inundation rate above 20%.

The majority of mapped inundation follows the river and creek lines in the Stoney Plains IBRA, with little in the sections of the Finke or Simpson Strzelecki Dunefields IBRAs within the study area. One of the areas with a high level of inundation was immediately west of the Cootanoorina Waterhole leaf water potential monitoring sites (Table 5-1), with rates of inundation as high as 40%.

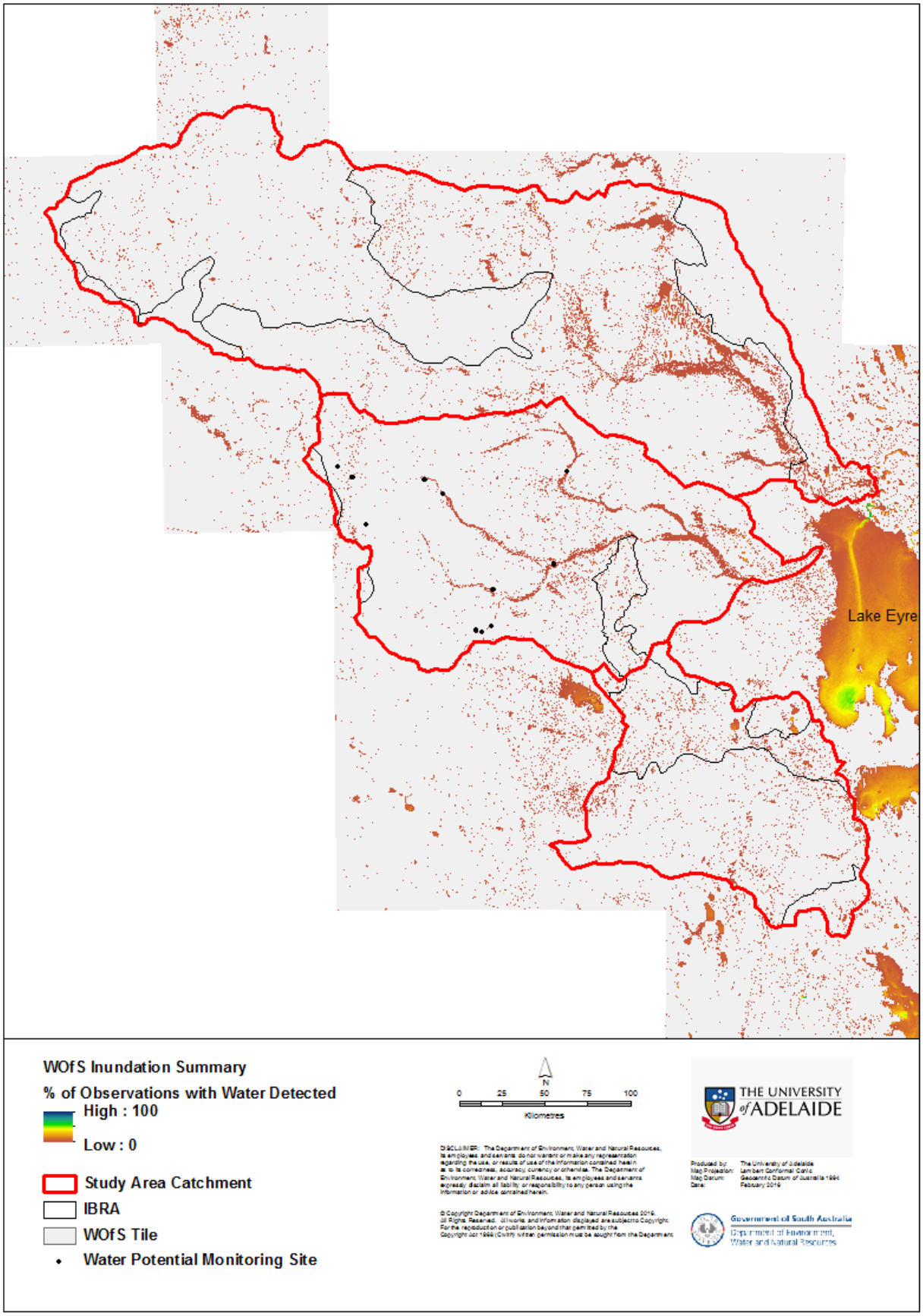

Figure 7-14: Water Observations from Space filtered summary inundation

8 References

Åberg, G Jacks, G and Hamilton, PJ, 1989. Weathering rates and $^{87}Sr/^{86}Sr$ ratios: an isotopic approach, Journal of Hydrology (109), pp. 65–78.

Ah Chee, D 2002, 'Indigenous people's connection with Kwatye (water) in the Great Artesian Basin', GAB FEST 2002: A resource under pressure, Great Artesian Basin Coordinating Committee, Toowoomba, Queensland.

Aggarwal, PK, Araguas-Araguas, L, Choudhry, M, van Duren, M and Froehlich, K. 2014, 'Lower groundwater ^{14}C age by atmospheric CO_2 uptake during sampling and analysis', *Groundwater*, vol. 52, issue 1, pp. 20–24.

Bowering, OJW, 1975. A summary of the Groundwater Resources within the Proposed Study Corridors – Stuart Highway Improvement Project. Department of Mines South Australia. Rep. Bk. No. 75/107, G.S No. 5640, Hyd. No. 2696, D.M. No. 854/74.

Bureau of Meteorology (BoM). 2016, Atlas of groundwater dependent ecosystems, Commonwealth of Australia, accessed on-line 12/02/2016, http://www.bom.gov.au/water/groundwater/gde/map.shtml

BoM. 2015a, Climate Data Online, Bureau of Meteorology. Available at http://www.bom.gov.au/climate/data/index.shtml

BoM. 2015b, Atlas of Groundwater Dependent Ecosystems, Bureau of Meteorology. Available at http://www.bom.gov.au/water/groundwater/gde/map.shtml

Clarke, K, Lawley, E, Raja Segaran, R & Lewis, M. 2014, Spatially-explicit environmental indicators for regional NRM planning for climate change. Technical report for Natural Resources SA Arid Lands by the University Of Adelaide, South Australia.

Costelloe, J. 2011, Hydrological assessment and analysis of the Neales Catchment, Report to the South Australian Arid Lands Natural Resources Management Board, Port Augusta.

Costelloe, JF. 2014, Arid zone sapflow monitoring update. Report to the South Australian Department of Environment, Water and Natural Resources. Department of Infrastructure Engineering, The University of Melbourne, Melbourne, September 2014.

Costelloe, JF. 2015, Arid zone sapflow monitoring: Finke and Neales Rivers. Report to the South Australian Department of Environment, Water and Natural Resources. Department of Infrastructure Engineering, The University of Melbourne, Melbourne, April 2015.

Costelloe, JF, Payne, EG, Woodrow, IE, Irvine, EC, Western, AW, Leaney, F. 2008, Water use by arid zone riparian trees in highly saline environments, Australia, Oecologia 156: 43-52. doi 10.1007/s00442-008-0975-4.

Croft, SJ, Pedler, JA and Milne, TI, 2005, Bushland Condition Monitoring Manual: Southern Mount Lofty Ranges. Nature Conservation Society of South Australia Inc., Adelaide.

Crosbie, R, Morrow, D, Cresswell, R, Leaney, F, Lamontagne, S, Lefournour, M 2012. New insights to the chemical and isotopic composition of rainfall across Australia. CSIRO Water for a Healthy Country Flagship, Australia.

Dunster, J, 1984. Pedological and Hydrological Study of Comalco Exploration Licences, central South Australia. Comalco Exploration. Department of State Development Open file Envelope No. 6259, pp. 1205-1225.

Eamus, D, Hatton, T, Cook, P and Colvin, C. 2006b, Ecohydrology: vegetation function, water and resource management, CSIRO Publishing, Collingwood.

Gat, JR, 1996, Oxygen and hydrogen isotopes in the hydrologic cycle. Annual Review of Earth and Planetary Sciences, 24: p.p. 225-262.

Habermehl, MA 1980. 'The Great Artesian Basin, Australia', BMR Journal of Geology and Geophysics, vol. 5, pp. 9–37.

Herraman, PD, 1976. Water Well Survey. Murloocoppie 1:250 000 Sheet. Department of Mines South Australia. Rep. Bk. No. 76/50, G.S. No. 5726, Hyd. No. 2724, D.M. No. 616/75.

Herraman, PD, and Safta, J, 1977. Wintinna 1:250 000 Sheet Water Well Survey. Department of Mines South Australia. Rep. Bk. No. 77/70, G.S. No. 5895, Eng. Geol. No. 77/55, D.M. No. 349/77.

International Atomic Energy Agency (IAEA), 2009, Laser Spectroscopic Analysis of Lquid Water Samples for Stable Hydrogen and Oxygen Isotopes. Training Course Series No. 35. Vienna 49p. < http://www.lgrinc.com/publications/TCS-35_web.pdf>

IAEA, 2013. Global Network of Isotopes in Precipitation (GNIP) last updated 22 May 2013. Viewed 2 May 2014. <http://www-naweb.iaea.org/napc/ih/IHS_resources_gnip.html>

Jones, DA, Wang, W and Fawcett, R, 2009, 'High-quality spatial climate data-sets for Australia', Australian Meteorological and Oceanographic Journal, vol. 58, pp. 233-248.

Jurgens, BC, Böhlke, JK and Eberts, SM, 2012, TracerLPM (Version 1): An Excel® Workbook for Interpreted Groundwater Age Distribution from Environmental Tracer Data. United States Geological Survey (USGS) Techniques and Methods Report 4-F3. 60 p.

Keppel, M, Wohling, D, Jensen-Schmidt, B and Sampson, L. 2015, *A hydrogeological characterisation of the Arckaringa Basin*, DEWNR technical report 2015/03, Department of Environment, Water and Natural Resources, Adelaide.

Lawley, EF, Lewis, MM and Ostendorf, B. 2011, Environmental zonation across the Australian arid region based on long-term vegetation dynamics, Journal of Arid Environments, 75(6): 576-585.

Leek, D 2002, 'Management of the Great Artesian Basin in South Australia: Looking Back, Looking Forward', GAB FEST 2002: A resource under pressure, Great Artesian Basin Co-ordinating Committee, Toowoomba, Queensland.

McMahon, TA, Murphy, RE, Peel, MC, Costelloe, JF and Chiew, FH. 2008a, Understanding the surface hydrology of Lake Eyre Basin – Part 1 Annual Rainfall. Journal of Arid Environments 72: 1853-1868.

Miles, CR and Costelloe, JF. 2015, Lake Eyre Basin (South Australia): mapping and conceptual models of shallow groundwater dependent ecosystems, DEWNR Technical note 2015/22, Government of South Australia, through the Department of Environment, Water and Natural Resources, Adelaide

Miles, C, Keppel, M, Osti, A and Foulkes J. 2015, Context Statement for the Arckaringa subregion. Product 1.1 for the Arckaringa subregion for the Lake Eyre Basin Bioregional Assessment. South Australian Department of Environment, Water and Natural Resources, Adelaide.

Miles, C and Miles, MW. 2015, South Australian Lake Eyre Basin aquatic ecosystem mapping and classification, DEWNR Technical report 2015/43, Government of South Australia, through Department of Environment, Water and Natural Resources, Adelaide

Mueller, N, Lewis, A, Roberts, D, Ring, S, Melrose, R, Sixsmith, J, Lymburner, L, McIntyre, A, Tan, P, Curnow, S and Ip, A. 2016, Water observations from space: Mapping surface water from 25 years of Landsat imagery across Australia, Remote Sensing of Environment, 174: 341-352.

O'Grady, AP., Cook, PG., Eamus, D, Duguid, A, Wischusen, JDH, Fass, T and Worldege, D, 2009, Convergence of tree water use within an arid-zone woodland. Oecologia (2009) 160: 643-655.

Phillips, FM. 2013, 'Chlorine-36 dating of old groundwater', in *Isotope methods for dating old groundwater*, International Atomic Energy Agency, Vienna, pp. 125–152.

Plummer, LN and Glynn, PD. 2013, 'Radiocarbon dating in groundwater systems', in *Isotope methods for dating old groundwater*, International Atomic Energy Agency, Vienna, pp. 33–73.

Richardson, S, Irvine, E, Froend, R, Boon, P, Barbe,r S and Bonneville, B. 2011, Australian groundwater-dependent ecosystem toolbox part 1: assessment framework, Waterlines report, National Water Commission, Canberra

Ryu, D, Costelloe, JF, Pipunic, R and Su, C-H. 2014, Rainfall-runoff modelling of the Neales River catchment, Report to the South Australian Department of Environment, Water and Natural Resources. Department of Infrastructure Engineering, The University of Melbourne, Melbourne.

Shand, P, Darbyshire, DPF, Love, AJ, Edmunds, WM 2009. Sr isotopes in natural waters: Applications to source characterisation and water-rock interaction in contrasting landscapes. Applied Geochemistry, 24, pp. 574–585.

Sinclair Knight Merz (SKM). 2012, Atlas of Groundwater Dependent Ecosystems (GDE Atlas), Phase 2: Task 5 Report: Identifying and mapping GDEs. Report to National Water Commission, Sinclair Knight Merz.

Smith, PC. 1976, Australian National Railways Tarcoola –Alice Springs Railway Groundwater Completion Report – Second Tender Progress Report No. 7. Report. Department of Mines South Australia, Geological Survey Engineering Division. Rep. Bk No. 46/65, G.S No. 5743, Eng. Geol. No. 76-29, D.M. No. 329/75.

United States Geological Survey (USGS) 2004. Resources on Isotopes: Periodic Table—Oxygen. Isotopic Tracers Project. Menlo Park, California. http://wwwrcamnl.wr.usgs.gov/isoig/period/o_iig.html>

Walker, G, Brunel, JP, Dighton, J, Holland, K, Leaney, F, McEwan, K, Mensforth, L, Thorburn, P and Walker, C. 2001, The use of stable isotopes for determining sources of water for plant transpiration. CSIRO Land and Water Technical Report 05/01.

9 Appendices

A. Mean Values of Daily Rainfall and NDVI 16-Day Composites for the Study Area from 2000 to 2015

Note: NDVI value is from a 16-day composite with the start date on the position of the marker

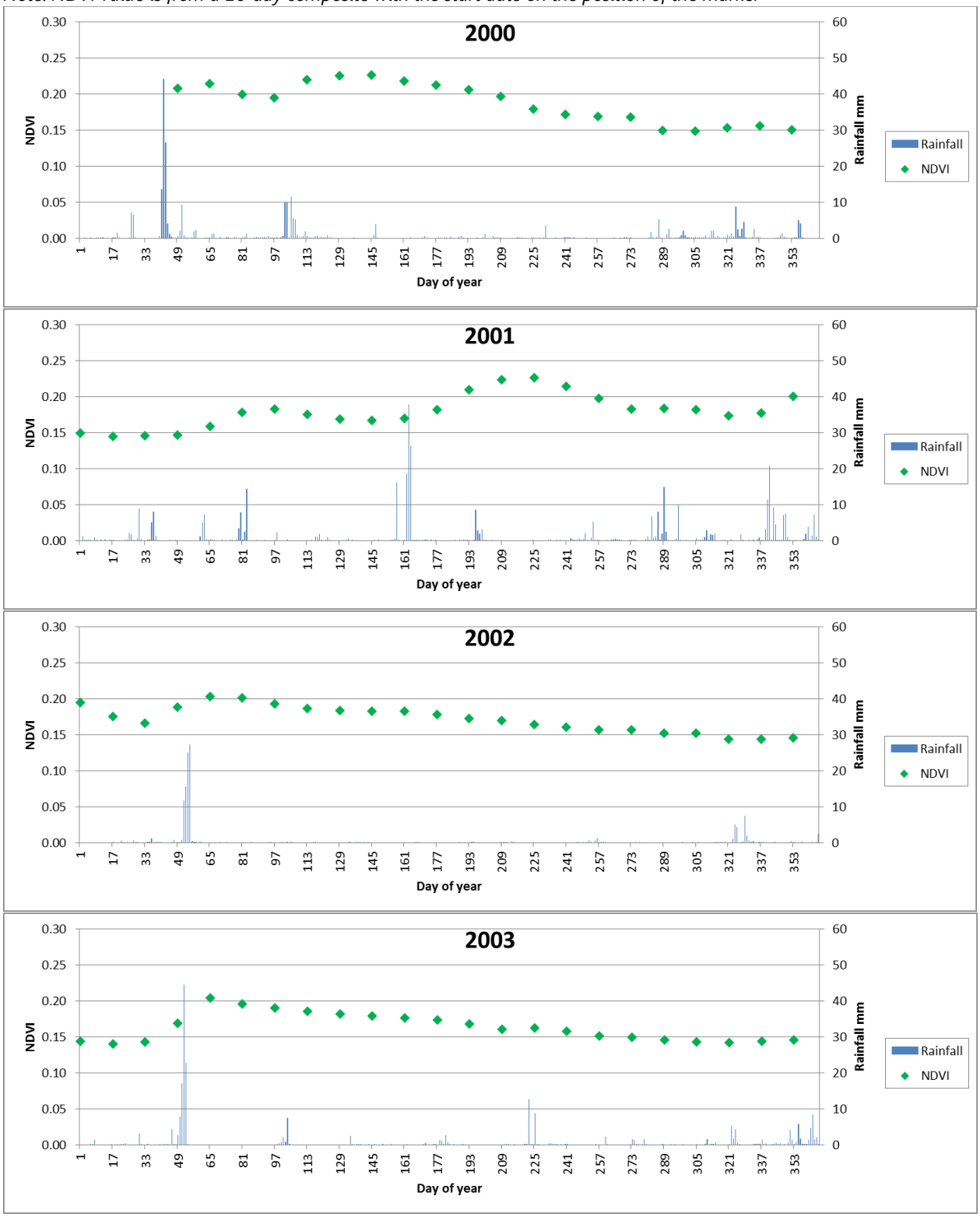

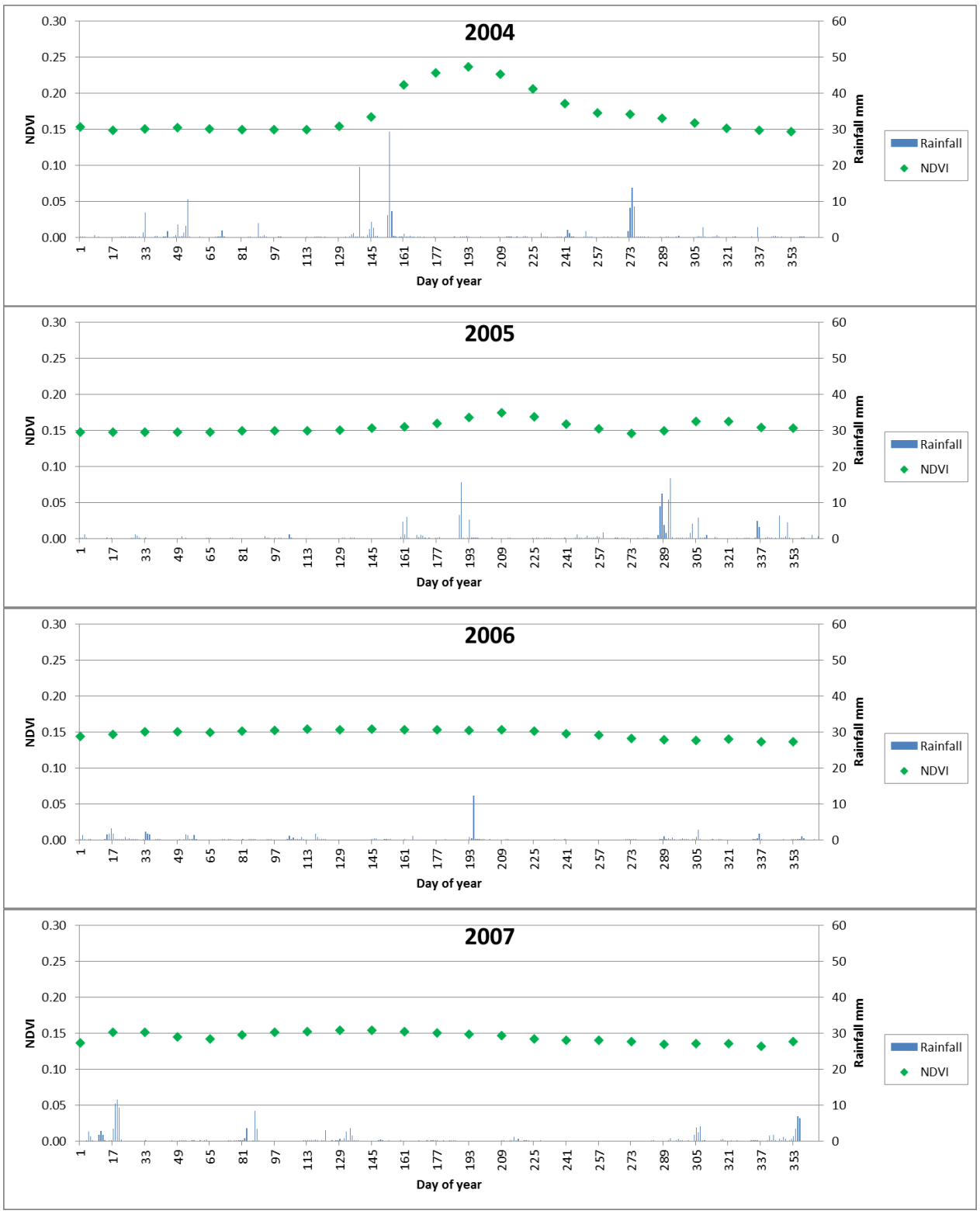
2004
2005
2006
2007
NDVI
Rainfall mm
Day of year
Rainfall
NDVI

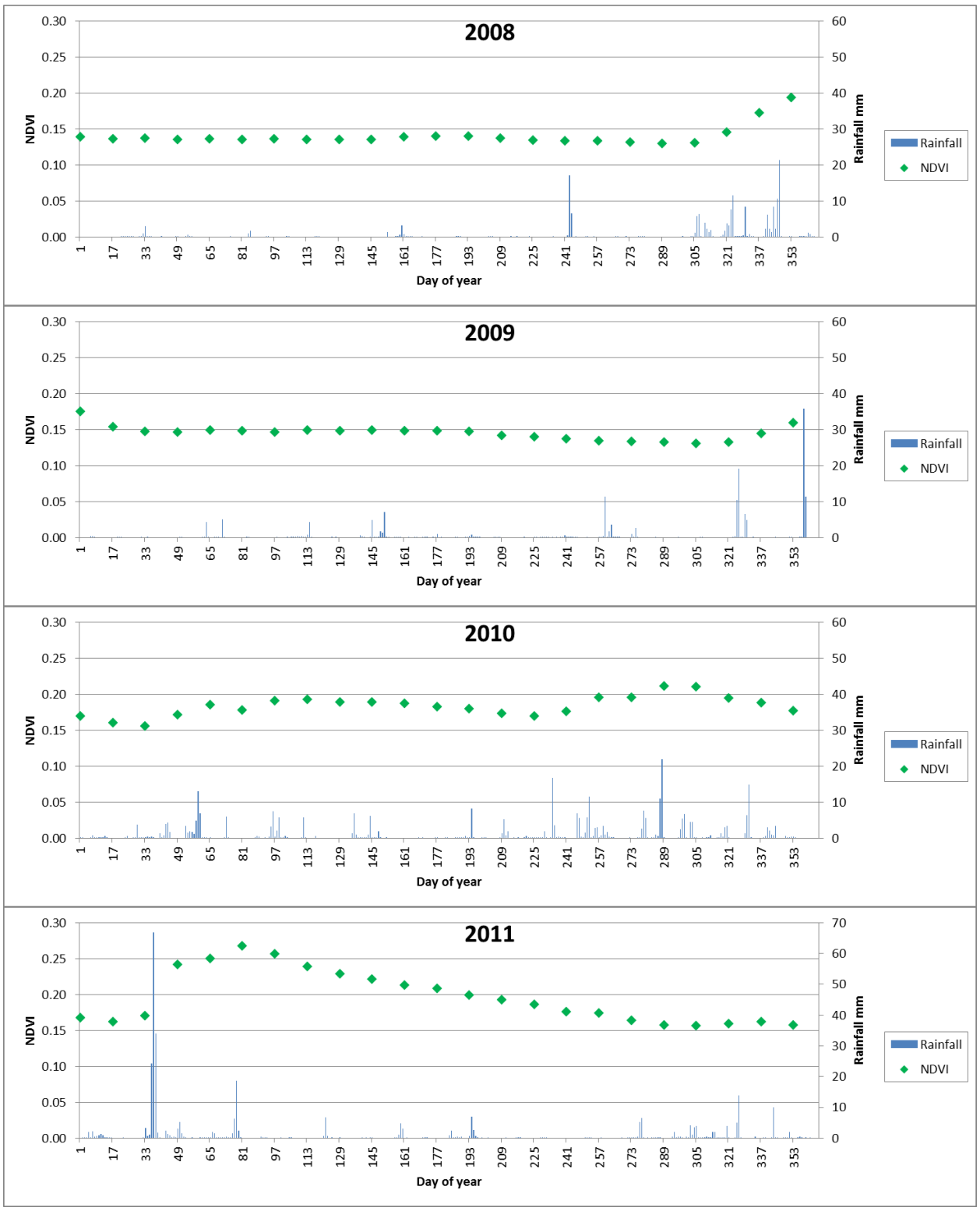
2008
2009
2010
2011
NDVI
Rainfall mm
Day of year
Rainfall
NDVI

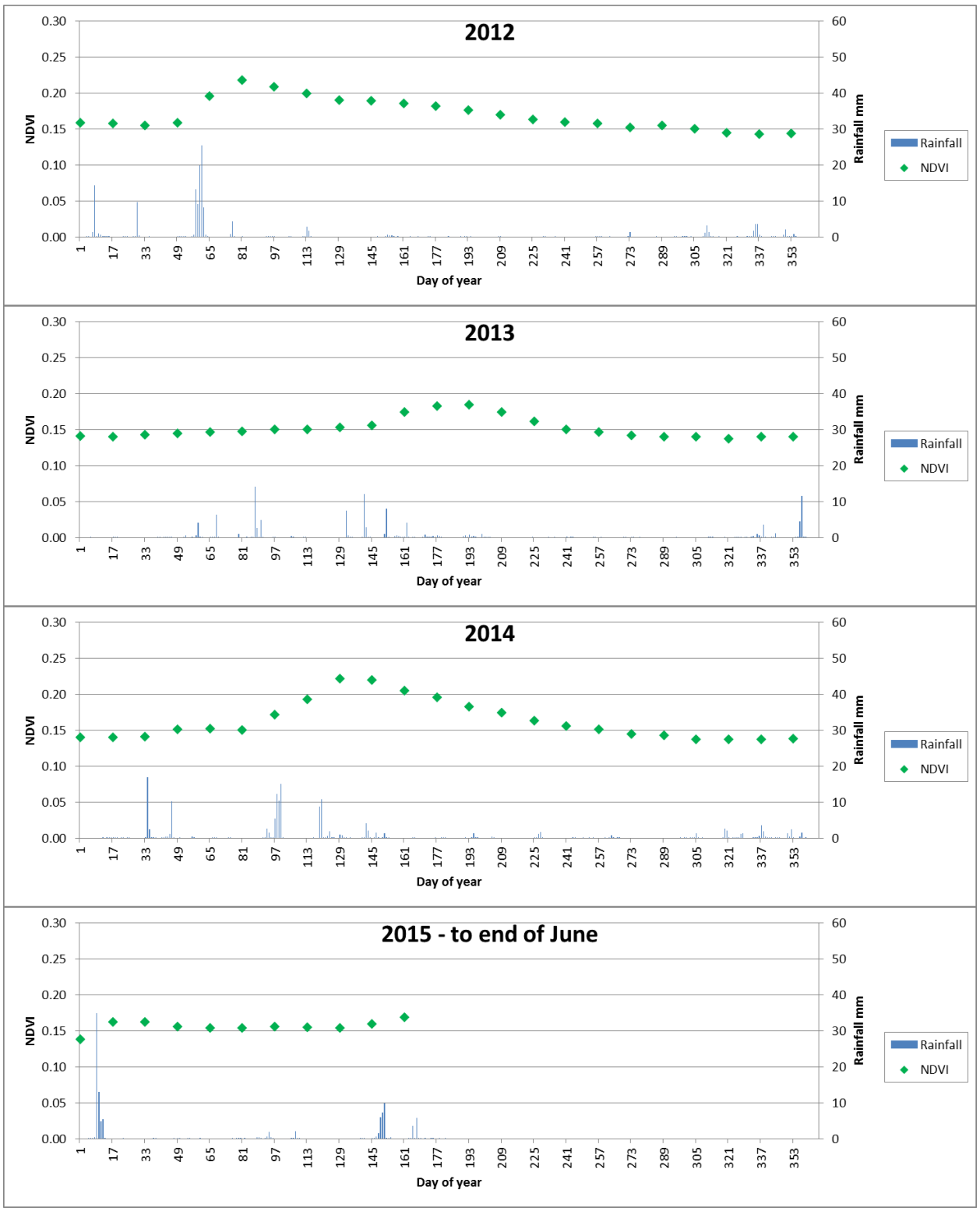
2012
2013
2014
2015 - to end of June
NDVI
Rainfall mm
Day of year
Rainfall
NDVI

Note: NDVI value is from a 16 day composite with the start date on the position of the marker

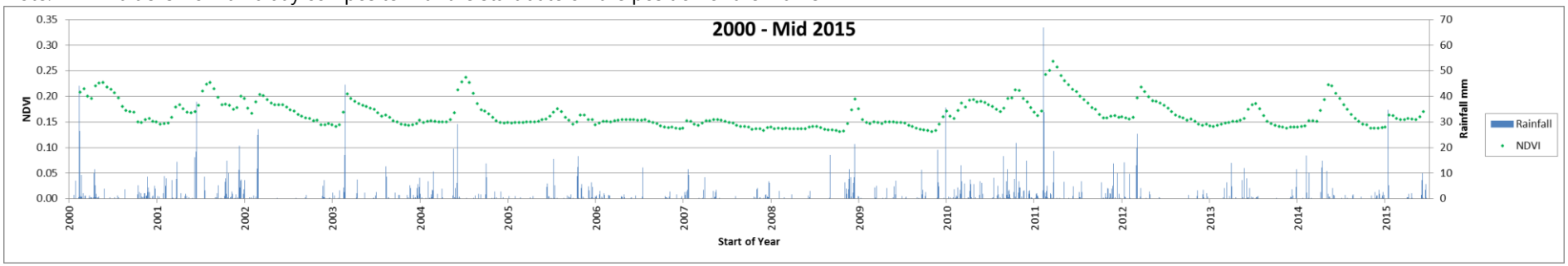

B. Metadata for GDE Index Tool by Processing Step

Step 1	
Processing	For each MODIS NDVI composite file, calculate which pixels equal or exceed the NDVI threshold input
Example of parameters	NDVI _Threshold = 0.2
Input subfolder	MODIS_NDVI 1 raster per 16 days 2000049.tif, 20000065.tif, … 2015161.tif (Note: Day number is the first day of the composite - e.g. 2000049 covers Feb 18th - Mar 5th 2000) Possible values: -1 to +1
Output subfolder	MODIS_NDVI_Point_2_Threshold 1 raster per 16 days 2000049.tif, 20000065.tif, … 2015161.tif Possible values: 0 if NDVI < 0.2 (NDVI_Threshold); 1 if NDVI >= 0.2 (i.e. = 1 if greener)
Step 2	
Processing	For each NDVI pixel location, calculate how many times it reached the NDVI threshold (i.e. sum the outputs of Step 1)
Example of parameters	NDVI_Threshold = 0.2
Input subfolder	MODIS_NDVI_Point_2_Threshold 1 raster per 16 days 2000049.tif, 20000065.tif, … 2015161.tif Possible values: 0 if NDVI < 0.2 (NDVI_Threshold); 1 if NDVI >= 0.2 (i.e. = 1 if greener)
Output subfolder	Periods_Green 1 raster Periods_Green_Point_2.tif Possible values: 0 to 353 (i.e. 0 to number of MODIS NDVI files)
Step 3	
Processing	For each day, calculate the cumulative rainfall for the previous 'x' days for each pixel (e.g. sum the previous 7 days rain)
Example of parameters	Rainfall_Days = 7
Input subfolder	Daily_Rainfall 1 raster per day 19980101.tif, 19980102.tif, … 20150630.tif Possible values: Rainfall amount (mm)
Output subfolder	Daily_Rainfall_Previous_7_Days 1 raster per day

	19980108.tif, 19980109.tif, … 20150630.tif (Note: first output file is 7 days after first input file) Possible values: Cumulative rainfall amount (mm)
Step 4	
Processing	For each day, calculate if the previous cumulative rainfall exceeded the rainfall threshold (i.e. was it a 'significant' rainfall event)
Example of parameters	Rainfall_Days = 7 Rainfall_Threshold = 25
Input subfolder	Daily_Rainfall_Previous_7_Days 1 raster per day 19980108.tif, 19980109.tif, … 20150630.tif (Note: first output file is 7 days after first input file) Possible values: Cumulative rainfall amount (mm)
Output subfolder	Daily_Rainfall_Previous_7_Days_25_mm_Threshold 1 raster per day 19980108.tif, 19980109.tif, … 20150630.tif (Note: first output file is 7 days after first rainfall data day) Possible values: 0 if previous 7 Days rainfall >= 25 (Rainfall_Threshold); 1 if previous 7 Days rainfall < 25 (i.e. = 1 if no 'significant' rain)
Step 5	
Processing	For each NDVI composite period, calculate if there were any significant rainfall events either within the dates of the 16 day composite or in the preceding dry period duration. Multiply the input rasters for the dates in question together. If ANY input raster pixel day = 0 (a significant rainfall event) the output pixel will be 0, otherwise it will be 1.
Example of parameters	Rainfall_Days = 7 Rainfall_Threshold = 25 Dry_Period = 180
Input subfolder	Daily_Rainfall_Previous_7_Days_25_mm_Threshold 1 raster per day 19980108.tif, 19980109.tif, … 20150630.tif (Note: first output file is 7 days after first rainfall data day) Possible values: 0 if previous 7 Days rainfall >= 25 (Rainfall_Threshold); 1 if previous 7 Days rainfall < 25 (i.e. = 1 if no 'significant' rain)
Output subfolder	Daily_Rainfall_Previous_7_Days_25_mm_Threshold_180_Dry_Days I raster per 16 days (Note: not for every individual day, same as NDVI composite dates) 2000049.tif, 20000065.tif, … 2015161.tif Possible values: 0 if at least one significant rainfall event (25 mm within 7 days), 1 if no significant rainfall events, in the previous 180 days or the NDVI composite dates.
Step 6	
Processing	For each NDVI composite date, resample the rainfall data from Step 5 (approximately 5 km cell size) to be the same cell size (approximately 250 metres) as the NDVI data and align (snap) to the NDVI data.

Example of parameters	Rainfall_Days = 7 Rainfall_Threshold = 25 Dry_Period = 180
Input subfolder	Daily_Rainfall_Previous_7_Days_25_mm_Threshold_180_Dry_Days I raster per 16 days (Note: not for every individual day, same as NDVI composite dates) 2000049.tif, 20000065.tif, … 2015161.tif Possible values: 0 if at least one significant rainfall event (25 mm within 7 days), 1 if no significant rainfall events, in the previous 180 days or the NDVI composite dates.
Output subfolder	Daily_Rainfall_Previous_7_Days_25_mm_Threshold_180_Dry_Days_Resampled I raster per 16 days (Note: Now the same cell size as the NDVI data (250 metres approx.), and aligned with the NDVI data) 2000049.tif, 20000065.tif, … 2015161.tif Possible values: 0 if at least one significant rainfall event (25 mm within 7 days) within in the 180 days or the NDVI composite dates, 1 if no significant rainfall events in the 180 days or the NDVI composite dates.
Step 7	
Processing	For each rainfall pixel location, calculate how many times it was in a dry period (i.e. sum the outputs of Step 6 – one file per NDVI composite period)
Example of parameters	Rainfall_Days = 7 Rainfall_Threshold = 25 Dry_Period = 180
Input subfolder	Daily_Rainfall_Previous_7_Days_25_mm_Threshold_180_Dry_Days_Resampled I raster per 16 days (Note: Now the same cell size as the NDVI data (250 metres approximately), and aligned with the NDVI data) 2000049.tif, 20000065.tif, … 2015161.tif Possible values: 0 if at least one significant rainfall event (25 mm within 7 days) within in the 180 days or the NDVI composite dates, 1 if no significant rainfall events in the 180 days or the NDVI composite dates.
Output subfolder	Periods_Dry 1 raster Periods_Dry_7_25_180.tif Possible values: 0 to 353 (i.e. 0 to number of MODIS NDVI files)
Step 8	
Processing	For each NDVI composite period, calculate when a pixel was in a dry period and also above the NDVI threshold i.e. persistent green i.e. Step 1 results = 1 (High NDVI) and Step 6 results = 1 (dry period)
Example of parameters	NDVI _Threshold = 0.2 Rainfall_Days = 7 Rainfall_Threshold = 25

	Dry_Period = 180
Input subfolders	MODIS_NDVI_Point_2_Threshold 1 raster per 16 days 2000049.tif, 20000065.tif, … 2015161.tif Possible values: 0 if NDVI < 0.2 (NDVI_Threshold); 1 if NDVI >= 0.2 (i.e. = 1 if greener) Daily_Rainfall_Previous_7_Days_25_mm_Threshold_180_Dry_Days_Resampled I raster per 16 days (Note: The same cell size as the NDVI data (250 metres approx.), and aligned with the NDVI data) 2000049.tif, 20000065.tif, … 2015161.tif Possible values: 0 if at least one significant rainfall event (25 mm within 7 days) within in the 180 days or the NDVI composite dates, 1 if no significant rainfall events in the 180 days or the NDVI composite dates.
Output subfolder	Green_ Point_2_In_Dry_7_25_180 1 raster per 16 days 2000049.tif, 20000065.tif, … 2015161.tif Possible values: 1 if green and dry, otherwise 0
Step 9	
Processing	For each NDVI pixel location, calculate how many times it was persistent green i.e. Sum the outputs from Step 8
Example of parameters	NDVI _Threshold = 0.2 Rainfall_Days = 7 Rainfall_Threshold = 25 Dry_Period = 180
Input subfolder	Green_ Point_2_In_Dry_7_25_180 1 raster per 16 days 2000049.tif, 20000065.tif, … 2015161.tif Possible values: 1 if green and dry, otherwise 0
Output subfolder	Periods_Green_In_Dry 1 raster Periods_Green_Point_2_In_Dry_7_25_180.tif Possible values: 0 to 353 (i.e. 0 to number of MODIS NDVI files)
Step 10	
Processing	For each NDVI pixel location, calculate the GDE Index i.e. What percentage of times were the dry periods above the NDVI_Threshold? i.e. (Step 9 / Step 7) x 100
Example of parameters	NDVI _Threshold = 0.2

	Rainfall_Days = 7 Rainfall_Threshold = 25 Dry_Period = 180
Input subfolders	Periods_Dry 1 raster Periods_Dry_7_25_180.tif Possible values: 0 to 353 (i.e. 0 to number of MODIS NDVI files) Periods_Green_In_Dry 1 raster Periods_Green_Point_2_In_Dry_7_25_180.tif Possible values: 0 to 353 (i.e. 0 to number of MODIS NDVI files)
Output subfolder	GDE_Index 1 raster GDE_Index_Green_Point_2_In_Dry_7_25_180.tif Possible values: 0 to 100 (percent) (i.e. ranging from never green after an extended dry period to always green)

Text in red is examples of the parameters which may be input by the user. They will change if different parameters are input.

Note: *The input NDVI and rainfall data must be stored in subdirectories (named Daily_Rainfall and MODIS_NDVI respectively) of the pathname entered. The output data will also be stored in subdirectories of this Root_Directory.*

C. Examples of Outputs from the GDE Index Tool

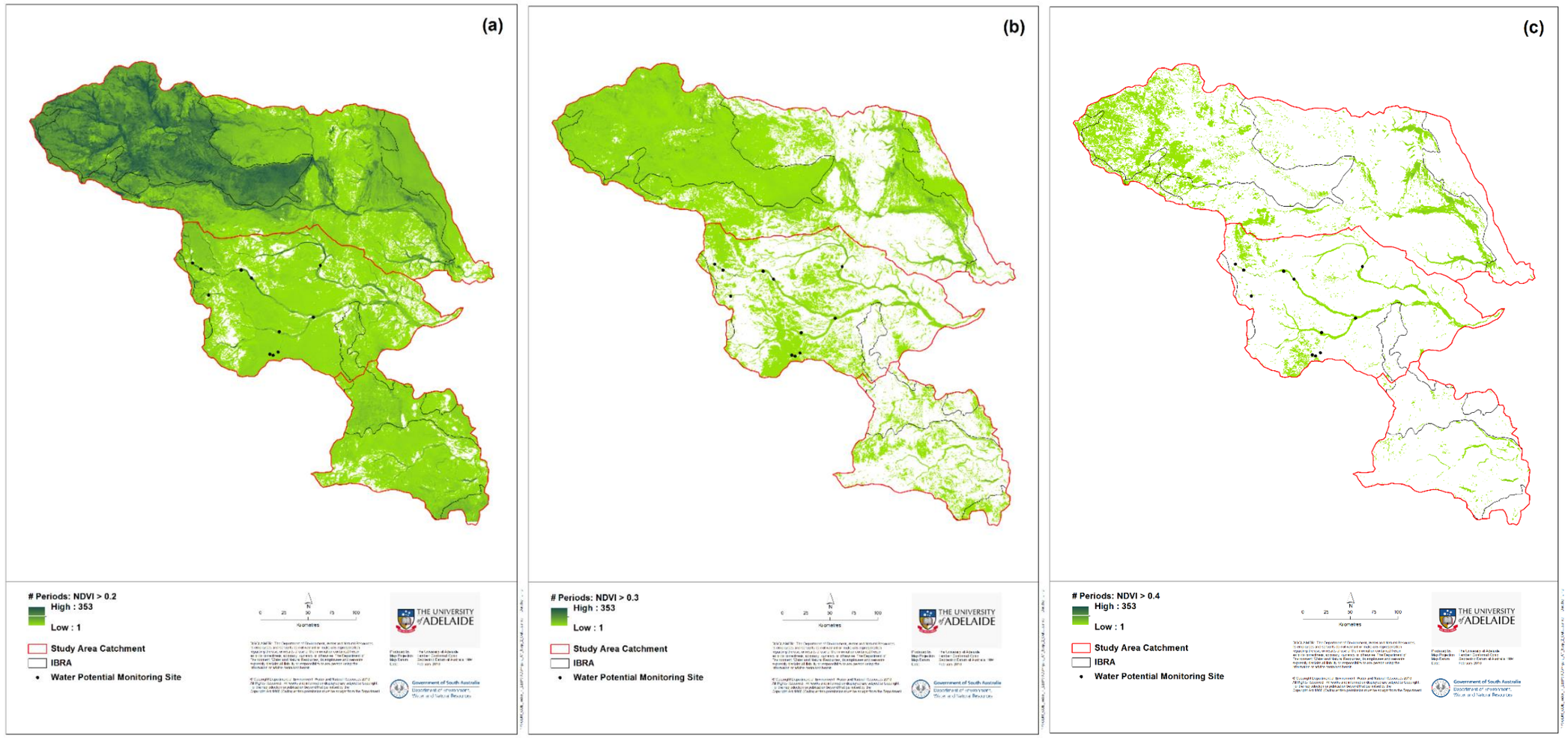

Figure C-1: Step 2 output. Number of times above NDVI threshold in 353 NDVI images (a) NDVI > 0.2 (b) NDVI > 0.3 (c) NDVI > 0.4.

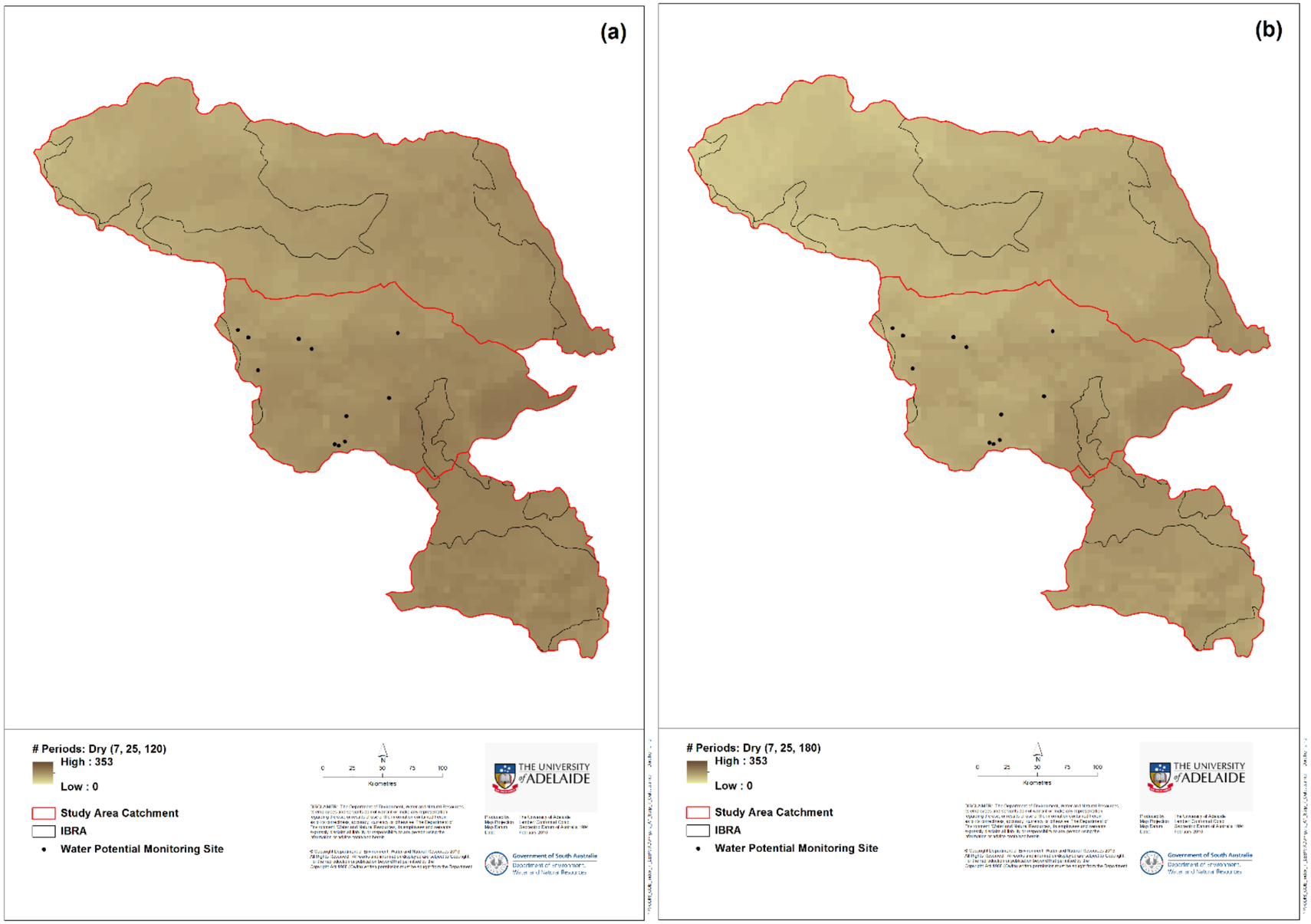

Figure C-2: Step 7 output. Number of dry periods out of a possible 353 (a) 120 days with no 7 days > 25 mm rain (lowest pixel value = 62 periods, highest =243 periods) (b) 180 days with no 7 days > 25 mm rain (lowest pixel value = 28 periods, highest = 205 periods).

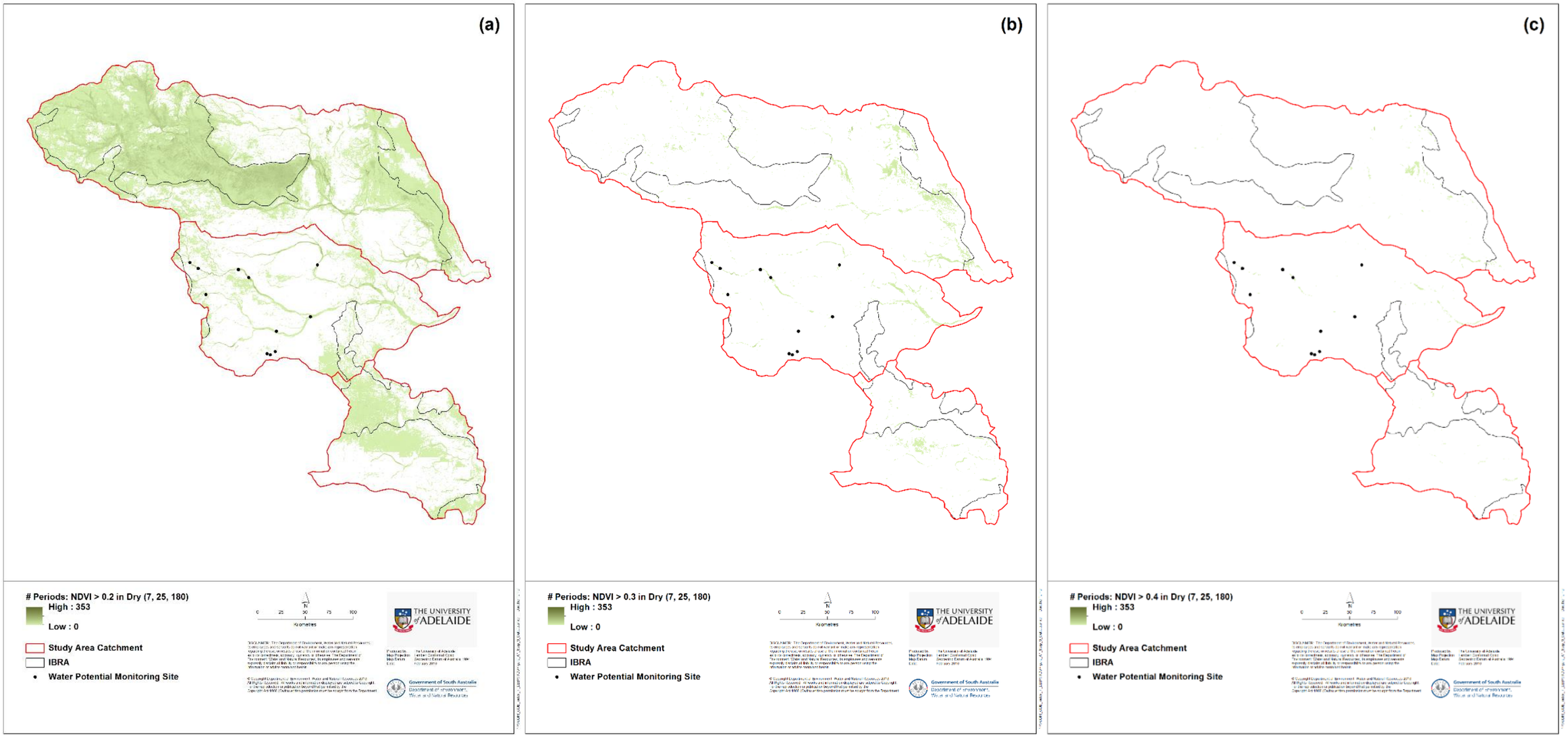

Figure C-3: Step 9 output. Number of times above NDVI threshold in dry periods. Dry period =180 days with no 7 days > 25 mm rain (a) NDVI > 0.2 (b) NDVI > 0.3 (c) NDVI > 0.4.

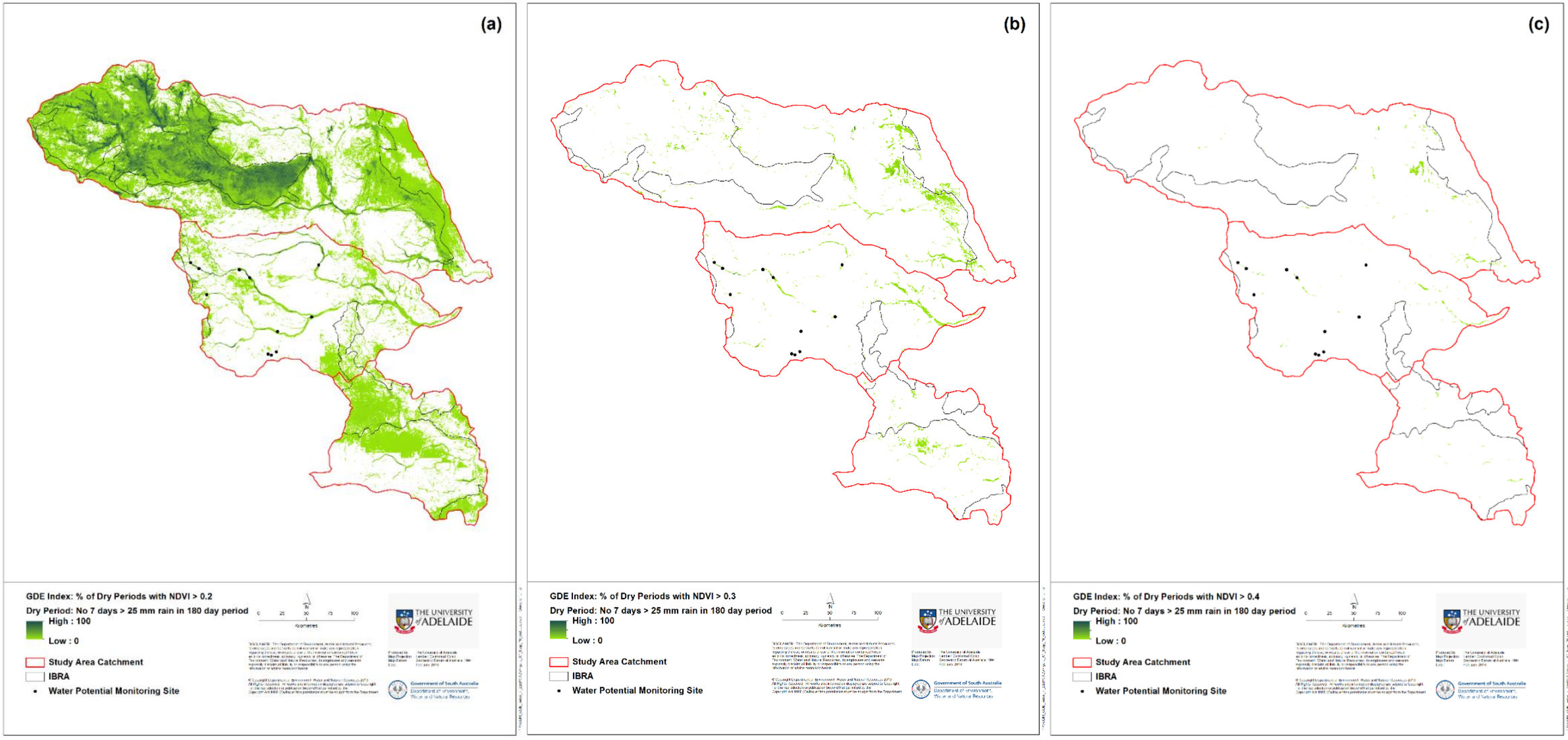

Figure C-4: Step 10 output. GDE Index (1 to 100). Dry period =180 days with no 7 days > 25 mm rain (a) NDVI > 0.2 (b) NDVI > 0.3 (c) NDVI > 0.4.

D. Leaf water potential monitoring sites 1:20 000; 1:20 000 with the GDE Index; 1:2000 enlargement

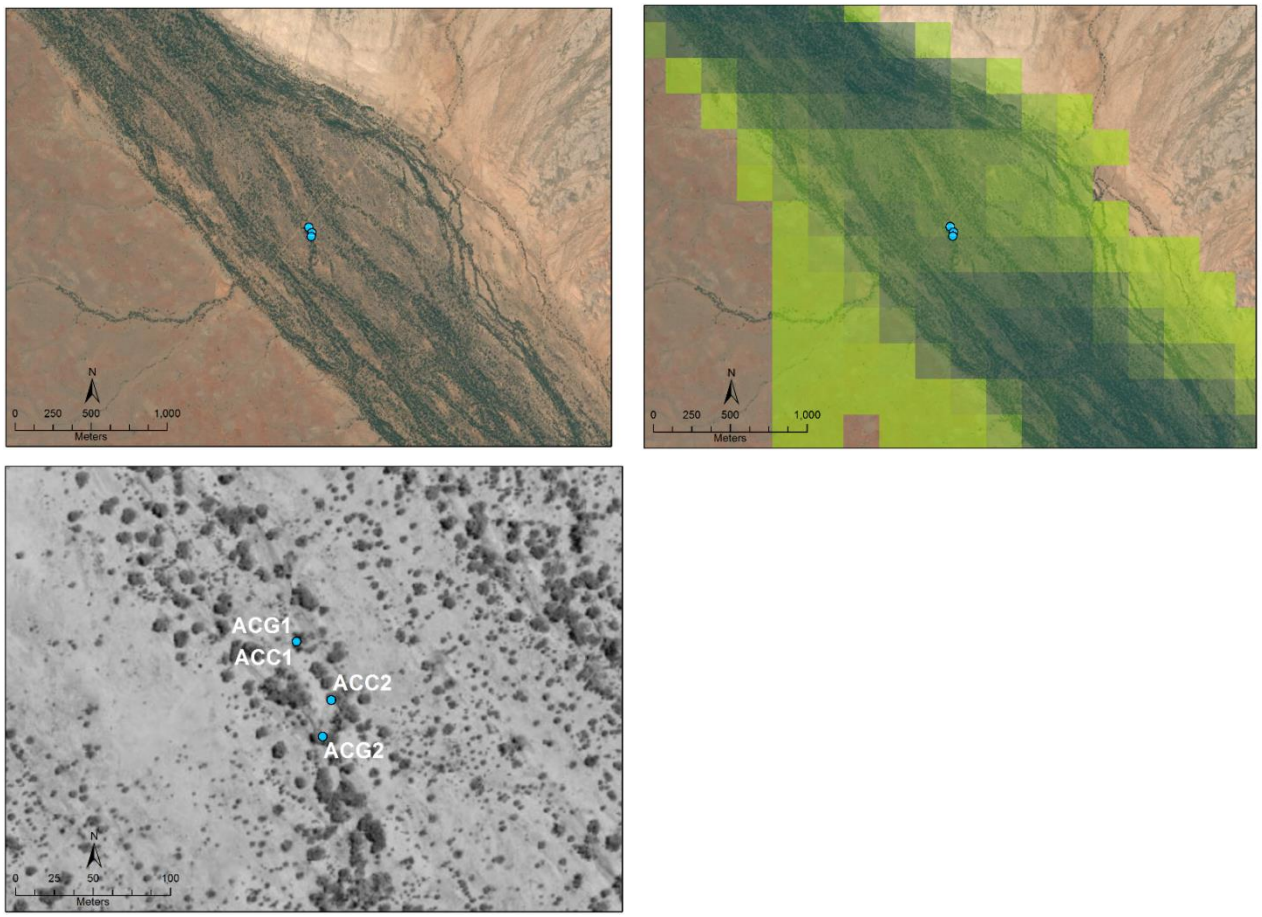

Figure D-1: Leaf water potential monitoring sites, Arckaringa

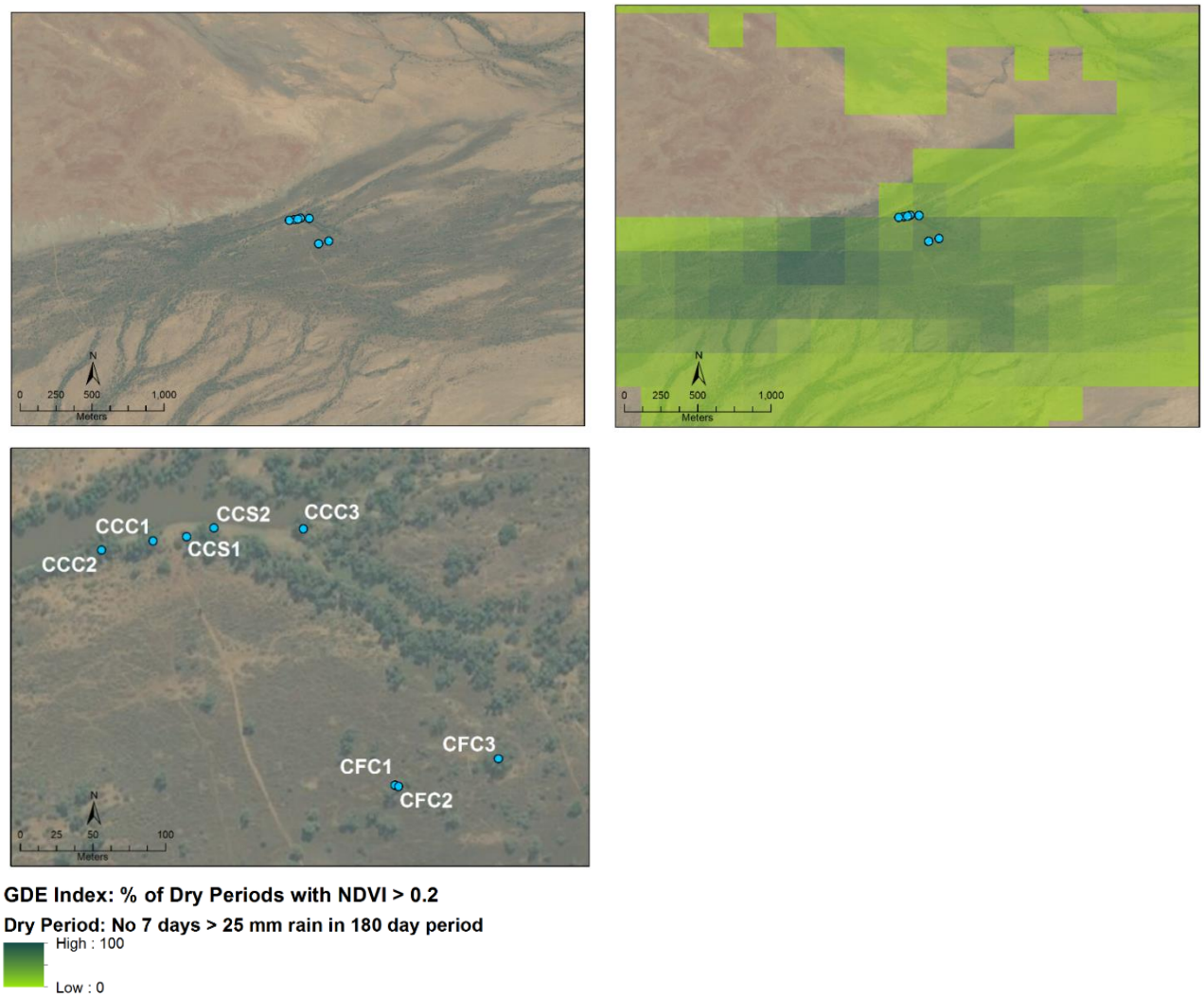

Figure D-2: Leaf water potential monitoring sites, Cootanoorina Waterhole

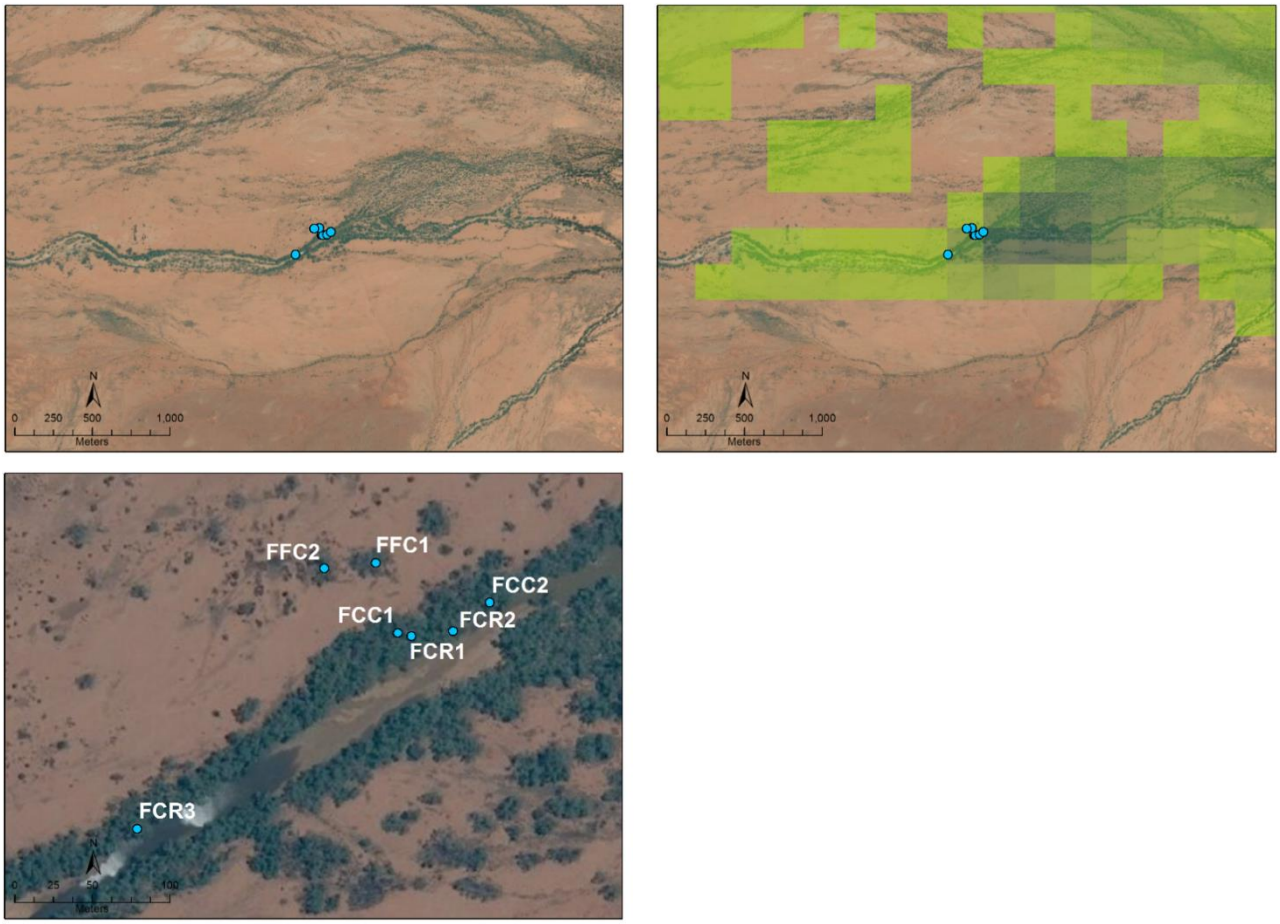

Figure D-3: Leaf water potential monitoring sites, Francis Camp Waterhole

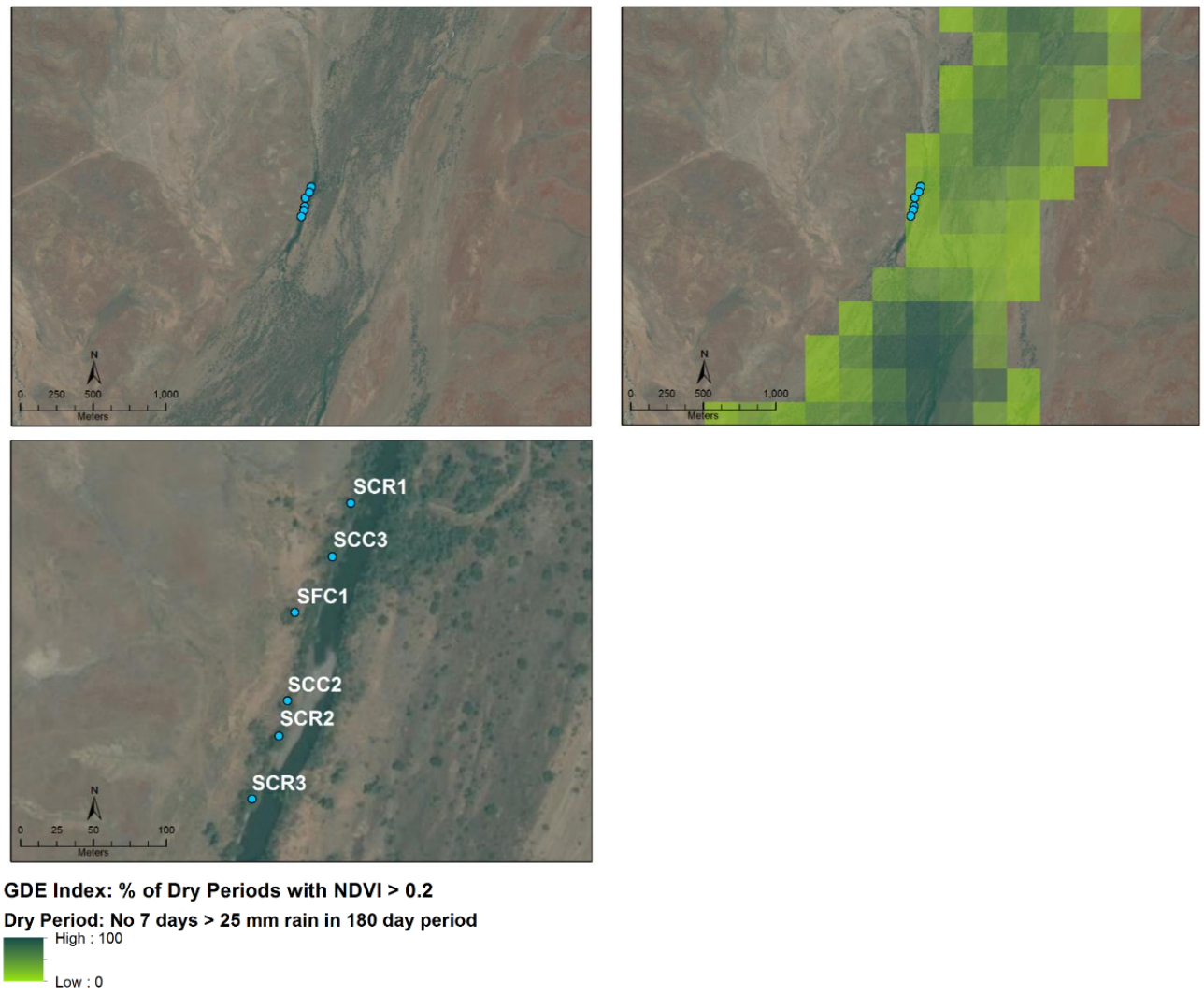

Figure D-4: Leaf water potential monitoring sites, Stewart Waterhole

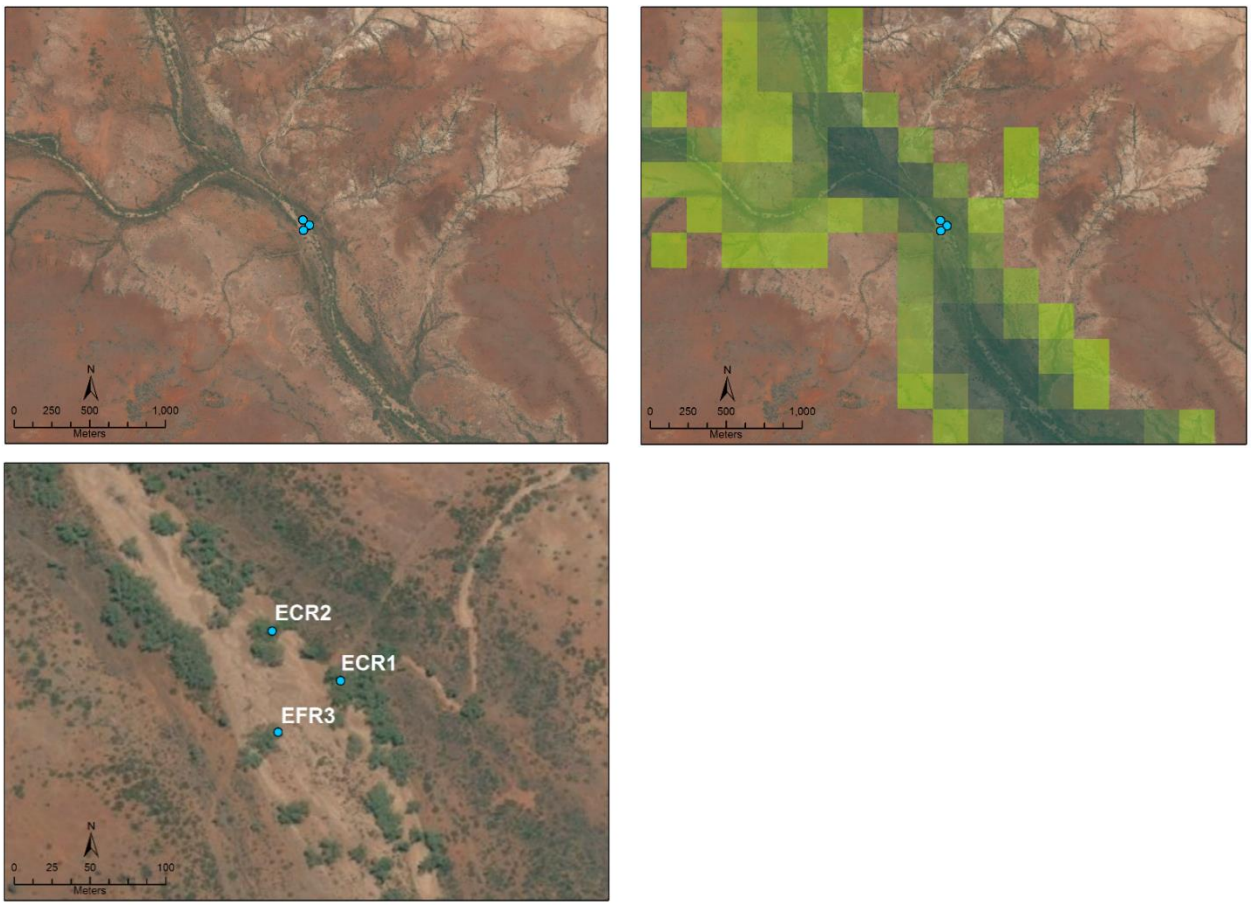

Figure D 5: Leaf water potential monitoring sites (e) Wintinna Homestead, Ethel Well

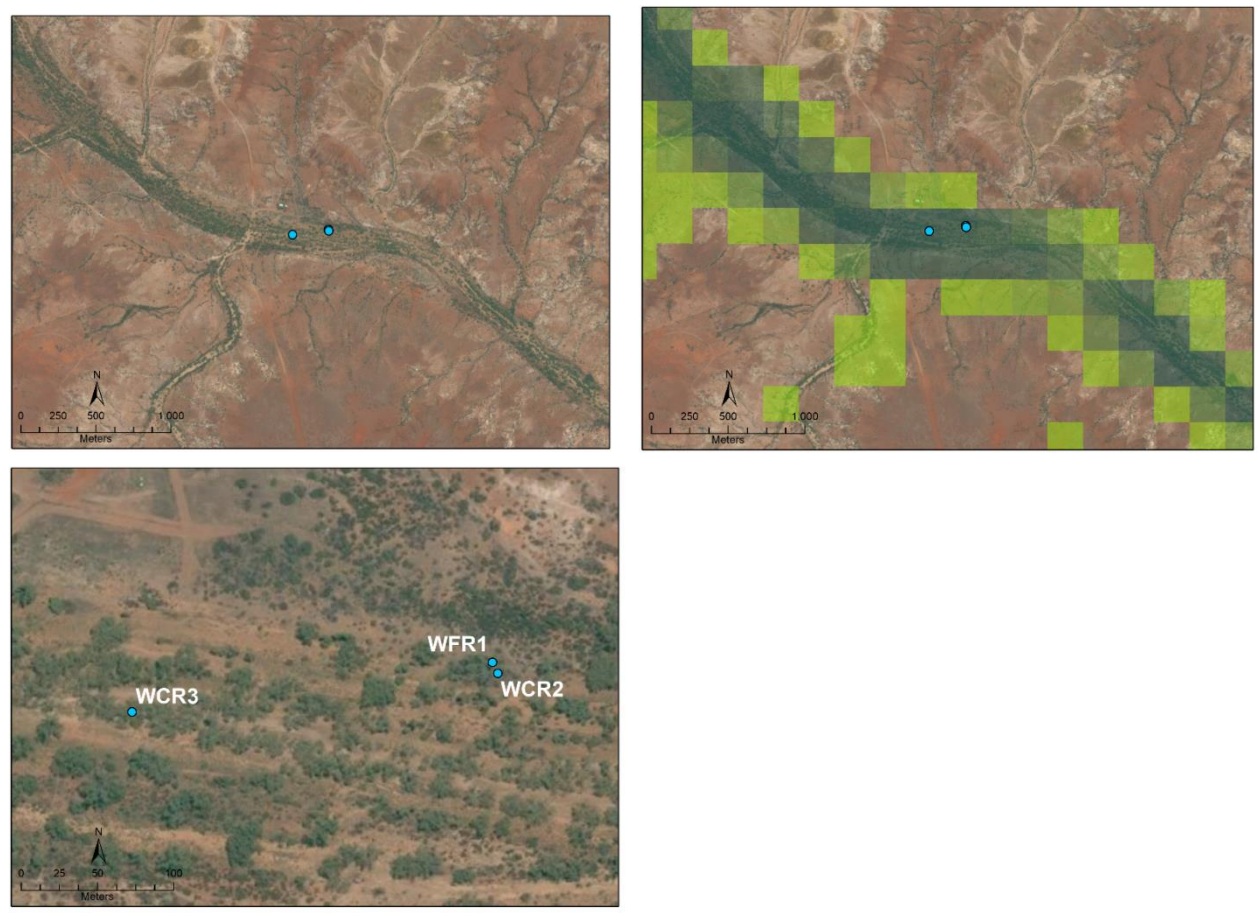

Figure D-6: Leaf water potential monitoring sites, Wintinna Homestead

E. GDE Index and WOfS inundation

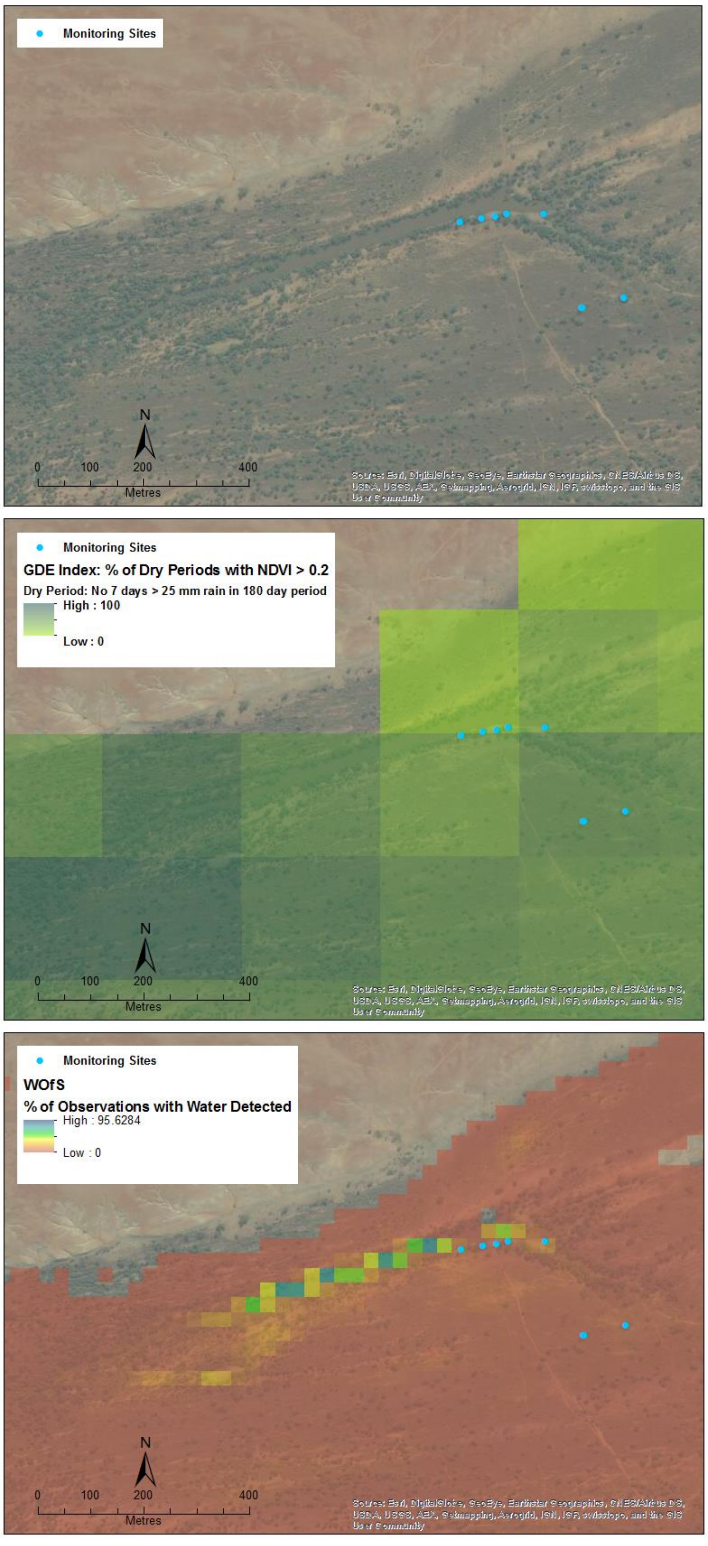

Figure E-1: Cootanoorina Waterhole (a) Leaf water potential monitoring sites, (b) GDE_Index, (c) WOfS inundation

Government of South Australia
Department of Environment,
Water and Natural Resources